

Washington University in St. Louis
Washington University Open Scholarship

All Theses and Dissertations (ETDs)

1-1-2011

Single chain MHC trimer-based DNA vaccines for pathogen protection

Sojung Kim

Washington University in St. Louis

Follow this and additional works at: <https://openscholarship.wustl.edu/etd>

Recommended Citation

Kim, Sojung, "Single chain MHC trimer-based DNA vaccines for pathogen protection" (2011). *All Theses and Dissertations (ETDs)*. 598.

<https://openscholarship.wustl.edu/etd/598>

This Dissertation is brought to you for free and open access by Washington University Open Scholarship. It has been accepted for inclusion in All Theses and Dissertations (ETDs) by an authorized administrator of Washington University Open Scholarship. For more information, please contact digital@wumail.wustl.edu.

WASHINGTON UNIVERSITY IN ST. LOUIS

Division of Biology and Biomedical Sciences

Immunology

Dissertation Examination Committee;

Ted Hansen, Chair

Paul M. Allen

Janet M. Connolly

Michael S. Diamond

Daved H. Fremont

Chyi-Song Hsieh

Wayne M. Yokoyama

SINGLE CHAIN MHC TRIMER (SCT)-BASED DNA VACCINES FOR PATHOGEN

PROTECTION

by

Sojung Kim

A dissertation presented to the
Graduate School of Arts and Sciences
of Washington University in
partial fulfillment of the
requirements for the degree
of Doctor of Philosophy

August 2011

Saint Louis, Missouri

Abstract

CD8⁺ T cells play a major role in controlling infection and disease progression in many infectious diseases. Upon infection, antigen-specific CD8⁺ T cells are generated and mainly through their cytotoxic activity remove infected cells, therefore, pathogens. Ongoing research has identified antigenic epitopes in a vast number of pathogens and, using the identified epitopes, the induction of CD8⁺ T cell immune responses has been an important strategy for successful vaccines. However, most immunization approaches with class I binding peptides have failed to induce CD8⁺ T cell responses strong enough to prevent disease. This failure has been attributed to the lack of CD4⁺ T cell help and difficulty in maintaining a sufficient level of antigen presentation required for CD8⁺ T cell activation. To circumvent these limitations, we have developed fully assembled MHC molecules that can be expressed as membrane-bound proteins on the cell surface, termed single chain trimers (SCTs). SCTs are composed of an immunodominant peptide, β 2m, and MHC I heavy chain covalently linked by 15-20 amino acid flexible linkers. Because SCTs are expressed as a single polypeptide chain, they do not require peptide processing, or chaperone-assisted peptide loading in the ER. Furthermore, antigen presentation by the SCT bypasses the need to compete with an extensive pool of endogenous peptides for peptide loading. SCTs are folded properly and T cells see SCTs comparably to native peptide/MHC I complexes. Various human and mouse class Ia and Ib MHC molecules have been engineered with epitope peptides into SCTs and proven as useful tools to

monitor and modulate immune responses. Thus, SCT engineering offers a great potential as a platform for antigen-specific DNA vaccines. Although there have been several reports of SCT-based DNA vaccines generating antigen-specific CTL responses, there have been no reports of pathogen protection after DNA vaccine expression of SCTs. In this thesis, I examined the efficacy of SCT DNA vaccines for the first time in pathogen infection models. First, we developed a clinically relevant human HLA-A2 transgenic mouse model of West Nile virus (WNV) infection and demonstrated protective efficacy of a HLA-A2 SCT DNA vaccine against lethal viral infection. Second, I validated the potency of a SCT DNA vaccine using the BALB/c model of *Listeria monocytogenes* infection, which indicated that SCT DNA vaccines also provide protective immunity against bacterial infection. Lastly, I demonstrated that further engineering of SCTs (dtSCT) using a disulfide trap to better accommodate epitopes can potentiate the capacity of SCTs to stimulate CD8⁺ T cells, suggesting broad application of SCTs even with low immunogenic peptides. I also used disulfide trap- or chimeric SCTs to test the mechanism of antigen presentation after DNA vaccination. My studies showed that SCTs are presented to T cells as intact molecules after DNA immunization, suggesting direct presentation by transfected DCs or cross-dressing as a major mechanism of the antigen presentation by DNA vaccine. In summary, these dissertation studies demonstrated that SCT-based DNA vaccines can provide pathogen protection and SCTs are effective probes for dissecting mechanisms of antigen presentation.

Acknowledgements

It is a pleasure to thank those who made this thesis possible and I could never have finished this work without the help, support, guidance and efforts of them.

Firstly, I am heartily thankful to my advisor, Ted Hansen, for his support, patience, and friendship throughout my graduate studies. It is not often that one finds an advisor that always has a lot of genuine interest and understanding for my work and for my life. His advice was essential to the completion of this dissertation and has taught me innumerable lessons and insights on the workings of academic research as well as the life. I am also deeply grateful to Dr. Janet Connolly for her support, helpful criticism, and friendship throughout my graduate studies in the lab.

This thesis work would not have been possible without successful collaborations with colleagues here at Washington University. I would like to thank the chair of my thesis committee, Dr. Michael Diamond and his West Nile virus research group for support and guidance over the years. I would also like to thank to Dr. Daved Fremont for his encouragement and valuable advice for the SCT study as well as the MR1 study which unfortunately was not able to be put into this thesis. I am also grateful to Drs. Emil Unanue and Javier Carrero for their help and advice for the SCT vaccine study in the Listeria model. I would like to thank Dr. Chyi-Song Hsieh for his support and valuable suggestions for this thesis work as well as the MR1 study. I am very grateful to my

committee members, Drs. Paul Allen and Wayne Yokoyama for their constructive suggestions throughout my thesis work.

My thanks also go to the past and present members of the Hansen/Connolly lab who supported me in many respects of the science during my graduate studies; Nancy Myers, Tina Primeau, Xiaoli Wang, Weijen Chua, Roger Herr, Shouxiong Huang, and Lawrence Yu. Thanks also go out to our collaborators, Drs. Beatriz Carreno (Medical Oncology), William Gillanders, and Lijin Li (Surgery) for their help and valuable advice.

Last, I would like to thank my husband, Sanghun Lee for his support, encouragement, and love. I am also thankful to my loving son, Ryan, and feel blessed to be a mother. I thank and express my deepest respect and love to my parents, Young-qu and Hyea-soon, and sister, Soyoun, for their dedication and the many years of support and concern.

Table of Contents

Abstract	ii
Acknowledgements	iv
Table of Contents	vi
List of Tables and Figures	viii
Chapter 1. Background and Significance	1
Chapter 2. HLA-A2 SCT DNA vaccines and West Nile virus infection	14
2.1 Identification of the immunodominant CD8 ⁺ T cell epitope	25
2.2 Protection against infection	46
Chapter 3. H-2K ^d SCT DNA vaccines and <i>Listeria monocytogenes</i> infection	68
3.1 Protection against infection	78
3.2 Role of cognate vs. non-cognate CD4 ⁺ T cell help for protection	86
Chapter 4. Mechanisms of SCT-based DNA vaccines	107
4.1 Trapping peptide by disulfide bond can potentiate difficult SCTs	111
4.2 SCTs are presented as intact structures	119

Chapter 5. Concluding Remarks and Future Directions	133
References	141
CV	164

List of Tables and Figures

Table 1. Six identified WNV-derived peptides bound to HLA-A*0201	38
Figure 1. Identification of an immunodominant WNV epitope bound to HLA-A2 in HHDI mice	39
Figure 2. Presentation of viral epitope/HLA-A2 complexes at the HeLa cell surface after WNV infection	40
Figure 3. Presentation of viral epitopes, SVG9 and SLF9, at the human DC surface after WNV infection	41
Figure 4. Schematic illustration of a WNV polyprotein expressed at the ER membrane	42
Figure 5. Presentation of viral epitopes at the cell surface is dependent on TAP function.	43
Figure 6. WNV infection generates SVG9-specific CTLs	44
Figure 7. Adoptively transferred SVG9-specific CTLs provide protection against lethal WNV infection	45
Figure 8. Expression of A2/SVG9 SCT and recognition by SVG9-specific T cells	56
Figure 9. Induction of a strong CD8 ⁺ T cell response by HLA-A2/SVG9 SCT DNA immunization	57

Figure 10. HLA-A2/SVG9 SCT DNA immunization provides mice protection against lethal WNV infection	58
Figure 11. Co-expression of a CD4 ⁺ helper T cell epitope enhances protective efficacy of SCTs	59
Figure 12. HLA-A2/SVG9 SCT DNA immunization lowers viral burden in the brain but has no effect on humoral responses.	60
Figure 13. SCT DNA immunization induces non-sterilizing immunity	61
Figure 14. SCT DNA vaccine generates functional memory T cell immunity and provides long-term protection	62
Figure 15. Expression and recognition of K ^d / LLO ₉₁₋₉₉ SCTs by CD8 ⁺ T cells	83
Figure 16. K ^d /LLO ₉₁₋₉₉ SCT DNA immunization induces peptide-specific CD8 ⁺ T cells	84
Figure 17. A K ^d /LLO ₉₁₋₉₉ SCT DNA vaccine lowers bacterial burden in lethal <i>L. monocytogenes</i> infection	85
Figure 18. A SCT DNA vaccine develops memory CD8 ⁺ T cells	93
Figure 19. A SCT DNA vaccine develops functional memory CD8 ⁺ T cells	94
Figure 20. Co-expression of a CD4 ⁺ T cell epitope does not affect primary CD8 ⁺ T cell responses	95
Figure 21. Co-expression of a CD4 ⁺ T cell epitope increases memory CD8 ⁺ T cell	

responses	96
Figure 22. Co-expression of a CD4 ⁺ T cell epitope enhances protective efficacy of a SCT DNA vaccine	97
Figure 23. K ^b /WNVp3 SCTs are expressed but do not activate peptide-specific CD8 ⁺ T cells	116
Figure 24. Diagram of the H-2K ^b /OVAp dtSCT	117
Figure 25. A disulfide trap improves stability and T cell recognition of K ^b /WNVp3 SCTs	118
Figure 26. Chimeric HLA-A2/D ^b α3 SCTs induce stronger CD8 ⁺ T cell responses than intact HLA-A2 SCTs in HHDII mice	125
Figure 27. H-2K ^b /OVAp5Y SCT DNA but not OVAp5Y cDNA immunization primes CD8 ⁺ T cells	126
Figure 28. H-2K ^b /WNVp3 dtSCTs induce a more robust CD8 ⁺ T cell response than the H-2K ^b /WNVp3 SCTs.	127

Chapter 1

Background and Significance

Vaccination is the most effective method of preventing infectious diseases. Most of the vaccines developed to date have focused on humoral immunity, i.e. production of antibodies for neutralizing viruses and toxins or opsonizing bacteria. However, there are many cases in which the antibody response is not the best effector arm of the immune system to protect against pathogens. This is where T cell immunity comes into play. CD8⁺ T cells also have a significant function in immunity against pathogens. Cytotoxic CD8⁺ T lymphocytes (CTLs) kill the infected cells and/or release cytokines that inhibit growth of the microbe or impair the ability of the pathogen to survive inside the cell. For example, cytotoxic memory CD8⁺ T cells have been found in several model systems to have prominent roles in the clearance of virus by producing antiviral cytokines or lysing virus-infected cells. Thus efforts have been made to generate vaccines that can elicit effective CD8⁺ T cell responses [1, 2]. Mechanistically generation of effective CD8⁺ T cell responses requires the delivery of antigen into the appropriate antigen presentation pathway to stimulate major histocompatibility complex I (MHC class I)-restricted CTL responses. Although it is possible to elicit CD8⁺ T cell responses against intact or attenuated pathogens, this approach rarely elicits optimal CD8⁺ T cell responses. Alternatively, it is considered more attractive to immunize only against the specific antigens that elicits efficacious anti-pathogen CD8⁺ T cell immune responses. However this approach requires knowing the immunodominant pathogen-specific antigens

presented by MHC-disparate individuals. Fortunately, there are now several computer programs that reliably predict peptide binding to different MHC alleles, and the genomes of several pathogens have continued to be sequenced. Thus bioinformatic analysis of a pathogen genome can be used to comprehensively identify pathogen-specific potential epitopes for CD8⁺ T cells *in silico*. Such predicted epitopes for CD8⁺ T cells can then be tested experimentally by showing they are capable of specific *ex vivo* re-activation of CD8⁺ T cells from infected patients or animals. However, unfortunately, immunodominant peptides have not been particularly effective in stimulating primary CD8⁺ T cell immune responses *in vivo*, thus limiting their vaccine applications. There are no currently available peptide-based or plasmid DNA vaccines encoding only immunodominant CD8⁺ T cell epitopes. However, using tumor models there is recent evidence by Melief and colleagues that long peptides extended beyond the minimal MHC-binding epitope may be effective as vaccines because of prolonged, dendritic cell-focused antigen presentation [3-8].

Failure to elicit a robust CD8⁺ T cell response after immunization with class I peptide epitopes in part stems from the lack of concomitant help from CD4⁺ T cells. In several experimental systems CD4⁺ T cell help is required for generating and sustaining long term CD8⁺ T cell memory. An additional problem with immunizing with class I binding peptides by themselves is the difficulty in maintaining a sufficient level of antigen presentation required for CD8⁺ T cell activation. As briefly mentioned above, CD8⁺ T cells see antigens in a form of MHC I/peptide complexes. MHC molecules are composed of a heavy chain and β 2-microglobulin (β 2m) and bind peptides from self or

from pathogen-infected or transformed cells, and present them on the cell surface to CD8⁺ T cells. Multiple cellular and molecular processes are required for cell surface expression of MHC I/peptide complexes [9]. Peptides suitable for MHC I binding are generated in the cytosol by the proteasome which generates peptides of 10-20 amino acids that are transported into the endoplasmic reticulum (ER) via TAP 1/2 (transporter associated with antigen processing). In the ER, peptides can be further trimmed at the N-terminus by aminopeptidases for MHC I binding. Then the peptide loading complex (PLC) in the ER facilitates assembly of the MHC I/peptide complex and consists of TAP, ERp57, and the molecular chaperones, tapasin and calreticulin along with MHC I heavy chain and β 2 microglobulin. Once a suitable peptide, typically 8-10 amino acids, binds to the binding groove of MHC I, the complex is released from the PLC and transits to the cell surface. Because this antigen processing and presentation pathway involves several complex molecular interactions, it can be inefficient, particularly for certain MHCI/peptide complexes. Furthermore, MHC molecules do not discriminate self from non-self peptides, and the antigenic peptide must compete with an extensive pool of endogenous peptides for loading onto MHC class I molecules and presentation to CD8⁺ T cells. Furthermore, peptide dissociation can occur post ER assembly, which lowers the steady state level of specific MHCI/peptide complexes at the plasma membrane. This results in insufficient MHC I/peptide complexes displayed at the cell surface for CD8⁺ T cell priming after epitope vaccines. Thus, antigenicity of vaccines for T cell responses can be enhanced by improving processing, abundance, or MHC binding of peptides.

To circumvent limitations of antigen processing and presentation, we and others have engineered fully assembled MHC molecules that can be expressed as membrane proteins on the cell surface [10, 11]. These fully assembled MHC molecules, termed single chain trimers (SCTs), are composed of an immunodominant peptide, a flexible linker of 15 or 20 amino acids that connects the C terminus of the peptide to the N terminus of $\beta 2m$, and a second flexible linker that connects the C terminus of $\beta 2m$ to the N terminus of the heavy chain of a given class I MHC molecule. We chose to attach the components in this order because i) based on the crystal structures, the C-terminus of peptide ligand is more accessible than the N-terminus deeply buried in the peptide binding groove and unusual peptides with a few additional residues at the C-terminal end have been isolated, ii) the crystal structure of MHC I predicts a more direct path for the linker from the peptide to the N terminus of $\beta 2m$ than to heavy chain [10-12]. Flexible linkers are based on the Gly-Gly-Gly-Gly-Ser motif that was used previously to produce single chain MHC molecules or immunoglobulins by others [10, 13]. Lengths of the linkers were determined, also based on the crystal structure, to be 10-20 amino acids and the study in our lab showed that the linker combination of 15 and 20 amino acids results in better recognition by T cells [11]. While coupling of peptide ligand to the heavy chain [10] and peptide to free $\beta 2m$ [12, 14, 15] have been previously reported by others, it was applicable only to select MHC I/peptide complexes and is not clear how efficiently it can exclude the binding of competing peptides. On the contrary, our SCTs have been successfully applied to most mouse, rat and human MHC I/peptide complexes tested so far, suggesting its application is universal. However, in this thesis work, we found that the

SCT construct does not work with every MHC I/peptide complex and this exception raised questions about whether SCTs with difficult peptides can be improved, which is important for vaccines for diseases where antigenic peptides have poor immunogenicity.

To probe structural and functional properties of SCTs, our lab has used the H-2K^b/OVAp SCT as a model. These comprehensive characterizations of the K^b/OVAp SCT have shown that the SCT has several properties described below that have potentiated their use as DNA vaccines as well as in studies of lymphocyte biology [11, 16-24]. Cell surface staining with a monoclonal antibody (mAb) specific for folded K^b as well as mAb 25D-1.16 that specifically recognizes K^b/OVAp complexes showed that SCTs are expressed at a high level with native folding at the cell surface[11]. OT-1 T cells that are specific for K^b/OVAp also recognized SCTs. Biochemical analyses using western blot revealed that SCTs maintain their intact covalent structure in cells. Covalent peptide binding in the SCT makes it less accessible to loading by exogenous competitor peptides. As a result, K^b/OVAp SCTs were very resistant to displacement by a high concentration of exogenous peptide in a peptide competition assay. They are also more stable at the cell surface than native MHC I/peptide complexes and exhibit an extended cell surface half-life. In vivo, K^b/OVAp SCTs retained their native MHC/peptide structure, and were thus able to stimulate antibody specific for K^b/OVAp by DNA vaccination. Cells expressing SCTs were detected by CTLs generated to native MHC I/peptide complexes, and CTLs generated to cells expressing SCT detect target cells expressing native MHC I/peptide complexes. Furthermore tetramers constructed with SCTs reliably stained the same T

cells as conventional tetramers. Thus T cells appear to detect SCTs indistinguishably compared to native MHC I/peptide complexes.

The MHC I peptide binding groove formed between the $\alpha 1$ and $\alpha 2$ domains of the heavy chain is closed and accommodates a certain length of peptides that does not extend beyond the binding groove. Because the interactions between the C terminus of peptide and conserved residues of heavy chain at the end of the binding groove are critical for stable peptide anchoring, in SCTs a linker extended from the C terminus of the peptide is predicted to abolish these conserved interactions and interfere with optimal peptide anchoring. In fact, K^b /OVAp SCTs exhibit lower reactivity with the antibody specific for K^b /OVAp complexes than native K^b loaded with exogenous OVAp. Also OVAp in the SCTs was more easily displaced with a high concentration of competing peptides than was the peptide bound to native K^b . Despite this impaired peptide binding, K^b /OVAp SCT is more stable than native MHC I/peptide complexes and exhibits a high level of steady state peptide occupancy because the covalently attached peptide efficiently rebinds after dissociation. Although this was not a problem for tight binding peptides like OVAp, weak binding peptides would be more dependent on peptide rebinding. Thus our lab in collaboration with the Fremont lab took a structure based approach to understand how the SCT binds peptide and accommodates the linker with the purpose to use this knowledge to engineer improvements to the SCT.

The crystal structure of K^b /OVAp SCT revealed that OVA peptide is bound in the MHC I peptide binding groove in a canonical manner where the anchoring residues, P2, P5, and P8 are buried and pointed toward the β -sheet platform of the groove. However, in

the F pocket of the peptide binding groove of the SCT, the peptide- β 2m linker extrudes from the C terminal end of the groove and extends over a conserved TCR recognition region. Tyr⁸⁴ in the K^b heavy chain, which creates the C-terminal wall in the F pocket and is involved in closing the C terminal end of the groove, precludes optimal linker positioning in the K^b/OVAp SCT. Mutation of Tyr⁸⁴ to Ala opened the C terminal end of the binding groove and created a channel to accommodate the peptide- β 2m linker without a big conformational change. This SCT^{Y84A} displayed enhanced surface stability with comparable T cell recognition to SCT^{WT} or native MHC I/peptide complexes [22, 25]. Our lab in collaboration with the Fremont lab further engineered SCTs by incorporating a disulfide trap in the F pocket area. Two mutations of Tyr⁸⁴ to Cys and Gly² of the peptide- β 2m linker to Cys generated a disulfide bond that creates a unique F pocket hydrogen bond network without disturbing overall conformation of the complexes [23]. This disulfide trapped SCT (dtSCT) better accommodates the peptide- β 2m linker and very efficiently excludes competitor peptides from the peptide binding groove and preserves TCR interactions [23-25]. The disulfide trap engineering of SCT is also applicable to human MHC class I, HLA because Tyr⁸⁴ is well conserved [24]. Thus the improved stability of dtSCT would have advantages over the original SCT (SCT^{WT}) in the case of weak-binding peptides. Importantly, various human and mouse MHC class Ia and class Ib molecules have been engineered with epitope peptides into SCT and proven as useful tools to monitor and modulate immune responses [24, 26-33].

Universal SCT engineering offers great potential as a platform for antigen-specific DNA vaccines. Plasmid DNA as vaccine vectors has been developed and applied

against various pathogens because of its advantages; easy manipulation, relatively generic construction and production, fewer safety issues than other vectors such as viral vectors, and potential for sustained antigen delivery. However, despite its great success in small animal studies, DNA vaccines performed poorly in larger animal models including human clinical trials [2, 34-39]. While efforts have been made to improve antigen expression, potency and immunogenicity of DNA vaccines, SCTs have several properties that could potentiate the use of DNA vaccines. SCTs have been proven strongly immunogenic as DNA vaccines. When expressed by DNA immunization, SCTs elicit robust antigen specific CD8⁺ T cell responses in mouse model systems. The potency of SCT DNA vaccines has been convincingly demonstrated in mouse tumor models [30, 40, 41]. For example, in a collaborative study between our lab and T. C. Wu and colleagues at Johns Hopkins university [30], mice vaccinated with DNA encoding a SCT of an immunodominant CTL epitope of human papilloma virus type 16 (HPV-16) E6 antigen and H-2K^b were protected against a lethal challenge of E6-expressing TC-1 tumor cells. Importantly, SCT-based DNA vaccines appeared more effective at generating CD8⁺ T cell immunity than subunit or epitope-only DNA vaccines even when targeted to the ER lumen, due to incorporation of a preprocessed and preloaded peptide [21, 30, 31]. Furthermore, studies have demonstrated the flexibility of the SCT platform by combining it with other strategies to enhance DNA vaccine potency. For example, SCTs were co-expressed with a universal CD4 helper T cell epitope to stimulate T helper cells that resulted in enhanced CD8⁺ T cell responses and anti-tumor effects [41]. However, tumor models used in those studies are not necessarily clinically relevant since the tumor cells

for mouse challenge were generated by transfection of cells with the protein that includes tumor antigens. Under physiological conditions, tumor cells can downregulate expression of MHC and target antigens to evade host immunity [34].

Despite promising studies in tumor models, there have been no reports of pathogen protection after DNA vaccine expression of SCTs. K. Gould et al. showed that a recombinant vaccinia virus (rVV) expressing a H-2D^b SCT with influenza virus nucleoprotein [42] epitope can more efficiently prime peptide-specific CD8 T cells than rVVs expressing other forms of NP antigen [31]. But protection provided by SCT against pathogen infection has never been tested. A SCT platform as a DNA vaccine against pathogen infection is particularly attractive because antigen expression as a SCT is not susceptible to immune evasion mechanisms employed by pathogens. Pathogens have evolved mechanisms by which they can evade immune surveillance of the host. For example, human cytomegalovirus (HCMV) encodes the US3 protein, which binds to tapasin, a chaperone molecule in the peptide loading complex, and retains MHC I complexes in the ER [43, 44]. Thus down-regulation of surface MHC I molecules leads to decreased CD8⁺ T cell responses and benefits survival of virus in the host. Because expression of SCTs bypasses antigen processing and peptide transport, SCT DNA vaccines are expected to be resistant to several viral immune evasion mechanisms.

Efficacy of DNA vaccines can be further increased by targeting the antigen expression to the compartment that plays a critical role in priming T cells. The exact mechanism by which DNA leads to antigen presentation capable of eliciting a T cell immune response has yet to be fully defined. Generally professional antigen presenting

cells, dendritic cells (DCs), are thought to present antigens and prime naïve CD8⁺ T cells after DNA vaccination, because DCs are equipped with co-stimulatory molecules which can activate naïve T cells in combination with TCR engagement [45-48]. However, it remains unclear whether T cell priming depends on antigen produced by DCs directly transfected with DNA that traffic to the draining lymph nodes to present antigens to T cells, antigen cross-presented by DCs that take up the antigens from transfected cells such as keratinocytes or myocytes, or antigen presented by both mechanisms. For example, Germain *et al.* demonstrated that after gene gun delivery of DNA, a small number of directly transfected DCs present in draining lymph nodes were predominantly involved in the induction of a T cell response. They showed this by using a β -gal plasmid as an indicator of direct transfection and by examining whether the same cells required co-expression of the antigen and co-stimulatory molecule to prime T cells [49]. On the other hand, DC-specific antigen expression using a CD11c promoter was not sufficient to induce T cell responses [50]. This is in agreement with a report that antigenic peptides expressed predominantly in nonlymphoid tissues are transferred to APCs to optimally stimulate immune responses [51]. More recent studies have focused on the importance of a subset of DCs, CD8 α ⁺ DCs that are capable of cross-presenting antigens in the induction of a T cell response [52-55]. The importance of CD8 α ⁺ DCs has been emphasized by studies examining CD8⁺ T cell priming in skin infection with herpes simplex virus type 1 (HSV-1). Among a variety of DC subsets, CD8 α ⁺ DCs were shown to be the only population responsible for antigen presentation in the draining lymph nodes after infection [55, 56]. Importantly, Murphy *et al.* demonstrated that DCs from

mice deficient in CD8 α^+ DCs by depletion of transcription factor *Batf3*, are defective in cross-presentation and these mice exhibit impaired anti-viral CTL responses and anti-tumor responses, suggesting an important role of cross-presentation by CD8 α^+ DCs in induction of CTL responses [54]. Also it was reported that migratory Langerin $^+$ CD103 $^+$ dermal DCs are able to cross-present viral and self-antigens and this subset was proposed to be related to splenic CD8 α^+ DCs [54, 57]. Thus, antigen cross-presentation by CD8 α^+ DCs might also be a mechanism for DNA vaccines. Indeed, our colleagues showed that *Batf3* $^{-/-}$ mice do not mount T cell responses after DNA vaccination (Lijin Li, personal communication).

As mentioned above, there are several studies that suggest that the pre-assembled nature of SCT makes it superior to non-processed or unassembled antigenic peptide alone as vaccines. One might envision that the SCT format would not be advantageous if cross-presentation is the predominant mechanism of Ag presentation after DNA vaccination. However, this may not be the case. Interestingly, Bevan *et al.* recently demonstrated that DCs can obtain pre-formed MHC I/antigens complexes from the surface of virus infected cells and present them to T cells *in vivo* [58]. This alternative way of antigen presentation is referred to as ‘cross-dressing’ and has previously been shown *in vitro* [59-63]. Moreover, the transfer of plasma membrane fragments including proteins between lymphocytes, called trans-endocytosis or trogocytosis, has long been reported [64, 65]. This process allows rapid transfer of intact cell surface proteins between cells in contact with one another and transfer of intact MHC/peptide complexes from APC to T cells has been demonstrated although the molecular processes involved need to be clarified. Cross-

cross-dressing as a mechanism of antigen presentation of DNA vaccines is very attractive because many studies have implied that both direct- and cross-presentation occurs and antigen-expressing nonlymphoid cells influence the magnitude of a primary response [50, 51, 66]. Also, Heath *et al.* demonstrated that blocking egress of migratory dermal DCs that do not present antigens substantially inhibits HSV-1 specific CTL priming after infection, suggesting that migratory dermal DCs transport and transfer antigens to lymph node resident CD8 α^+ DCs for presentation [56]. If cross-dressing serves a critical mechanism in inducing T cell responses by DNA vaccines, usage of the SCT platform will greatly enhance vaccine efficacy. Therefore, elucidating the antigen presentation mechanism after DNA immunization is of importance in that it allows optimization of the potency of DNA vaccines by targeting the right compartment as well as choosing the suitable form for antigen delivery.

In this thesis, I examined the efficacy of SCT DNA vaccines for the first time in pathogen infection models. First, we developed a clinically relevant human HLA-A2 transgenic mouse model of West Nile virus (WNV) infection and demonstrated the protective efficacy of a HLA-A2 SCT DNA vaccine against lethal viral infection. Second, I validated the potency of SCT DNA vaccines using H-2K^d SCTs in the BALB/c model of *Listeria monocytogenes* infection, which indicates that SCT DNA vaccines also provide protective immunity against bacterial infection. Lastly, I demonstrated that further engineering of SCTs (dtSCT) using a disulfide trap to better accommodate epitopes can improve the capacity of SCTs to stimulate CD8⁺ T cells, suggesting a broad application of SCTs even with low immunogenic peptides. Also, using a disulfide trap- or chimeric

SCT in order to distinguish whether it's being cross-presented, I also demonstrated that a SCT is presented to T cells as an intact molecule after DNA immunization, suggesting direct presentation by transfected DCs or cross-dressing as a major mechanism of antigen presentation by DNA vaccines. Therefore, these dissertation studies demonstrate that SCTs serve as a potent DNA vaccine platform as well as effective probes for dissecting mechanisms of antigen presentation.

Chapter 2

HLA-A2 SCT DNA vaccines in WNV infection

Introduction

To study the vaccine efficacy of SCTs against pathogen infection, we developed a HLA-A2 transgenic mouse model of West Nile virus infection (WNV). WNV is a mosquito-borne Flavivirus with an 11 kilobase single stranded RNA genome and contains a single open reading frame [67-71]. Infection in humans and other vertebrate animals can progress to paralysis, meningitis, encephalitis and death, especially in the elderly and immunocompromised individuals while the majority of infections are either asymptomatic or produce a mild febrile illness. Although the continued threat of WNV epidemics has stimulated vaccine development, there are currently no commercial human vaccines available. Both innate and adaptive immunity are implicated in protection against WNV. Cytotoxic T lymphocytes (CTL) play an important role in control and clearance of WNV infection, and recent studies in a murine model have suggested that induction of a strong CD8⁺ T cell immune response can enhance the protective activity of a WNV vaccine against challenge. Thus vaccines targeting CD8⁺ T cell immunity to WNV are clearly relevant and therefore WNV infection serves as a good animal model to test efficacy and probe the mechanism of SCT DNA vaccine to induce CD8⁺ T cell immunity for protection.

Despite prior studies suggesting the protective role of CD8⁺ T cells against WNV infection, CD8⁺ T cell recognition epitopes were not reported until recently. A

collaborative study between the Diamond, Hansen and Fremont labs as well as a study by the Nikolich-Žugich lab defined dominant H-2D^b and H-2K^b epitopes of WNV antigens [72, 73]. More specifically, a D^b-restricted WNV epitope derived from the NS4B protein and a K^b-restricted epitope from the envelope (E) protein were identified. Adoptive transfer of CTLs specific for these epitopes conferred partial protection against WNV infection in C57BL/6 mice. To extend these findings to humans, our collaborators in the Hildebrand lab at the University of Oklahoma eluted peptides from HLA-A0201 molecules of WNV-infected HeLa cells [74]. Mass spectrometry approaches were then used to identify six WNV-derived peptides bound to HLA-A2. These six peptides were derived from five different WNV proteins demonstrating broad presentation of epitopes from the WNV proteome (Table 1). When tested with T cells from HLA-A2⁺ patients post WNV infection, one peptide was found to be immunodominant, two subdominant and three demonstrated no significant CTL response. The immunodominant peptide of WNV recognized by patients' CTLs was SVGGVFTSV (designated as SVG9) that is derived from the E protein of WNV.

To test the efficacy of an SCT-based vaccine incorporating the human WNV epitopes, we used the HLA-A2 transgenic mouse (HHDII) model. HHDII mice express a chimeric monochain of HLA-A*0201 ($\alpha 1/\alpha 2$ domains), mouse H-2 D^b ($\alpha 3$ domain) and linker-attached human $\beta 2m$ [75]. The mouse $\alpha 3$ domain was incorporated into the monochain to optimize interaction with mouse CD8⁺ T cells, whereas the human $\beta 2m$ was incorporated into the monochain to facilitate HLA-A2 expression. To restrict the development of CD8⁺ T cells to only HLA-A2, HHDII mice are also genetically deficient

in D^b and mouse β 2m. Thus these mice develop relatively few CD8⁺ T cells, but the CD8⁺ T cells that HHDII mice do develop are largely HLA-A2-restricted. HHDII mice have been widely used for preclinical vaccine studies against tumors and viruses.

I show in this chapter that the SVG9 peptide of WNV demonstrates striking immunodominance in the HHDII mouse model in concordance with the published studies of HLA-A2⁺ patients with previous WNV infections. This concordance validates the HHDII model system for studies of SCT-based vaccine efficacy as well as factors that determine the immunodominance of viral epitopes detected by CD8⁺ T cells during viral infection. I also show in this chapter that the SVG9 peptide can be incorporated into a SCT format, that vaccination with plasmid DNA encoding the HLA-A2/SVG9 SCT stimulates a robust CD8⁺ T cell response, and this response confers protective immunity against lethal WNV infection in the absence of pre-existing antibody. These findings were published in a featured article in the Journal of Immunology and represent the first demonstration of the efficacy of SCTs in pathogen protection. Also included in this chapter is unpublished data using novel T cell receptor (TCR)-mimic monoclonal antibodies to show that antigen presentation of WNV epitopes expressed in the ER lumen, such as SVG9, is TAP-dependent. This is an interesting finding because it suggests that SVG9 is not processed by cellular ER proteases, but by the proteasome in the cytosol.

Materials and Methods

1. Viruses and Mice

The WNV strain 3000.0259 was isolated in New York in 2000 and passaged once in C6/36 cells. The WNV-KUN strain (16-532) propagated in C6/36 cells has been described previously [73]. HHDII transgenic (B6; Cg-B2M^{tm1Unc} H2-D1^{tm1Bpe}Tg (HLA-A/H2-D/B2M)1Bpe) mice were obtained from Dr. Beatriz Carreno with permission of Dr. François A. Lemonnier (18). These mice express the transgene, Tg (HLA-A/H2-D/B2M)1Bpe, in a mixed background involving B2M^{tm1Unc/tm1Unc} and H2-D1^{tm1Bpe/tm1Bpe}. For simplicity, these mice are designated HHDII mice for the rest of this dissertation. All mice were bred and housed at Washington University Animal Facility and all animal procedures were approved by the Animal Studies Committee at the Washington University.

2. Virus infection

For inoculation of mice, virus was diluted in Hanks' balanced salt solution (HBSS) containing 1% heat inactivated fetal bovine serum (FBS). Mice were infected with 10²PFU of WNV subcutaneously by footpad injection. To detect viral epitopes presented after infection, primary human monocyte-derived dendritic cells at day 7 in culture with GM-CSF and IL-4 were plated at 1x10⁶ cells/mL/well in a non-tissue culture treated 6 well plate. The following day, cells were infected with WNV at a MOI (Multiplicity of Infection) of 3 for 48 hours before performing cell staining. HeLa or

HeLa A2 cells were plated at 2×10^5 cells/well in a 6 well plate and, on the same day, infected with WNV at a MOI of 0.3 or 3 for 48 hours before staining.

3. Antibodies and peptides

The following mAbs were purchased from eBiosciences or BD Biosciences: anti-mCD8 α (53-6.7), rat IgG2a isotype control, anti-IFN γ , rat IgG1 isotype control, and PE-conjugated goat anti-mouse Ig. PE-conjugated SVG9 peptide/HLA-A*0201 and control tetramer were obtained from the National Institute of Allergy and Infectious Diseases tetramer facility (Emory University, Atlanta, GA). T cell receptor mimic monoclonal antibodies (TCRm) that are specific for peptide/HLA-A2 complexes were generated by immunization of mice with tetramers of peptide/ HLA-A2: RL4D, RL14C, RL15A, or RL26A (Receptor Logic, Abilene, TX). Peptides were synthesized by and purchased from Sigma-Aldrich (St. Louis, MO).

4. Flow cytometry

IFN γ production and tetramer binding of splenocytes and surface expression of viral epitope/HLA-A2 complexes on virus-infected cells were monitored by flow cytometry. For intracellular IFN γ staining, splenocytes were stimulated in vitro with each peptide at 0.1 μ g/mL in the presence of GolgiPlug (BD Biosciences, San Jose, CA) for 4 hours at 37°C. Cells were washed, stained with FITC-conjugated anti-CD8 α mAb or rat IgG2a, and fixed with 1% paraformaldehyde (PFA). After washing twice with buffer containing 0.1% saponin, cells were stained with APC-conjugated anti-IFN γ mAb or rat IgG1. For tetramer staining, cells were stained with tetramers for 40 min at 37°C, and

subsequently FITC-conjugated anti-CD8 α mAb was added for an additional 20 min at 4°C. Propidium iodide (PI) was added shortly before flow cytometry to gate out dead cells. Cells were acquired on FACSCalibur and data were analyzed with FlowJo software (Tree Star, Ashland, OR).

5. Detection of Viral Epitope/HLA-A2 complex Expression

For controls, 10 μ M of peptide was added to uninfected cells for the last hour. Cells were washed three times and incubated with TCRm, RL4D, RL14C, RL15A, or RL26A (mIgG2a) for 40 min on ice. After washing, cells were stained with PE-conjugated goat anti-mouse Ig antibody (BD Biosciences). To confirm the infection, aliquots of cells were stained with anti-WNV envelope mAb, E24. Prior to flow cytometry, cells were fixed with 2% PFA.

6. Generation of ICP47-expressing cell line

Stable cell lines expressing ICP47 were generated with HeLa or HeLa A2 cells using retrovirus transduction. As an internal control for TAP function, the HLA-A2 binding peptide, GVLPALPQV derived from human chorionic gonadotropin (hCG)- β , was expressed in the cytosol by attaching ubiquitins in front of the peptide. Expression of this peptide in combination with HLA-A2 at the surface was detected by specific TCR mimic monoclonal antibody, RL4D. To produce retrovirus, human embryonic kidney cells 293T were transiently transfected with plasmids using Lipofectamine 2000 (Invitrogen, Carlsbad, CA) according to manufacturer's instruction and cell culture

supernatant containing retrovirus was collected. HeLa or HeLa A2 cells were selected and maintained under geneticin or puromycin (Life Technologies, Grand Island, NY) post-transduction. All cells were maintained in DMEM (Invitrogen) supplemented with 10% FBS (HyClone Laboratories, Logan, UT), 2mM L-glutamine, 0.1mM non-essential amino acids, 1.25mM HEPES, 1mM sodium pyruvate, and 100U/mL penicillin/streptomycin (all from the Tissue Culture Support Center, Washington University School of Medicine, St. Louis, MO).

7. CTL Assays

For *in vitro* CTL assay, CTLs were generated from WNV-KUN immunized HHDII spleen cells after *in vitro* SVG9 peptide stimulation for 2-4 weeks. To perform a ^{51}Cr release assay, target cells labeled with 0.2 mCi of ^{51}Cr (PerkinElmer Life Sciences, Wellesley, MA) were incubated with CTLs with or without peptides for 4 ½ hours at 37°C. To determine maximum lysis, Triton-X 100 was added to control wells. To determine spontaneous lysis, target cells were incubated without CTLs. Supernatants were collected and read by an Isomedic γ -counter (ICN Biomedicals, Huntsville, AL). The percentage of ^{51}Cr release was calculated by [(experimental ^{51}Cr release-spontaneous ^{51}Cr release)/(maximum ^{51}Cr release-spontaneous ^{51}Cr release)] x100. For *in vivo* CTL assay, recipient HHDII mice were left uninfected or challenged with 10^2 PFU of WNV-NY a week before adoptive transfer of target cells. For target cells, naïve HHDII splenocytes were stained with 2 μM of PKH26 (Sigma, St. Louis, MO) and incubated with 1 μM of SVG9 or control peptide for 1 hour at 37°C. After washing, SVG9- or

control peptide-pulsed cells were labeled with 1 μ M or 50nM CFSE, respectively. Equal numbers of SVG9- and control peptide-pulsed cells were mixed in HBSS and 2x10⁷ total labeled target cells were transferred intravenously into the recipient mice. 6 hours later, spleen cells were harvested, fixed with PFA, and evaluated by flow cytometry. Target cells were distinguished from recipient cells based on PKH26 staining and from one another based on CFSE labeling. Gating on PKH26⁺ cells, the percentage of killing was calculated as follows: $[1-(r_{naive}/r_{infected})] \times 100$, where $r = \%CFSE^{low} \text{ cells} / \%CFSE^{hi} \text{ cells}$.

8. Single Chain Trimer (SCT) DNA Constructs

The SVG9/HLA-A2*0201 SCT consists of the leader sequence of β_2m followed by the SVGGVFTSV sequence, then a linker of 15 residues (G₄S)₃, and the mature human β_2m sequence. The β_2m was followed by the second linker of 20 residues (G₄S)₄ and the chimeric HLA-A*0201 sequence of which the α_3 domain was replaced by that of H-2K^b. To generate SVG9/HLA-A2 SCTs, OVA.hb2m.HLA-A2 in an expression vector pIRESneo was used as a template. First, nucleotide oligos encoding SVG9 peptide flanked by restriction enzyme sites, Age1 and Nhe1 were designed in order to replace the existing OVA peptide;

5'-
CCGGTTTGTATGCTAGCGTGGGCGGCGTGTTTACCAGCGTGGGAGGAGGTG-3'

and

5'-
CTAGCACCTCCTCCCACGCTGGTAAACACGCCGCCACGCTAGCATACAAAA-3'.

Oligos were annealed to form a double strand and inserted into the vector cut with Age1 and Nhe1, which generated a pIRESneo.SVG9/HLA-A2 SCT with α_3 domain of A2.

Next, to swap the $\alpha 3$ domain with H-2K^b, the plasmid was cut with BamH1 which resulted in the whole heavy chain excised from the plasmid. The fragment encoding A2/Kb $\alpha 3$ was prepared from pCR2.1topo.CMV. chimeric SCT (a kind gift from Dr. Beatriz Carreno, Washington University in St. Louis) and ligated into the vector, which generated pIRESneo.SVG9/A2/K^b $\alpha 3$ chimeric SCT. The correct sequence was confirmed by DNA sequencing using BigDye3.1 (Washington University in St. Louis). For a control SCT, the SVG9 sequence was replaced with the mammoglobin A epitope, LIYDSSLCDL, sequence using similar cloning methods. To express a helper epitope, the Pan HLA-DR reactive epitope (PADRE) sequence (AKFVAAWTLKAAA) flanked by ATG and TAA was inserted before the leader sequence. For immunization, DNA was prepared using Plasmid Maxi Prep kit (Qiagen, Valencia, CA) according to the manufacturer's instructions

9. DNA Immunization

DNA-coated gold particle-mediated DNA vaccination was performed using a helium-driven gene gun (Bio-Rad, Hercules, CA). DNA-coated gold particles (diameter, 1 μ m) and cartridges were prepared according to the manufacturer's instructions so that each cartridge contained 1 μ g of DNA. The DNA-coated gold particles were delivered to the shaved abdomen of mice with a discharge pressure of 200 psi. Mice were immunized with 4 μ g of DNA three times at 3 day intervals.

10. IFN γ ELISpot assay

Spleens were harvested from mice 5 days after the last DNA immunization. After RBC lysis, single cell suspensions were incubated with 1 μ g/mL SVG9 or control peptides in a PVDF filter plate (Millipore, Billerica, MA) pre-coated with 15 μ g/mL of anti-IFN γ capture antibody (AN18, Mabtech Inc, Cincinnati, OH). After overnight stimulation, cells were removed and the plate was incubated with biotinylated anti-IFN γ detection antibody (R4-6A2) and subsequently with streptavidin-ALP. Then spots were developed by adding substrate solution (BCIP/NBT) and counted with an automated ELISpot reader (CTL, Shaker Heights, OH).

11. Detection of WNV-specific Antibodies in Serum

WNV-specific antibody titer was measured by ELISA. Serum was collected and added to the 96 well plates pre-absorbed with purified recombinant WNV E protein (5 μ g/mL). After wash with washing buffer, PBS containing 0.05% Tween-20 (Sigma), plates were incubated with primary (biotinylated anti-mouse IgG or IgM, Sigma) and, subsequently with streptavidin-HRP for 1 hour. Then color was developed by adding TMB substrate (eBiosciences) and the reaction was stopped with 2N sulfuric acid. Plates were read on a plate reader (Bio-Rad) at 450nm. Endpoint titers were determined using GraphPad Prism 5.

12. Quantification of Viral Burden

For analysis of virus, brains were recovered after cardiac perfusion with PBS, homogenized, and titrated for virus by a plaque assay using BHK21 cells [76]. 10-fold

dilutions of a tissue homogenate were prepared, and 150 μ L aliquots were inoculated onto BHK21 cell monolayers that were prepared overnight. After a 1-2 hour incubation period, the monolayers were covered with a medium containing 1% agar and incubated for 3 days. The cells were fixed with 10% formaldehyde and stained with 1% crystal violet after agarose plugs were removed. Virus concentrations were determined as PFU/g.

Chapter 2.1

Identification of the immunodominant WNV CD8⁺ T cell epitope

Results

Identification of an immunodominant peptide in HLA-A2 transgenic mice

To identify WNV-derived peptides presented by HLA-A2 class I MHC molecules after infection, members of our group previously eluted peptides from affinity-purified HLA-A2 molecules isolated from uninfected or infected HeLa cells [74]. Comparative analyses using HPLC and tandem mass spectrometry (MS/MS) identified six virus-derived peptides binding to HLA-A2 (Table 1). When tested in reactivation assays using CD8⁺ T cells from infected individuals, the WNV E-derived peptide (SVG9) was immunodominant. To develop the mouse model of WNV infection to study SCT vaccines, I determined whether these findings could be replicated in the HLA-A2 transgenic (HHDII) mouse model of WNV infection by comparing CD8⁺ T cell responses to these six WNV peptides.

To assess the T cell responses against the six WNV peptides, HHDII mice were infected with 10² PFU of a North American isolate of WNV (strain New York 1999 (WNV-NY)). At 7 days after infection, splenocytes were harvested and stimulated *ex vivo* with each peptide for 4 hours and then stained for levels of intracellular IFN γ . Only the SVG9 peptide induced a strong IFN γ response in CD8⁺ T cells from infected mice (Fig. 1A). On average, ~ 3% of CD8⁺ T cells produced IFN γ after restimulation with the SVG9 peptide, whereas a much smaller percentage of CD8⁺ T cells produced IFN γ in response

to other peptides. Consistent with this finding, staining with SVG9 peptide/HLA-A2 tetramers confirmed the presence of SVG9-specific CD8⁺ T cells in infected spleens (Fig. 1B). Thus, of the six viral peptides bound to HLA-A2, the SVG9 peptide is immunodominant in HHDII mice, results that parallel what was observed in infected humans [74]. This concordance supports the relevance of using the HLA-A2 transgenic mouse model to test vaccine efficacy for protection against WNV. Importantly, the SVG9 (SVGGVFTSV) sequence is completely conserved in most contemporary and historical WNV isolates available in the NCBI database, including WNV-KUN, Egypt 101, the original Uganda 1937 lineage 2 isolate, and all Western Hemisphere strains that have been sequenced to date. Thus, this epitope is an excellent candidate to develop a CD8⁺ T cell-based WNV vaccine for HLA-A2 individuals. Thus, the immunodominant SVG9 peptide was chosen to be incorporated into a SCT as a DNA vaccine hereafter.

Epitope expression after WNV infection

The high immunodominance of the SVG9 peptide suggests that it might be expressed at high levels on virus-infected cells. The six viral peptides listed in Table I, including the immunodominant SVG9 peptide, had been isolated from HLA-A2/peptide complexes secreted by WNV infected human HeLa tumor cells which had previously been transfected with a soluble HLA-A2 molecule. Thus it may not exactly recapitulate the actual antigen presentation that follows natural infection. I monitored actual antigen presentation of viral epitopes on the cell surface after infection using a novel TCR-mimic monoclonal antibody. TCR-mimic mAbs are specific for peptide/HLA-A2 complexes and

were generated by immunization of C57BL/6 mice with tetramers of peptide/HLA-A2 [77, 78]. Three TCR-mimic mAbs with different specificities, RL15A, RL14C, and RL26A were used in this study. RL15A recognizes the SVG9/HLA-A2, RL14C the SLF9/HLA-A2, and RL26A the YTM9/HLA-A2 complex.

HeLa or HeLa A2 cells that had been transfected with HLA-A2 were infected *in vitro* with WNV for 48 hours and stained with TCR-mimic mAbs. As a positive control, uninfected HeLa A2 were pulsed with each peptide for 4 hours prior to staining; as expected, the TCR-mimic mAbs bound to peptide-pulsed uninfected HeLa A2 cells but not to uninfected HeLa A2 cells or uninfected or infected HeLa cells (Fig. 2A). The degree of virus infection was confirmed using an anti-WNV envelope (E) protein antibody, E24 (Fig. 2B). All of the three SVG9/, SLF9/, and YTM9/HLA-A2 complexes were detected on the cell surface of infected HeLa A2 cells at high levels, but not on uninfected cells (Fig. 2B).

I then decided to monitor the epitope presentation in a more physiologically relevant cell type, human dendritic cells (DCs) from HLA-A2 positive individuals. Human DCs are professional antigen presenting cells and known to likely be a primary cell type infected by WNV *in vivo* [79, 80]. Human DCs derived from the peripheral blood mononuclear cells of HLA-A2 positive individuals were cultured with GM-CSF and IL-4 and, at day 7 of the culture, infected *in vitro* with WNV for 48 hours and stained with TCR-mimic mAbs, RL15A and RL14C. As a positive control, uninfected DCs were pulsed with each peptide prior to staining. Consistent with the result from the experiment with HeLa cells, both SVG9/ and SLF9/HLA-A2 complexes were detected at high levels

on the cell surface of infected DCs, but not on uninfected cells (Fig. 3). Therefore, I confirmed that the immunodominant epitope SVG9 as well as the non-immunodominant epitopes are processed and presented in the context of HLA-A2 on the surface of antigen-presenting cells after virus infection. Interestingly, I noticed that after infection the surface expression of SLF9/HLA-A2 is consistently higher than that of SVG9/HLA-A2 in both HeLa A2 and human DCs, although SVG9 is more immunodominant than SLF9. Thus my data suggest that the level of epitope presentation on the APC alone does not explain immunodominance.

TAP-dependency of viral antigen presentation

To bind MHC I, a peptide should meet certain criteria; 8-10 amino acids in length and a hydrophobic or basic amino acid at its C-terminus [9]. The initial processing of the MHCI epitopes occurs in the cytosol by the proteasome after which peptides of 10-20 amino acids are transported into the ER by TAP. Within the ER further trimming by the aminopeptidase (ERAAP) can occur prior to stable MHC I/peptide complex formation and subsequent ER exit to the plasma membrane. The relative importance of cytosolic processing can thus be determined by assessing TAP dependency of presentation of the epitope to T cells. Numerous epitopes detected by CD8⁺ T cells have been investigated and most have been found to be TAP-dependent suggesting their dependency on proteasomal processing. Regarding the importance of ER proteolysis for MHC I binding peptides, the processing and MHC binding of signal peptides is particularly relevant. A historical study first showed that in TAP deficient cells MHC I molecules are

predominantly loaded with signal peptides [81]. This finding implied that cleavage of signal peptides by signal peptidases, ERAAP and possibly other ER proteases is sufficient to generate MHC I binding peptides without access to the cytosol and proteasomes. However, it is noteworthy that there are exceptions to this conclusion. For example, the qdm signal peptide that binds to the mouse class Ib molecule Qa-1^b was found to be TAP-dependent, suggesting its proteasomal processing [82]. The model system we have developed in collaboration with the Diamond, Hildebrand, and Weidanz labs provides unique approaches to probe the host *vs.* viral proteases as well as the intracellular location of processing events that generate an immunodominant CD8⁺ T cell epitope during viral infection.

Flaviviruses including WNV enter target cells by receptor-mediated endocytosis and then traffic to early endosomes, where the acidic environment induces fusion between the virus and the host membrane resulting in RNA genome release [83, 84]. Replication occurs on the host cell ER membrane where a replication complex, which consists of viral RNA, viral proteins, and possibly host cell factors, is assembled. Translation of viral RNA is followed by processing of the resulting polyprotein by host and virus-encoded proteases. Immature, noninfectious virions assemble within the ER and move through the host secretory pathway, where virion maturation occurs. Mature infectious particles are then released by exocytosis into the extracellular medium. WNV RNA is translated as a single polyprotein in the ER membrane, which is processed into ten viral mature proteins by viral and cellular proteases. Fig. 4 schematically illustrates the cleavage sites and topology of structural and nonstructural (NS) proteins at the ER

membrane. While host signal peptidase is responsible for cleavages between C/preM, preM/E, E/NS1, and within NS4b, a virus-encoded serine protease is responsible for cleavages between NS2a/2b, NS2b/NS3, NS3/NS4a, and NS4b/NS5 junctions. The viral envelope protein from which the SVG9 peptide derives, as well as the part of NS4b that includes the SLF9 epitope, is predicted to reside in the ER lumen, while NS3 including the YTM9 epitope is predicted to reside in the cytosol.

The proteases that generate these aforementioned WNV epitopes are not known, but their identity is intriguing especially for the ones processing the SVG9 immunodominant peptide. As previously noted, my data show that the SVG9 peptide is displayed at a high level at the cell surface after *in vitro* WNV infection of DCs suggesting efficient processing and loading of the SVG9 epitope into HLA-A2 molecules. Yet the WNV sequence including the SVG9 resides inside the ER. Thus we considered it of interest to examine the TAP-dependency of the antigen presentation of the SVG9 epitope in comparison with the presentation of the SLF9 and YTM9 WNV epitopes. TAP-dependency was determined by overexpressing the TAP inhibitor ICP47 (an HSV immune evasion protein) in HLA-A2⁺ cells prior to WNV infection. HLA-A2/peptide complexes were then enumerated by flow cytometry using TCR mimic mAbs. More specifically, HeLa or HeLa A2 cells expressing ICP47 were generated by transduction of a retrovirus encoding ICP47 and selection with antibiotics. As a control for ICP47 blocking of TAP, an irrelevant HLA-A2 epitope (tumor peptide GVL) was expressed with an ubiquitin moiety and its HLA-A2 restricted expression was determined with a specific TCR mimic mAb (Fig. 5A). With ICP47 expressed, all of the three SVG9/, SLF9/, and

YTM9/HLA-A2 complexes were not presented at the cell surface after WNV infection (Fig. 5B). It was not because ICP47 affected MHC I expression itself, since total HLA-A2 expression at the cell surface was not affected by ICP47 expression (Fig. 5C). This finding is consistent with published reports that HLA-A2 surface expression is largely TAP-independent.

In summary data in this section indicate that antigen presentation of all three HLA-A2 restricted WNV epitopes examined here depends on TAP function. It is intriguing that TAP is required for the presentation of SVG9 and SLF9 WNV peptides which reside in the ER. Our findings suggest that these peptides are likely transported back to cytosol, processed by proteasomes and re-transported to the ER via TAP for binding to MHC I molecules. Host signal peptidases in the ER seem not to be able to process these peptides, rather viral proteases and/or proteasomes in the cytosol may be required. A mechanism for the efficient retro-transport of peptides from the ER is unknown and unexpected, but TAP functions only to introduce peptides into the ER. Alternatively, one might speculate that the SVG9 and SLF9 peptides are processed in post-ER endosomal compartments similar to mechanisms implicated in cross-presentation of certain CD8⁺ T cell epitopes using *in vitro* assays. However, if post-ER processing is implicated, it remains unclear where HLA-A2 loading would occur in a manner efficient enough to achieve high levels of surface HLA-A2/SVG9 expression after WNV infection. In any case the application of the TCR mimic mAbs and mAbs from the Diamond lab to the WNV E protein have the ability to define the precise location of processing and HLA-A2 loading of the SVG9 immunodominant WNV

peptide.

Cytotoxic T cells specific for the immunodominant epitope mediate partial protection against infection

It was determined whether functional cytolytic CD8⁺ T cells specific for the immunodominant epitope, SVG9, are induced during viral infection and the CTLs contribute to control infection. First, cytolytic activity of CD8⁺ T cells was tested *in vitro*. For *in vitro* killing assays, bulk CD8⁺ T cells were generated from WNV-Kunjin (WNV-KUN) immune spleen cells from HHDII mice after *in vitro* restimulation with SVG9 peptide. We used WNV-KUN because the mortality rate with WNV-NY approached 100% within 10 days of infection in the HHDII mice and so we were not able to obtain T cells to culture. WNV-KUN is a related lineage I WNV strain with reduced virulence in mice and humans and has 97.6% sequence identity with WNV-NY 1999, including 100% identity of the SVG9 peptide. In ⁵¹Cr-release assays, bulk CD8⁺ T cells from WNV-KUN immune mice lysed SVG9 peptide-loaded target cells as well as WNV-KUN infected cells (Fig. 6A). When these CD8⁺ T cells were incubated with target cells pulsed with SVG9 peptide in the presence of TCR-mimic antibody, RL15A or RL14C, RL15A completely blocked killing whereas RL14C which has the same IgG1 isotype did not alter killing (Fig. 6B). This indicates that SVG9-specific CD8⁺ T cells are cytotoxic. The cytotoxic activity was confirmed *in vivo*. A 1:1 mixture of differentially CFSE-labeled naïve syngeneic splenocytes pre-loaded with SVG9 or an irrelevant peptide was adoptively transferred into naïve HHDII mice or mice infected with WNV. Six hours later

the splenocytes were harvested and analyzed by flow cytometry for levels of CFSE expression. In naïve recipient mice, the 1:1 ratio of SVG9-loaded targets and irrelevant peptide-loaded targets remained the same (Fig. 6C). However, in infected mice, 58% of the SVG9-loaded targets were eliminated, but irrelevant peptide-loaded targets were not, indicating SVG9-specific killing of targets by T cells *in vivo*. Thus, during WNV infection, SVG9-specific CD8⁺ T cells are generated and lyse virus infected cells.

Previous studies have established that CD8⁺ T cells contribute to viral clearance of WNV infected mice. Mice lacking CD8⁺ T cells or class I MHC developed higher central nervous system viral burdens and increased mortality rates after infection [73, 85]. Based on these findings, I assessed whether SVG9-specific CD8⁺ T cells could control WNV infection *in vivo*. Initially, an adoptive transfer experiment of SVG9-specific CD8⁺ T cells into WNV infected mice was performed. Mice that received naïve CD8⁺ T cells had a 100% mortality rate within 10 days of infection (Fig. 7). In contrast, mice that received SVG9-restimulated CD8⁺ T cells exhibited a 40% survival rate ($p < 0.0005$, $n = 10-11$). Thus, enhanced CD8⁺ T cell responses specific for an immunodominant epitope SVG9 can provide protection against lethal WNV infection *in vivo*.

Figure Legends

Table 1. Six identified WNV-derived peptides bound to HLA-A*0201

Data was adapted from the previous publication by McMurtrey *et al.* [74]. NS, non-structural protein, Env, envelope protein. IC50 is the concentration of the peptide that is required for 50% inhibition of the reference peptide binding.

Figure 1. Identification of an immunodominant WNV epitope bound to HLA-A2 in HDDII mice

HDDII mice were infected with 10^2 PFU of WNV, and 7 days later spleen cells were harvested. (A) Cells were stimulated *in vitro* with peptides for 4 hours in the presence of golgi-blocking agent. Then cells were stained for CD8 and intracellular IFN γ . The percentages of IFN γ^+ CD8 $^+$ T cells after each peptide stimulation (*x*-axis) from infected (●) or naïve (Δ) mice are shown. *, $p < 0.05$ (unpaired *t* test). (B) Cells were stimulated *in vitro* with SVG9 peptide for 7 days, and stained with anti-CD8 mAb and SVG9/HLA-A*0201 or control tetramers. Cells were gated on PI negative events. Numbers indicate the percentage of cells in each quadrant of total cells.

Figure 2. Presentation of viral epitope/HLA-A2 complexes at the HeLa cell surface after WNV infection

(A) HeLa or HeLa A2 cells were incubated with SVG9, SLF9, or YTM9 peptide for 4 hours and stained with TCRm Ab, RL14C, RL15A, or RL26A. In each panel, shaded

histograms show staining of HeLa cells pulsed with each peptide and solid or dotted line shows HeLa A2 cells pulsed with an indicated or irrelevant peptide, respectively. (B) HeLa [86] or HeLa A2 (*lower*) cells were infected with WNV at a MOI of 1. 48 hours later, cells were stained with anti-WNV E24 or TCR mimic mAb. Shaded histograms show staining of uninfected cells and solid lines show infected cells.

Figure 3. Presentation of viral epitopes, SVG9 and SLF9, at the human DC surface after WNV infection

Primary dendritic cells derived from HLA-A2 positive PBMC were infected with WNV at a MOI of 1 for 48 hours. (A) Cells were stained with anti-WNV E24 (solid line) or isotype control mAb (dotted line). Shaded histogram, uninfected cells. (B) Uninfected (*left*) or infected [87] DCs were stained with RL14C (SLF9) [86] or RL15A (SVG9) (*lower*). Numbers indicate the percentages of TCRm positive cells.

Figure 4. Schematic illustration of a WNV polyprotein expressed at the ER membrane

The cleavage sites and topology of structural (in green) and nonstructural (NS) (in red) proteins at the endoplasmic reticulum (ER) membrane are illustrated schematically. The cleavage sites by host signalases or viral serine proteases were indicated with black or blue arrows, respectively. Approximate locations of the HLA-A2 binding epitopes in the viral polyprotein were indicated as yellow. C, capsid protein; E, envelope; preM, pre-membrane; NS, nonstructural protein.

Figure 5. Presentation of viral epitopes at the cell surface is dependent on TAP function.

(A) and (B) HeLa A2 cells expressing GVL peptide (solid line) or GVL and ICP47 (dotted line) were infected with WNV at a MOI of 1 for 48 hours. Cells were stained with the indicated TCR mimic mAb. (A) Shaded histograms show staining of HeLa A2 cells without GVL peptide transfected. (B) Shaded histograms show staining of uninfected HeLa A2 cells expressing GVL and ICP47. (C) Infected cells were stained with anti-HLA-A2 mAb, BB7.2 ; solid line, HeLa A2 cells expressing GVL peptide, dotted line, HeLa A2 cells expressing GVL and ICP47. A dashed line shows staining of uninfected HeLa A2 cells expressing GVL and ICP47 and a shaded histogram shows uninfected HeLa cells.

Figure 6. WNV infection generates SVG9-specific CTLs

(A) and (B) A ^{51}Cr -release assay was performed with SVG9-specific CTLs as effectors. SVG9-specific CTLs were generated from spleen cells of mice that had been infected with WNV-KUN for a month. (A) (*left*) HeLa A2 targets were incubated with CTLs for 4½ hours in the presence of 1 or 10µM of SVG9 peptide. [87] HeLa or HeLa A2 cells infected with WNV-KUN were used as targets. (B) A ^{51}Cr -release assay was performed in the presence of TCRm Ab. (C) An *in vivo* cytotoxic assay was performed. Histograms were gated on PKH26⁺ events (donor cells). The percentage of CFSE^{hi} or CFSE^{lo} population of PKH26⁺ cells is indicated in parentheses. All data are representative of at least two independent experiments with similar results.

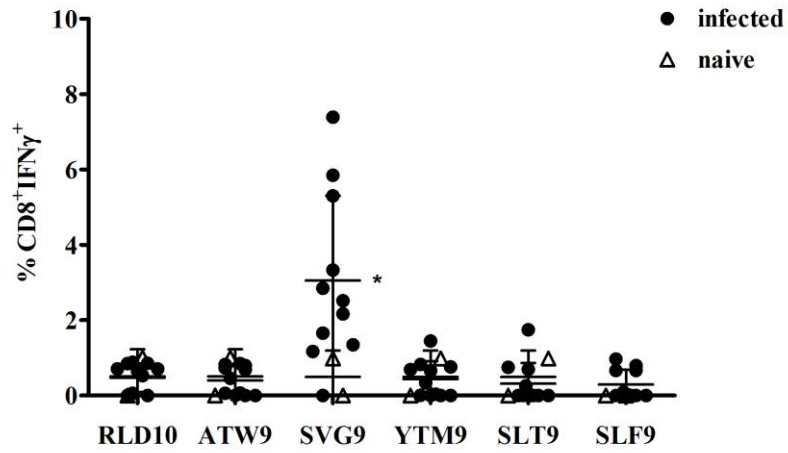
Figure 7. Adoptively transferred SVG9-specific CTLs provide protection against lethal WNV infection

Donor cells were obtained from HHDII mice that had been infected with 10^2 PFU of WNV. Cells were re-stimulated *in vitro* for 7 days with 0.1 μ M of SVG9 peptide. CD8⁺ T cells were then isolated by negative selection and transferred into HHDII mice at day 1 post-infection with 10^2 PFU of WNV (2×10^6 CD8⁺ T cells per mouse). Survival was monitored over 28 days. **, $p < 0.0005$ (log-rank test). The results were combined from two independent experiments ($n=10-11$ per group).

Table 1. Six identified WNV-derived peptides bound to HLA-A*0201			
Peptide	Sequence	Protein	IC₅₀(nM)
RLD10	RLDDDGNFQL	NS2b	847
ATW9	ATWAENIQV	NS5	780
SVG9	SVGGVFTSV	Env	247
YTM9	YTMDGEYRL	NS3	291
SLT9	SLTSINVQA	NS4b	503
SLF9	SLFGQRIEV	NS4b	204

Table 1. Six identified WNV-derived peptides bound to HLA-A*0201

A



B

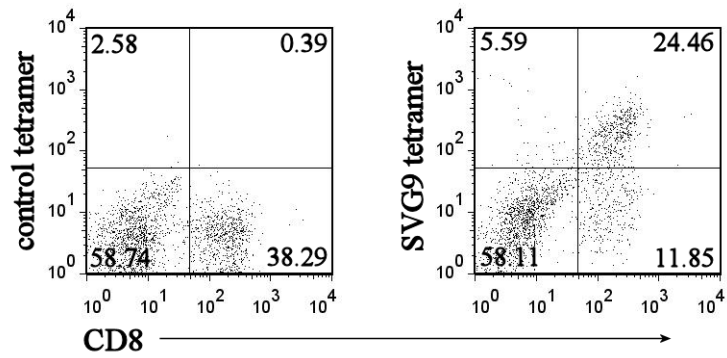
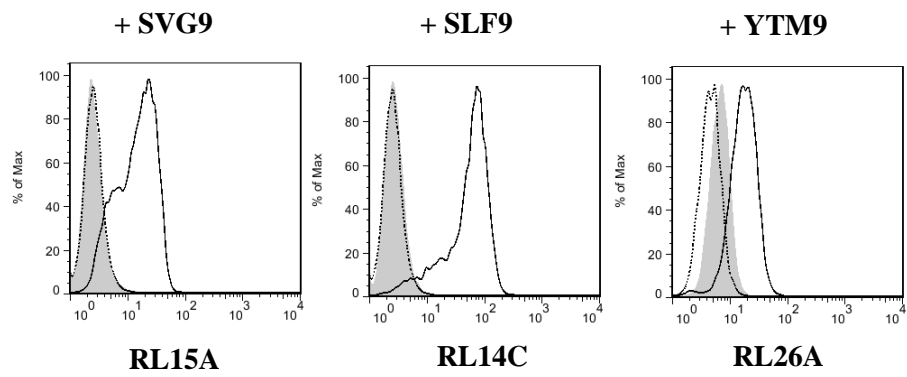


Figure 1. Identification of an immunodominant WNV epitope bound to HLA-A2 in HHDII mice

A



B

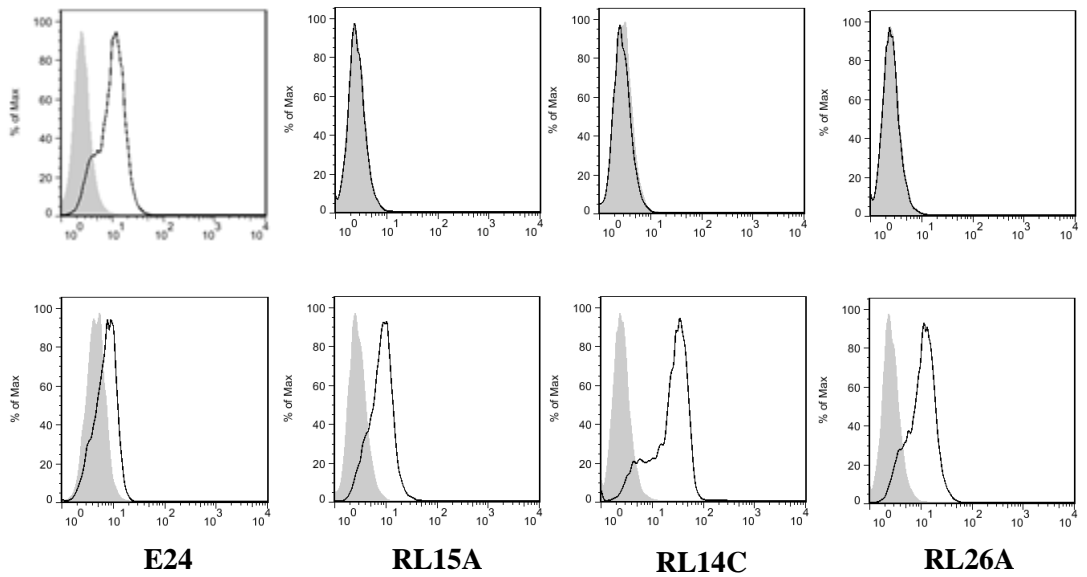
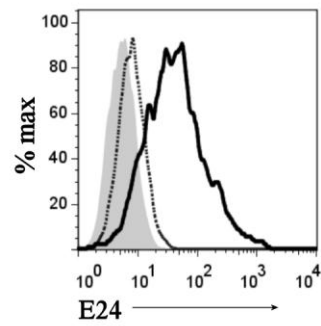


Figure 2. Presentation of viral epitope/HLA-A2 complexes at the HeLa cell surface after WNV infection

A



B

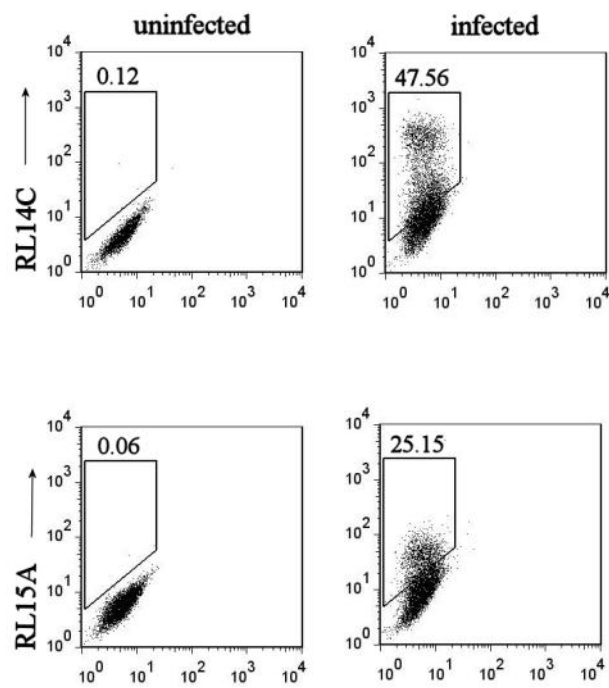


Figure 3. Presentation of viral epitopes, SVG9 and SLF9, at the human DC surface after WNV infection

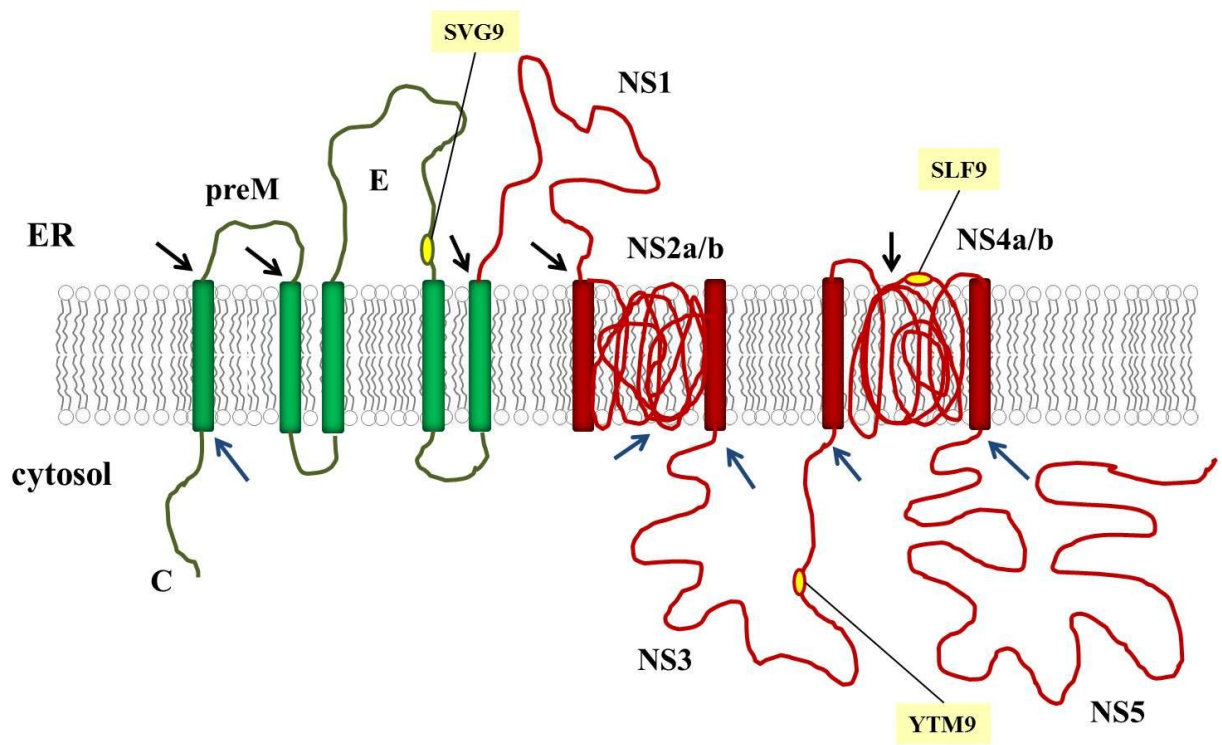


Figure 4. Schematic illustration of a WNV polyprotein expressed at the ER membrane

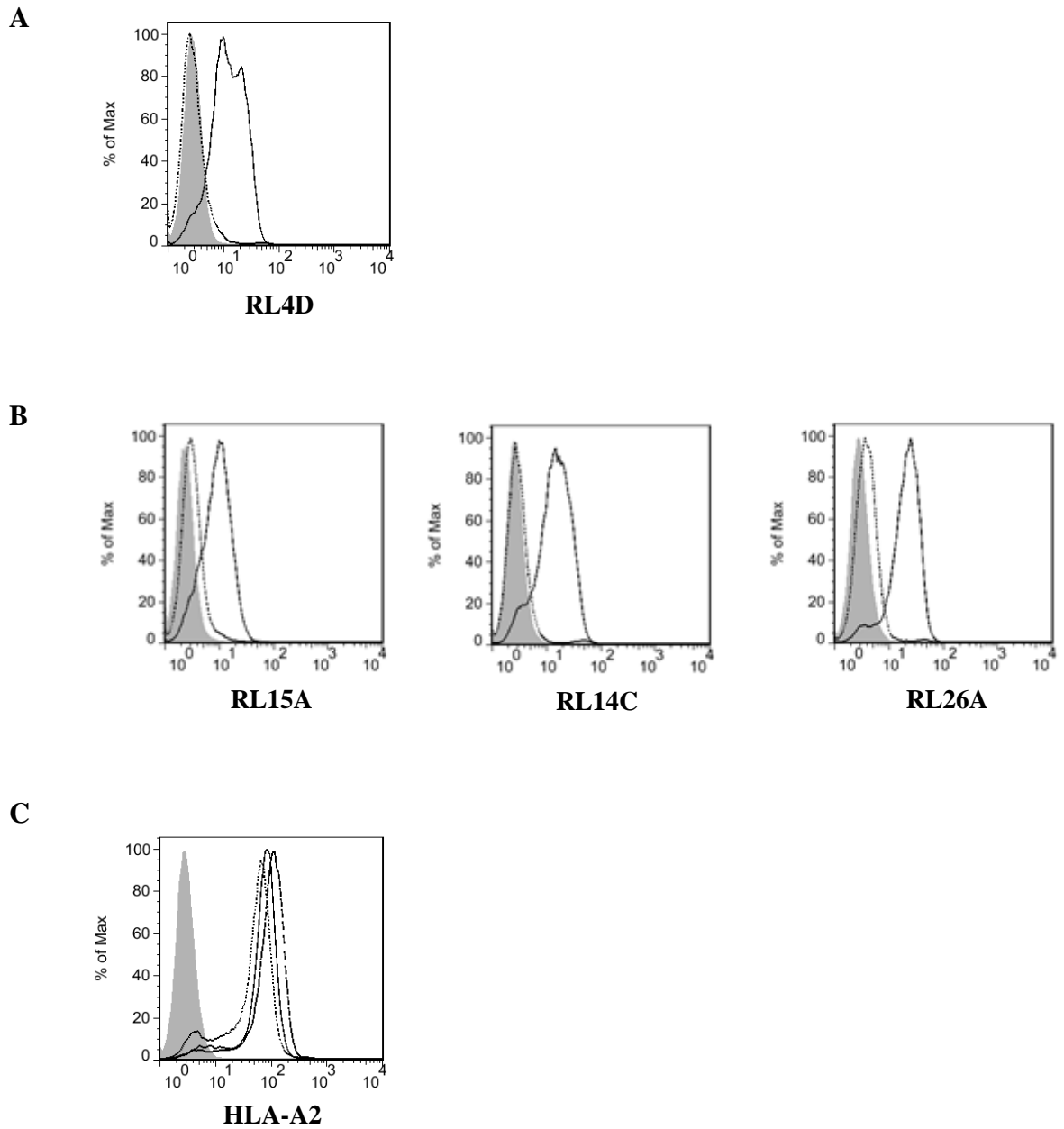
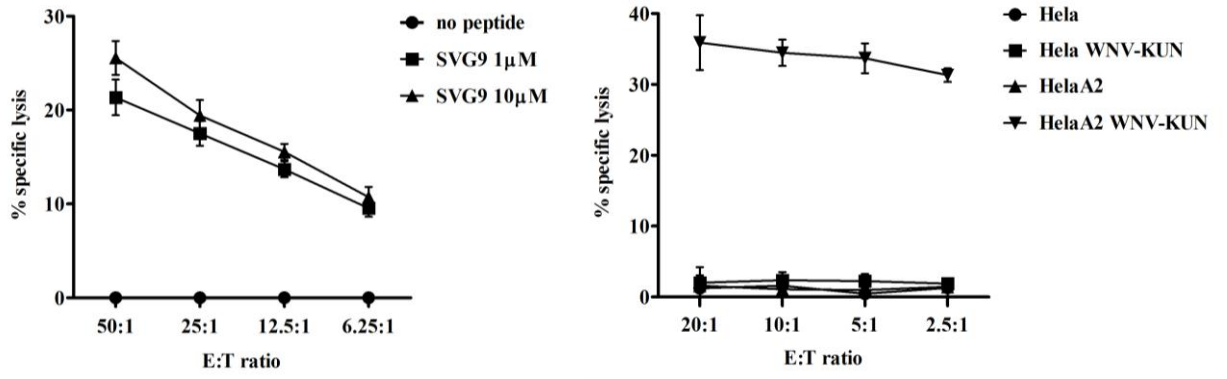
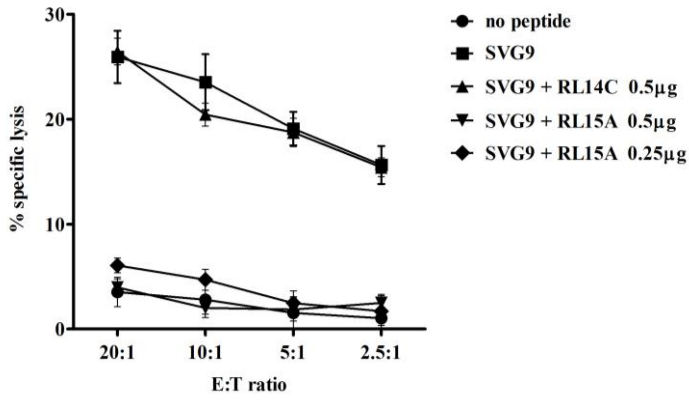


Figure 5. Presentation of viral epitopes at the cell surface is dependent on TAP function.

A



B



C

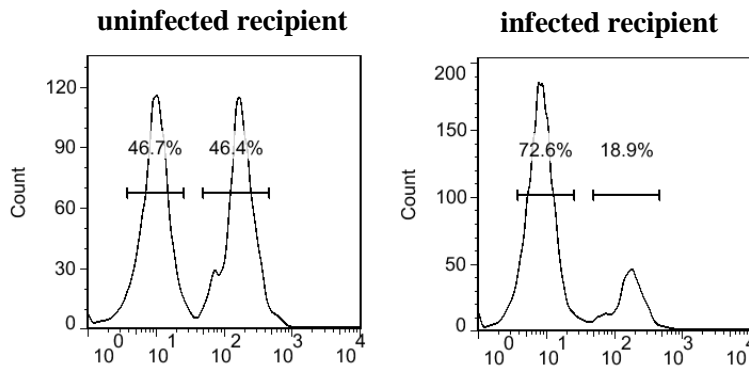


Figure 6. WNV infection generates SVG9-specific CTLs

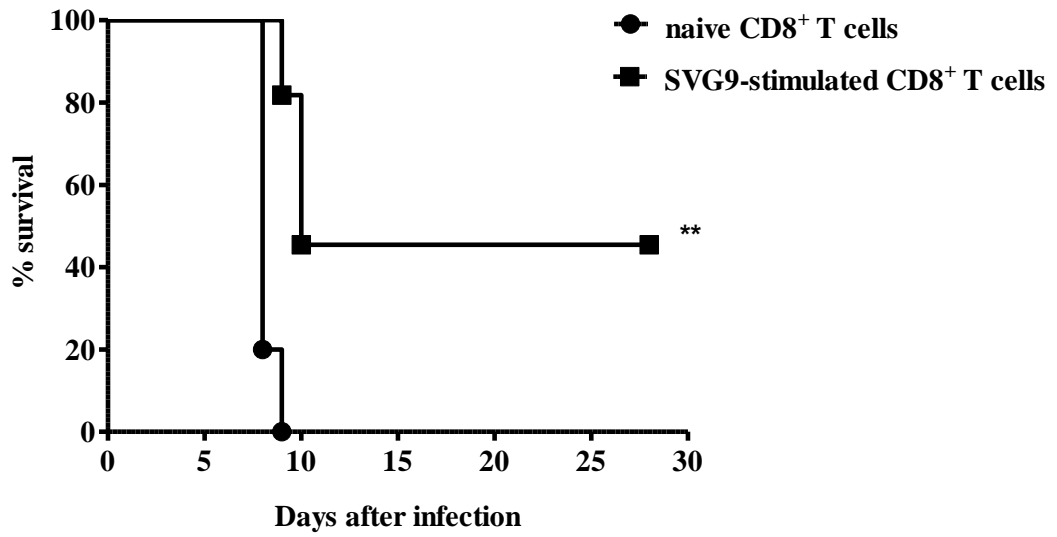


Figure 7. Adoptively transferred SVG9-specific CTLs provide protection against lethal WNV infection

Chapter 2.2

SCT DNA vaccine-mediated protection against infection

Results

*Generation of a SCT incorporating HLA-A*0201 and the SVG9 peptide*

To test the efficacy of SCTs as a DNA vaccine for viral infection, a SVG9/HLA-A*0201 SCT (A2/SVG9 SCT) DNA construct was generated. The SCT construct consisted of a short leader sequence followed by the SVG9 peptide, a 15-amino acid linker, human β 2m, a 20-amino acid linker, and a chimeric HLA-A2 heavy chain containing the α 3 domain of K^b (Fig. 8A) and expressed from the pIRES expression vector. We generated a chimeric heavy chain of HLA-A2 instead of an intact heavy chain, because HHDII mice also express chimeric HLA-A2 molecules. As a control SCT DNA, a mammoglobin A epitope, which is a human breast tumor antigen known to bind HLA-A2 [88], was inserted in place of the SVG9 sequence in the same plasmid. We also incorporated a CD4⁺ helper T cell epitope, PADRE (Pan MHCII reactive epitope), sequence into the construct to enhance CD8⁺ T cell responses. The pan CD4⁺ helper T cell epitope, PADRE (AKFVAAWTLKAA), is an engineered peptide that binds to multiple HLA-DR alleles, which also cross-reacts on mouse class II alleles [86]. Inclusion of this pan CD4 epitope in peptide or DNA vaccines has been shown to increase CD8⁺ T cell responses and vaccine efficacy in HHDII mice [41, 89-91].

To determine whether the A2/SVG9 SCTs are properly folded and expressed on the cell surface, HeLa cells were transfected with A2/SVG9 SCT DNA and stained with

anti-HLA-A2 antibody (BB7.2) or RL15A. A2/SVG9 complexes were detected on the cell surface by both antibodies (Fig. 8B), suggesting stable expression of the complexes with native folding. In addition, recognition of SCTs by T cells was examined in a cytotoxicity assay *in vitro*. A2/SVG9 SCT-expressing cells labeled with ^{51}Cr were incubated with SVG9-specific CD8^+ T cells for 4 hours and lysis was measured. SVG9-specific CD8^+ T cells lysed A2/SVG9 SCT-expressing target cells comparable to peptide-pulsed target cells (Fig. 8C), confirming that SCTs are recognized by antigen-specific CD8^+ T cells comparably to the native MHC/peptide complexes.

DNA immunization of HLA-A2/SVG9 SCTs induces strong CD8^+ T cell responses

I then tested whether immunization with A2/SVG9 SCT DNA can elicit specific CD8^+ T cell responses. A2/SVG9 or control SCT DNA plasmids were injected intradermally three times at three day intervals into the abdomen of naïve HHDII mice using a gene-gun approach [92]. Biolistic gene gun delivery involves adhering naked DNA to gold particles and shooting the particles through a high-pressured instrument. This system delivers DNA directly into skin and Langerhans cells in a highly efficient process. Gene gun immunization has been shown to induce a greater CD8^+ T cell response as well as require less vaccine to achieve immunity [2, 93]. A short-interval repetitive schedule has been developed to lead to rapid and sustained induction of T cell responses upon gene-gun vaccination which was shown to mediate the regression of established tumors and prevent virus-induced morbidity [92]. According to previous studies, CD8^+ T cell responses are at the peak around day 5 post-immunization by the

gene gun method. Thus, at day 5 after the last immunization, splenocytes were harvested and stained with SVG9/HLA-A2 tetramers or re-stimulated *in vitro* with SVG9 peptide to induce IFN γ production. Immunization with A2/SVG9 SCT DNA induced an average of 27% of splenic CD8⁺ T cells to become antigen-specific as judged by tetramer positive reactivity (Fig. 9A) and production of IFN γ from about 20% of splenic CD8⁺ T cells after SVG9 peptide stimulation while control SCTs induced no responses (Fig. 9B). These findings demonstrate that SVG9 SCT DNA vaccination induces a robust SVG9-specific CD8⁺ T cell response *in vivo*.

Protection against lethal WNV infection by SCT DNA vaccination

Next, whether CD8⁺ T cell responses induced by vaccination with SCT DNA can provide mice protection against lethal WNV infection was examined. Naïve HHDII mice were immunized with A2/SVG9 or control SCT DNA plasmids and subsequently infected with 10²PFU of WNV-NY at day 5 after the last immunization. Mice immunized with control SCT DNA developed the expected CNS disease symptoms such as tremors and limb paralysis beginning at day 8 until death, which occurred two to five days later (100% mortality rate) similar to naïve mice. In contrast, of mice immunized with A2/SVG9 SCT DNA, ~30% developed disease symptoms and 25% became moribund by day 10-13 after infection. The remainder of immunized mice never developed disease symptoms and were healthy for 60 days after infection (75% survival rate, Fig. 10). This result clearly establishes that T cell immunity induced by A2/SVG9 SCT DNA vaccination in the absence of a humoral response protects mice from lethal WNV infection.

Co-expression of CD4 helper epitope enhances protective efficacy of SCTs

I assessed whether co-expression of the CD4⁺ T cell helper epitope, PADRE, is required for SCT vaccine efficacy. Naïve HHDII mice were immunized as above with DNA encoding A2/SVG9 SCT with PADRE or A2/SVG9 SCT without PADRE (Fig. 11A). When T cell responses were compared at day 5 after the last immunization, interestingly, immunization of the A2/SVG9 SCT DNA with or without PADRE resulted in a comparable number of SVG9-specific T cells by IFN γ production (Fig. 11B). However, when survival rates upon lethal virus challenge were compared between two groups, co-expression of SCTs with PADRE was significantly more effective at conferring protective immunity (Fig. 11C; $p < 0.05$, $n = 8-9$) than SCTs without PADRE.

SCT DNA immunization lowers viral burden in the brain

WNV infection is thought to begin in Langerhans dendritic cells in the skin [67-71, 79, 80]. Infected dendritic cells migrate to draining lymph nodes where replication occurs and infectious virus enters the circulation via the efferent lymphatic system and thoracic duct. Following viremia, virus spreads to visceral organs (e.g. liver, kidney, spleen) and the brain and spinal cord. CNS disease is suggested to be caused by neuronal degeneration induced directly by viral infection and/or by immune responses to the pathogen. To define the mechanism of disease protection, the viral burden in the brains of A2/SVG9 SCT and control SCT-immunized mice were compared on day 8, the time point at which infected HHDII mice became noticeably ill. Consistent with the clinical phenotype and decreased lethality, A2/SVG9 SCT-immunized mice had 100-fold lower

levels of WNV in the brain than control SCT-immunized mice (Fig. 12A). This effect was independent of humoral responses because the levels of anti-WNV E (envelope) IgG and IgM in the serum were comparable between the two groups (Fig. 12B). This finding was expected because the chemical stability of the SCT makes it unlikely that the SVG9 epitope would be released to induce epitope-specific antibodies. Moreover, the SVG9 epitope, which is located beyond domain III at residues 430-438 of the E protein, is not part of any known B cell epitopes for neutralizing antibody in mice or humans [94-96]. Thus, these results suggest that CD8 T cell responses induced by A2/SVG9 SCT immunization increased survival rate by limiting virus spread to the brain and/or by accelerating virus clearance.

I also examined whether the SCT-immunized mice that survived viral infection developed memory CD8⁺ T cells and protective antibodies against the virus. Mice were vaccinated with A2/SVG9 SCT DNA, then infected with 10²PFU of WNV, and, at day 65, splenocytes and serum from the mice that survived were analyzed for the presence of SVG9/HLA-A2 tetramer positive cells and the ability to produce IFN γ upon restimulation with SVG9 peptide and for levels of specific antibodies against WNV E protein. About 12% of CD8⁺ T cells in the spleens of immunized mice stained positive with SVG9-specific tetramers and were CD44^{hi}, consistent with a memory phenotype (Fig. 13A). Accordingly, ~11% of CD8⁺ T cells produced IFN γ after restimulation with the SVG9 peptide (Fig. 13B). WNV E-specific IgG responses were detected in all A2/SVG9 SCT immunized mice, indicating non-sterilizing immunity and the induction of durable humoral responses after challenge (Fig. 13C).

Functional memory T cell responses develop after SCT DNA immunization

So far, I have shown that primary responses by SCT DNA immunization protect mice against virus infection. Finally, whether DNA vaccination provides long-lasting protective immunity was addressed. Mice were vaccinated with A2/SVG9 SCT or control SCT DNA with PADRE as described above, rested for 45 days, and then challenged with 10^2 PFU of WNV. Before virus challenge, A2/SVG9 SCT-immunized mice had SVG9/A2 tetramer positive, CD62L^{lo} and CD44^{hi} cells which consist of about 2% of CD8⁺ T cells in the spleen (Fig. 14A). Upon virus challenge, A2/SVG9 SCT-immunized mice developed greater CD8⁺ T cell responses than control mice. At day 7 after virus challenge, about 15% of splenic CD8⁺ T cells were SVG9/A2 tetramer positive and produced IFN γ in A2/SVG9 SCT-immunized mice, in contrast to about 2% in control mice (Fig. 14B). A2/SVG9 SCT DNA vaccination conferred 46% survival against lethal WNV infection (Fig. 14C; $p < 0.05$, $n = 11-13$), demonstrating functional memory T cell responses in vaccinated mice. Therefore, A2/SVG9 SCT DNA vaccination develops long-lasting CD8⁺ T cell immunity that can confer protection against infection.

Figure Legends

Figure 8. Expression of A2/SVG9 SCT and recognition by SVG9-specific T cells

(A) Diagram of the SCT DNA encoding SVG9 or mammoglobin A (mamA) peptide /chimeric HLA-A2 complex. PADRE, Pan HLA-DR reactive epitope. SS, signal sequence. (B) Cell surface expression of A2/SVG9 SCT. HeLa cells were transfected with A2/SVG9 SCT DNA and stained with anti-HLA-A2 mAb (BB7.2, dotted line), RL15A (solid line), or isotype control Ab (shaded histogram). (C) Lysis of target cells expressing A2/SVG9 SCT. A2/SVG9 SCT-expressing HeLa cells were used as targets in a ^{51}Cr -release assay with SVG9-specific CTLs. For controls, HeLa A2 cells or HeLa A2 cells pulsed with SVG9 peptide were also used as targets.

Figure 9. Induction of a strong CD8⁺ T cell response by HLA-A2/SVG9 SCT DNA immunization

HHdII mice were immunized with A2/SVG9 or control SCT DNA three times at 3 day intervals. At 5 days after the last immunization, splenocytes were harvested. (A) Splenocytes from control (*left*) or A2/SVG9 SCT immunized mice [87] were stained with anti-CD8 mAb and SVG9/HLA-A*0201 tetramers. Numbers indicate the percentage of tetramer positive cells among CD8⁺ cells. Representative figures of the flow cytometry data. (B) Splenocytes from each group were stimulated *in vitro* with SVG9 or irrelevant peptide overnight and IFN γ secretion was measured by ELISPOT. Error bars indicate SE

of the experiment. The data presented are from one representative experiment of two performed independently with each group containing 4~5 mice.

Figure 10. HLA-A2/SVG9 SCT DNA immunization provides mice protection against lethal WNV infection

HHDII mice were immunized with SVG9 or control SCT DNA with PADRE. At 5 days after the last immunization, mice were infected with 10^2 PFU of WNV. Mice were monitored over 60 days ($n=11-12$ per group). *, $p<0.05$ (log-rank test).

Figure 11. Co-expression of a CD4⁺ helper T cell epitope enhances protective efficacy of SCTs

(A) Diagram of a A2/SVG9 SCT DNA construct with or without an insertion of PADRE sequence. SS, signal sequence. (B) and (C) HHDII mice were immunized with A2/SVG9 SCT with or without PADRE or control SCT DNA. (B) At 5 days after the last immunization, splenocytes were stimulated *in vitro* with 1 μ M of SVG9 or irrelevant peptide overnight. IFN γ secretion was measured by ELISPOT. Error bars indicate SD with $n=5$ mice per group. *n.s.*, not significant (unpaired *t* test). (C) At 5 days after the last immunization, mice were infected with 10^2 PFU of WNV and monitored over 30 days ($n=8-9$ per group). *, $p<0.05$ (unpaired *t* test) compared with A2/SVG9 SCT without PADRE.

Figure 12. HLA-A2/SVG9 SCT DNA immunization lowers viral burden in the brain but has no effect on humoral responses.

Brain tissue and serum were collected at day 8 after viral challenge of HHDII mice that had been immunized with A2/SVG9 or control SCT DNA. (A) Viral burden in brain tissue was determined by a plaque assay. Naïve mice were used as a negative control. *, $p < 0.05$ (unpaired t test). (B) The levels of anti-WNV IgG (*left*) and IgM [87] in the serum were measured by ELISA. *n.s.*, not significant (unpaired t test).

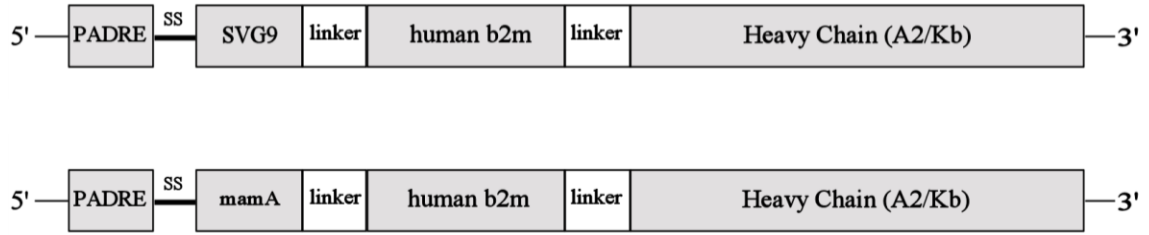
Figure 13. SCT DNA immunization induces non-sterilizing immunity

Spleen and serum samples were taken from A2/SVG9 SCT DNA-vaccinated mice at day 65 post-WNV infection. Naïve mice were used as a negative control. (A) Splenocytes were stained with anti-CD8, -CD44 mAb and SVG9/HLA-A*0201 tetramers. Percentage of tetramer⁺ CD44^{hi}CD8⁺ T cells of four mice in each group was shown. Error bars indicate SD. (B) Splenocytes were stained for CD8 and intracellular IFN γ after 4 hour stimulation *in vitro* with SVG9 or irrelevant peptide in the presence of Golgi-blocking agent. Percentage of CD3⁺CD8⁺IFN γ ⁺ cells is shown. Error bars indicate SD (C) WNV-specific IgG titers in the serum were measured by ELISA. Data were expressed as reciprocal log endpoint titers after regression analysis. *, $p < 0.05$ (unpaired t test).

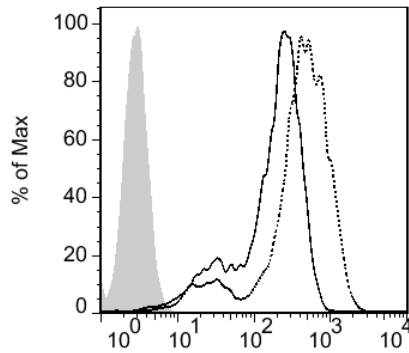
Figure 14. SCT DNA vaccine generates functional memory T cell immunity and provides long-term protection

HHDI mice were vaccinated with A2/SVG9 or control SCT DNA with PADRE as above and rested for 45 days before challenge with 10^2 PFU of WNV. (A) At day 45 post-immunization, splenocytes were stained with anti-CD8, -CD44, -CD62L mAb or SVG9/HLA-A*0201 tetramers. In all the panels, CD3 positive cells were gated and in the middle and right panels only CD8 positive cells were shown. (B) At day 7 after virus challenge, splenocytes were stained with SVG9/HLA-A*0201 tetramers and anti-CD8, -CD44, or -CD62L mAb or CD8 and intracellular IFN γ after 4 hour stimulation *in vitro* with SVG9 or irrelevant peptide in the presence of Golgi-blocking agent. In all the panels, CD3 positive cells were gated and in the middle two columns only CD8 positive cells were shown. Numbers indicate the percentage of cells in each quadrant among CD3⁺ CD8⁺ cells. Representative figures of the flow cytometry data. (C) After WNV challenge, mice were monitored over 25 days ($n=11-13$ per group). *, $p<0.05$ (log-rank test).

A



B



C

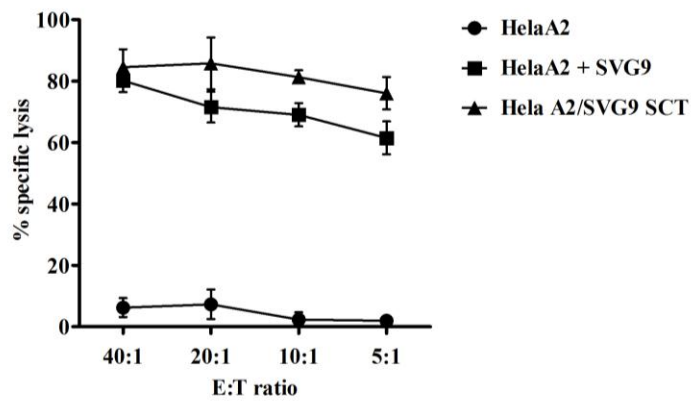
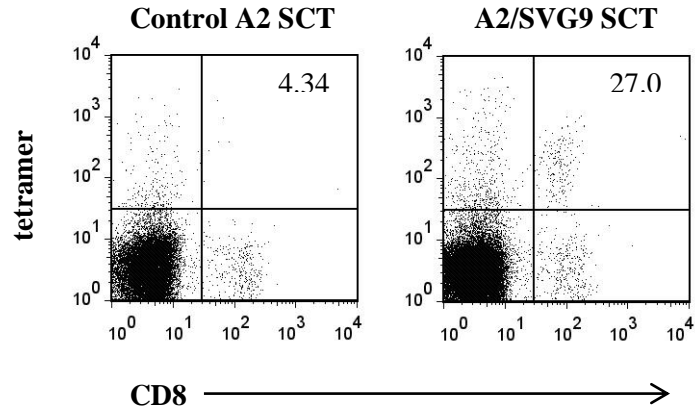


Figure 8. Expression of A2/SVG9 SCT and recognition by SVG9-specific T cells

A



B

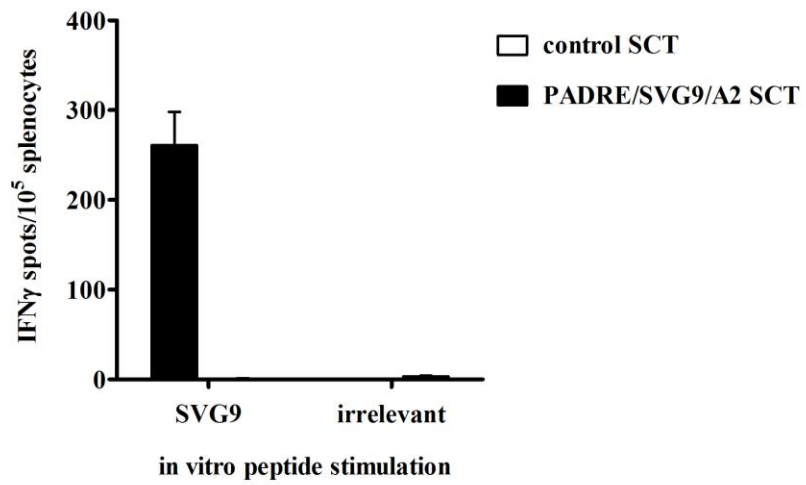


Figure 9. Induction of a strong CD8⁺ T cell response by HLA-A2/SVG9 SCT DNA immunization

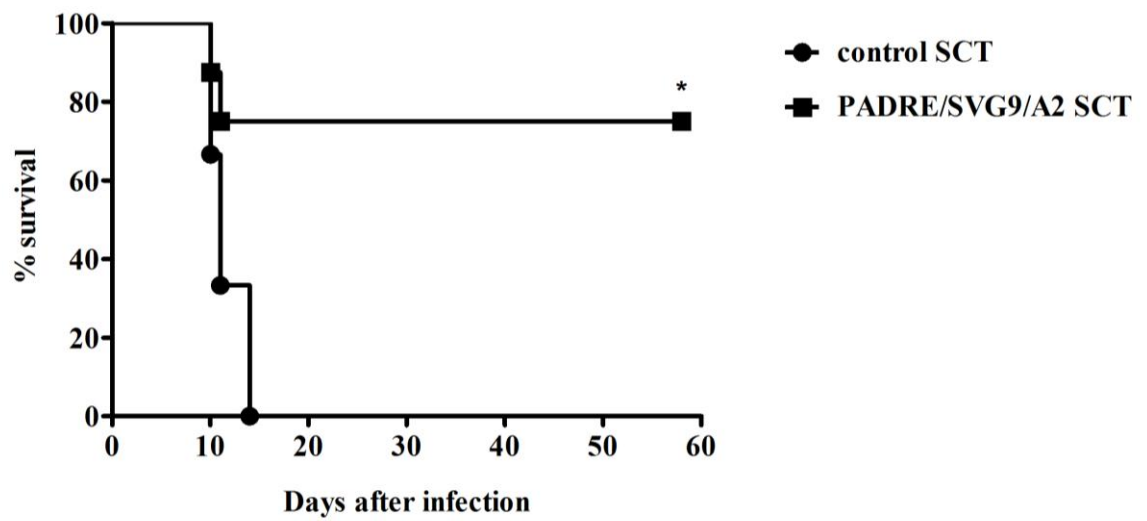
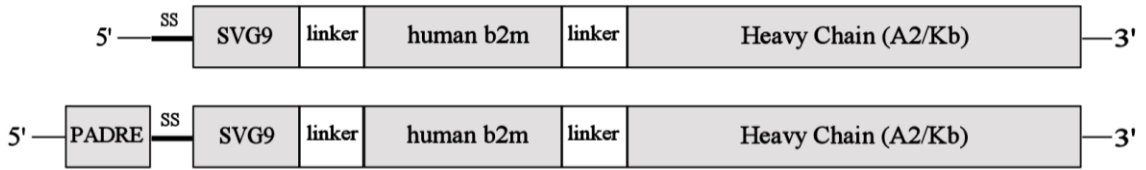
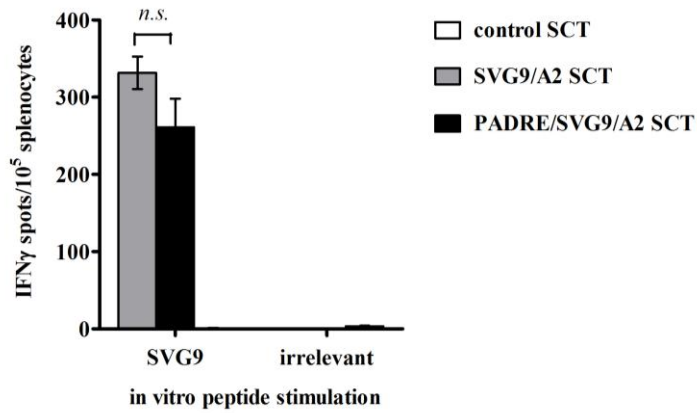


Figure 10. HLA-A2/SVG9 SCT DNA immunization provides mice protection against lethal WNV infection

A



B



C

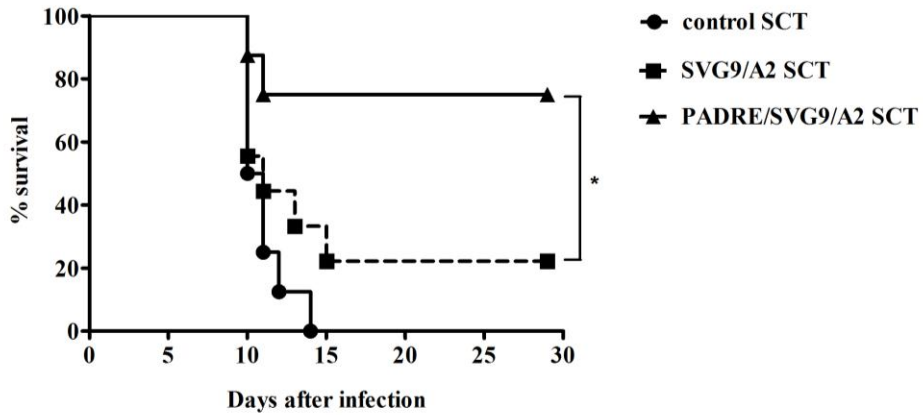


Figure 11. Co-expression of a CD4⁺ helper T cell epitope enhances protective efficacy of SCTs

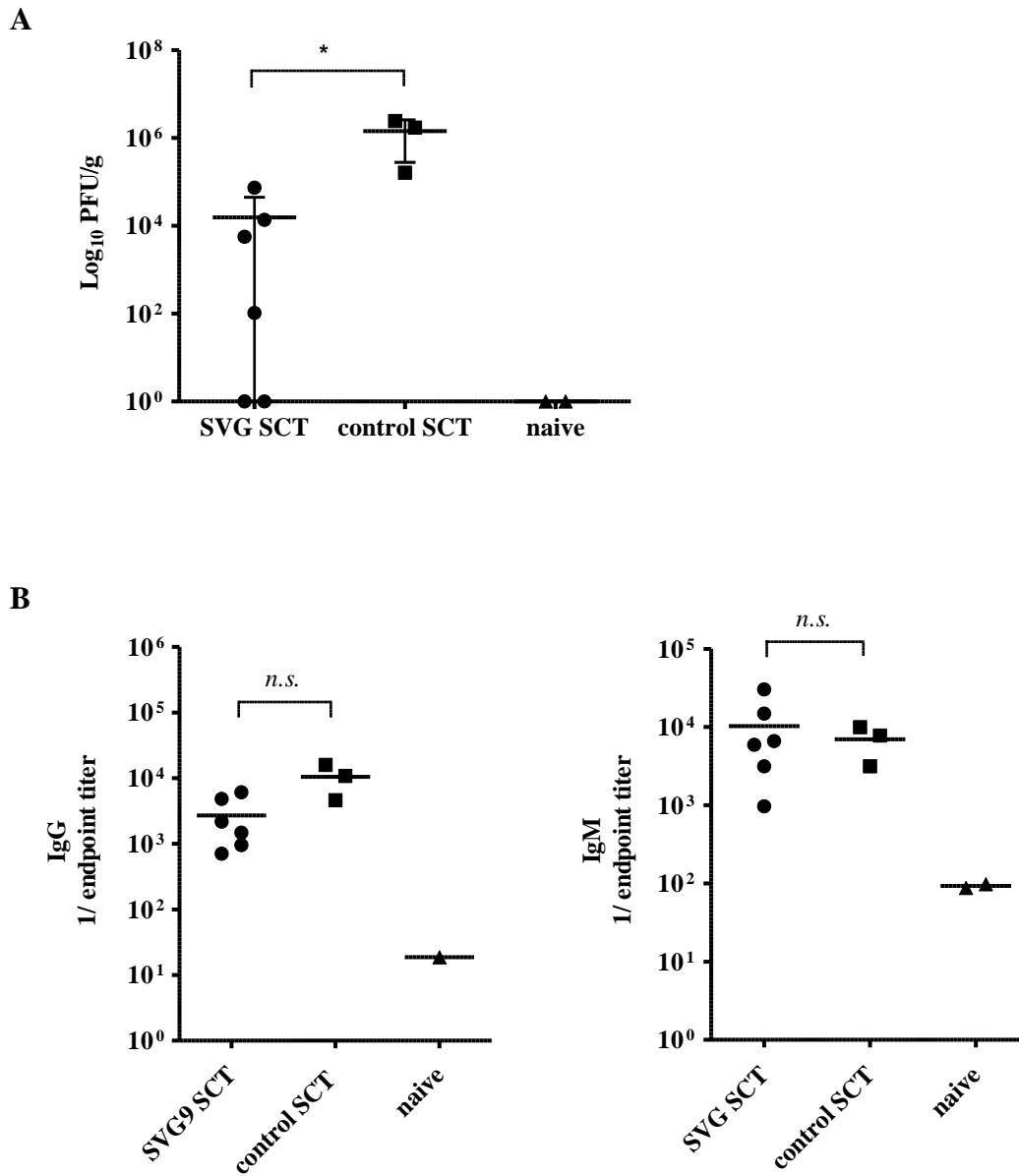


Figure 12. HLA-A2/SVG9 SCT DNA immunization lowers viral burden in the brain but has no effect on humoral responses.

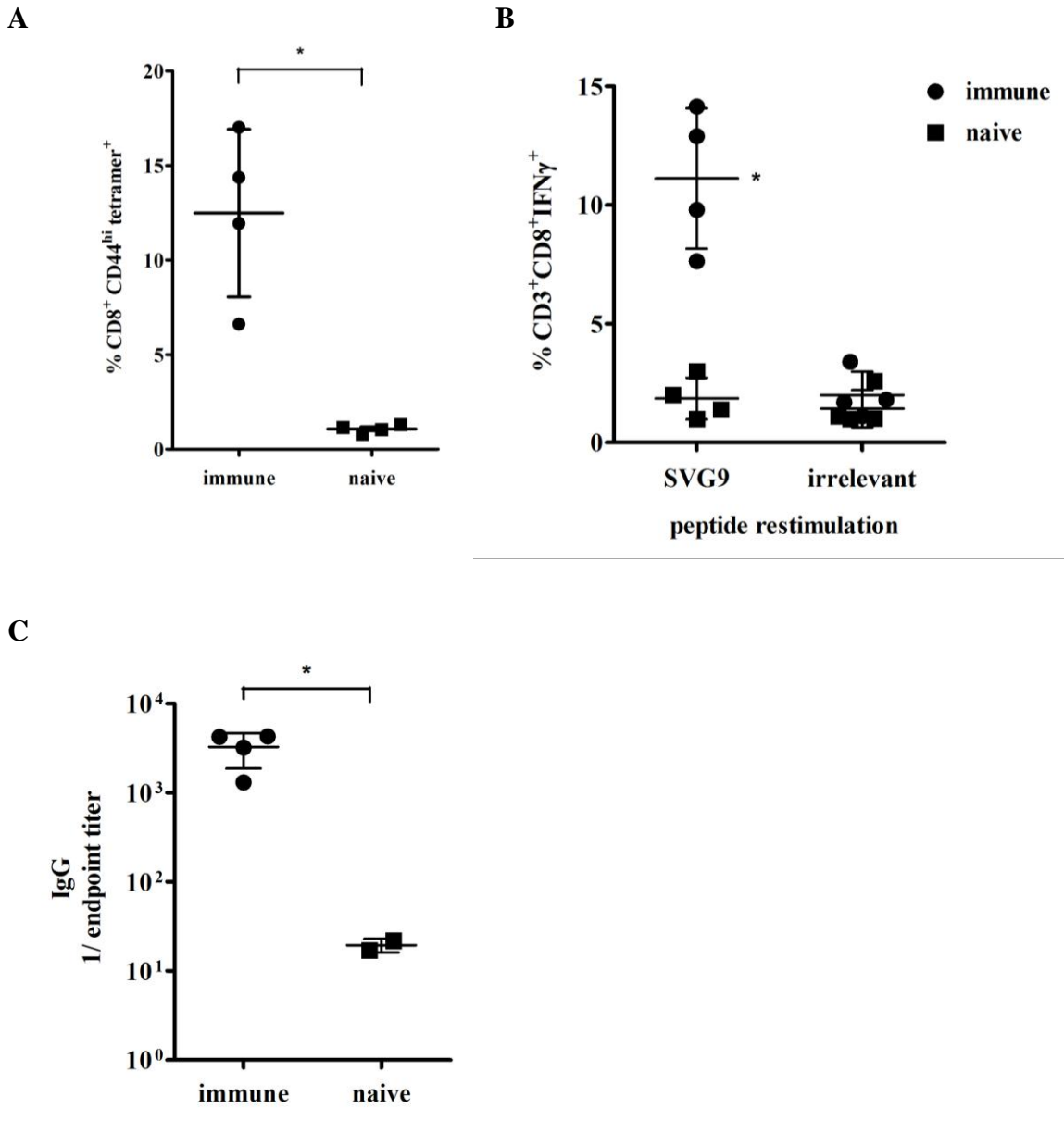


Figure 13. SCT DNA immunization induces non-sterilizing immunity

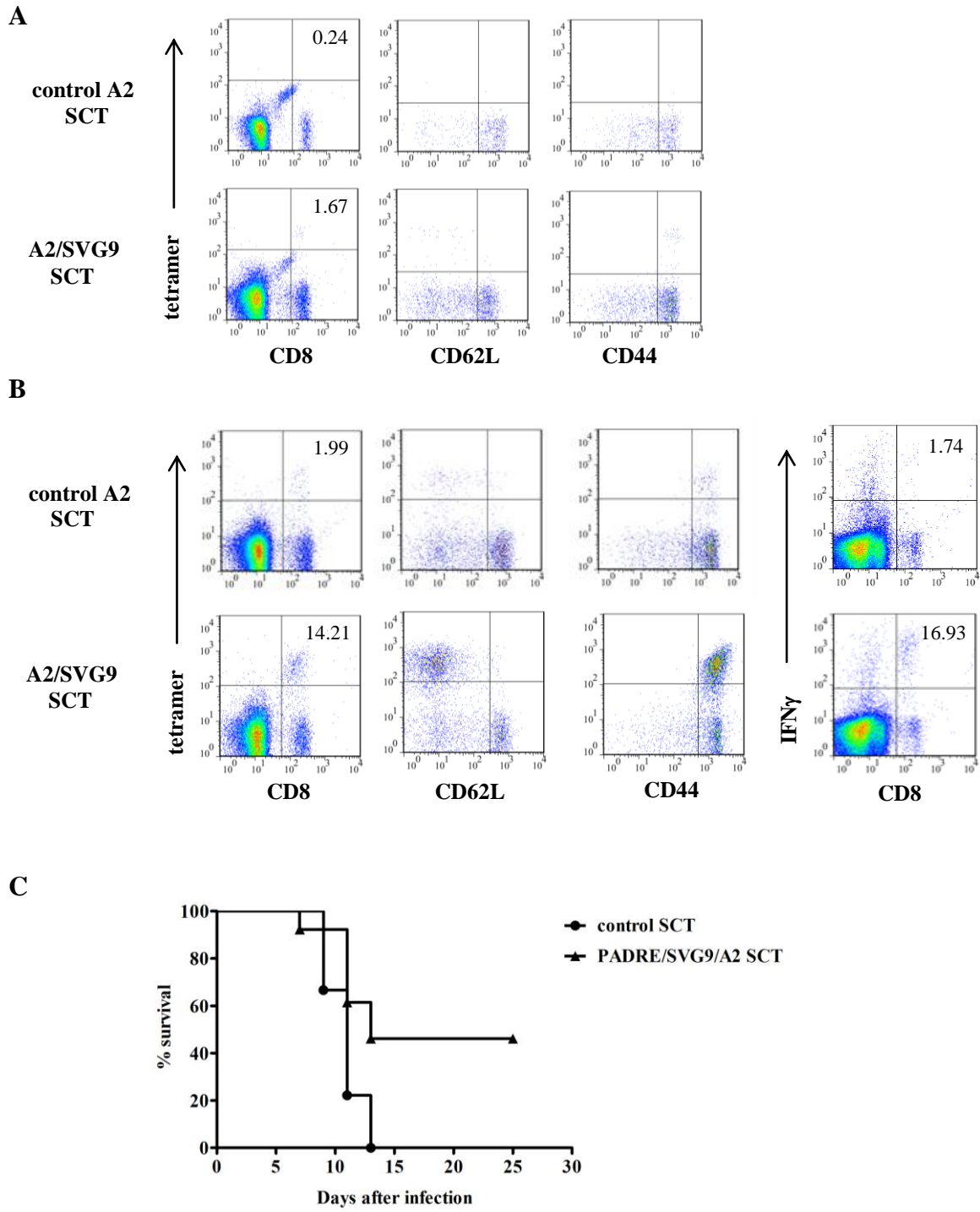


Figure 14. SCT DNA vaccine generates functional memory T cell immunity and provides long-term protection

Discussion

A DNA vaccine is an attractive approach to generate humoral and cellular immunity because plasmids are relatively safe, easy to produce, and readily amenable to technological improvements [2]. Of particular relevance for pathogen immunity, DNA vaccines induce CD8⁺ T cell immunity that may not be elicited by inactivated pathogen or protein subunit based vaccine platforms. DNA vaccines do not have the risks associated with production of live attenuated viral vaccines, especially for administration to the elderly or immunocompromised, the likely targets of diseases of many severe acute infections including WNV and seasonal influenza. Within the last few years several technical innovations in DNA vaccination have occurred including more effective delivery strategies, immune enhancements using adjuvants, and targeting to specific intracellular pathways. Even with these advances, a major hurdle for improving DNA vaccines is increasing immunogenicity. This issue is particularly relevant for larger animals and humans where the DNA platform has proven less effective than in mice. Here, we utilized a unique approach to improve CD8⁺ T cell responses by targeting an immunodominant WNV epitope to the class I MHC antigen presentation pathway with SCT based technology.

Several properties of SCTs likely contribute to their effectiveness in eliciting a CD8⁺ T cell response. The expressed SCT polypeptide includes all three MHC class I components, peptide, β 2m and heavy chain attached sequentially with flexible linkers [11]. The SCT platform appears readily applicable to different mouse and human MHCI/peptide complexes [24, 31]. The preassembled nature of SCTs allows them to

rapidly fold, exclude the binding of competitive peptides, and expediently transit to the cell surface. Furthermore, the linker controlled peptide occupancy renders the SCT stable at the cell surface. Once on the cell surface, SCTs are recognized by CD8⁺ T cells in a manner comparable to native class I/peptide complexes [11]. Thus, immunization with SCTs induces the stable display of specific class I/peptide complexes for a duration sufficient to elicit a robust CD8⁺ T cell response. Indeed, there are now several published examples of plasmids encoding SCTs that elicit robust CD8⁺ T cell responses in model systems and SCT based vaccines confer protection against tumor challenge in mice [30, 31]. Although SCTs incorporating viral epitopes have been shown to elicit CD8⁺ T cells, prior to our study, no previous reports have documented the utility of SCT-based vaccines in conferring protection against lethal challenge by a pathogen. Application of SCTs to pathogen immunity is attractive given that CD8⁺ T cells detect unique pathogen-derived epitopes, whereas tumor-associated epitopes are typically over-expressed self-proteins. It is also notable that immune evasion mechanisms can mitigate CD8⁺ T cell responses to pathogens by mechanisms that include blocking antigen presentation. Indeed, commonly used viral immune evasion mechanisms prevent peptide generation by inhibiting proteasome function or peptide loading by inhibiting TAP function [97]. The preprocessed and preassembled nature of the SCT makes their expression impervious to these mechanisms of immune evasion [98].

The ongoing discovery of pathogen-derived peptide epitopes presented by different HLA molecules will allow construction of tailored SCT based vaccines. The effectiveness of SCT vaccines may be related to the immunodominance of particular

CD8⁺ T cell epitopes. Mechanistically, immunodominance is believed to be affected by (i) peptide abundance as determined by the turnover rate of the donor protein and the peptide processing efficiency, (ii) peptide binding affinity to class I MHC molecules, and (iii) the CD8⁺ T cell repertoire, which is determined during thymic selection. Although six different WNV peptides were eluted from HLA-A2 molecules, the E derived peptide SVG9 was immunodominant in HLA-A2 transgenic mice and in humans. This concordance suggests that the SVG9 peptide is efficiently processed and presented by both mouse and human APCs. Taking advantage of TCR-mimic antibodies, I was able to show that high levels of SVG9/HLA-A2 complexes were displayed on the surface of mouse or human cells infected *in vitro* with WNV. Interestingly, comparably high levels of HLA-A2 bound by the SLF9 and YTM9 peptide were also displayed on the cell surface of WNV infected cells (see Fig. 3B and Fig. 4B), even though few if any SLF9- or YTM9-specific CD8⁺ T cells were detected in re-stimulation assays. Presentation of all the three epitopes at the cell surface was dependent on TAP, regardless of its location in the cells. Thus, the level of epitope presentation on the APC alone does not explain immunodominance. It is consistent with a previous report that the magnitude of the CD8⁺ T cell response to different epitopes is only minimally affected by their abundance in infected cells [99]. After a threshold quantity of antigen has been presented, the magnitude of the T cell response is unaffected by increased presentation of antigen. We speculate the T cell repertoire must also contribute to the immunodominance of the SVG9 peptide.

Plasmid DNA encoding a SCT with the SVG9 peptide elicited a robust CD8⁺ T cell response as determined by intracellular IFN γ production and protective immunity against WNV infection. Co-expression of a helper epitope with the SCT did not affect the level of SVG9-specific T cells, but was required for optimal protective immunity. This observation is consistent with the previous findings showing that CD4-deficiency did not affect the primary CD8⁺ T responses but did compromise the responses at later time points after WNV infection [100]. This study demonstrated that re-stimulation of WNV-specific CD8⁺ T cells and the number of CD8⁺ T cells in the CNS of CD4-deficient mice were compromised only late during infection, suggesting that CD4⁺ T cells play a role in sustaining primary responses and the level of CD8⁺ T cells in the CNS. Also CD4-deficiency resulted in increased lethality. The mechanism through which CD4⁺ T cells provide help to CD8⁺ T cells is as yet unclear. CD4⁺ T cells may secrete cytokines to sustain or increase CD8⁺ T cell numbers. Also, it has been reported that whereas CD4⁺ T cell help does not modify the initial response of naïve CD8⁺ T cells, it appears to be fundamental for generation of efficient memory cells [101-103]. Thus the inclusion of the helper epitope in the SCT likely facilitates development of central and effector memory or the presence of memory T cells in tissues. Our results prove that the flexibility of the SCT platform can combine with other strategies to enhance DNA vaccine potency. Our studies also confirm the importance of CD8⁺ T cells in controlling WNV during primary infection [85, 104-106]. Indeed, the induction of WNV-specific CD8⁺ T cells was sufficient to control infection in the complete absence of humoral immunity. These findings also extend earlier studies in which adoptive transfer of bulk CD8⁺ T cells from

infected mice protected naïve mice from WNV challenge and immunization with a D^b-restricted immunodominant NS4b peptide limited WNV-induced disease and mortality [72, 73].

Although SCT vaccines elicit antigen-specific CD8⁺ T cells, it is likely that their effectiveness can be enhanced once the immune response to DNA vaccination is better understood. For example, the identity of the critical cells expressing antigens after DNA vaccination remains controversial as well as the relative importance of direct versus cross-presentation for CD8⁺ T cell activation [2, 45, 48]. To realize the full potential of SCT vaccine approaches it will be necessary to define the precise cellular and molecular mechanism of antigen presentation after DNA plasmid vaccination. Then, expression of the SCT can be targeted to appropriate cell types to provide maximal CD8⁺ T responses. In summary, SCT-based DNA vaccines have the potential to induce pathogen-specific CD8⁺ T cell responses. Incorporation of an SCT vaccine with other classical approaches that elicit robust humoral immunity may provide a focused approach to stimulating both arms of the adaptive response and generating protective immunity against a range of infectious diseases.

Chapter 3

H-2K^d SCT DNA vaccines and *Listeria* infection

Introduction

In the previous study using HLA-A*0201 SCTs in the mouse model of West Nile virus infection, I demonstrated for the first time that SCT DNA vaccination induces protective T cell immunity against virus infection. This suggested that the SCT platform can be incorporated into a composite vaccine targeting multiple aspects of immunity against viral infection and opened the possibility that SCT-based DNA vaccines may be applied to other infectious disease models. The HLA-A2 transgenic mouse model of WNV infection was unique in that the immunodominance of the SVG9 epitope is very strong. However, this immunodominance may partially be attributed to the fact that relatively few CD8⁺ T cells developed in HHDII mice due to impaired heterologous interactions of host mouse proteins with the chimeric HLA-A2 transgene [107]. Thus we next wanted to extend these findings in the more physiologic C57BL/6 model. Such an approach was made possible by a recent collaborative study between the Diamond, Hansen and Fremont labs as well as studies by the Nikolich-Žugich lab that defined immunodominant WNV epitopes presented by D^b and K^b molecules [72, 73]. Unexpectedly, however, construction of SCTs with these immunodominant WNV epitopes and mouse K^b or D^b was problematic (discussed in Chapter 4 and 5). Therefore as an alternate plan to test pathogen protection of SCT-based vaccines in a non-transgenic model, we chose to use the BALB/c infection model of *Listeria monocytogenes*. The

advantage of using the BALB/c *Listeria* model is that the immunodominant epitopes detected by CD8⁺ T cells are well documented and CD8⁺ T cells are known to play a prominent role in pathogen protection. In addition, the modest contribution of help seen in our SCT-based vaccine to WNV in the HHDII mice was unexpected, so we wanted to extend this observation to a model system where the role of help was well documented. Advantageously, the Unanue lab has considerable expertise using the BALB/c model to study *Listeria* immunity and we are grateful to Drs. Javier Carrero and Emil Unanue for their help with these experiments.

Listeria monocytogenes is a gram positive intracellular bacterium that can cause human disease, listeriosis, particularly in immunocompromised individuals. *L. monocytogenes* infects a broad range of hosts and is often used to study the mammalian immune response to infection because it is easy to culture, safe to work with, and causes a highly predictable infection in mice [108, 109]. Mouse models of *Listeria* infection have been well established and provided several insights into the immune responses to bacterial infection [109]. Although innate immune cells are critical for control of early stages of *L. monocytogenes* infection, they are unable to eliminate bacteria from the mouse. *L. monocytogenes* infection elicits a robust T cell response that clears the pathogen from infected mice and provides long-lasting immunity while humoral immunity provides only a small contribution to protect mice. CD8⁺ T cells play a more substantial role than CD4⁺ T cells in conferring long term protective immunity particularly in the BALB/c mouse model [110, 111]. The BALB/c model has been informative in that immunodominant CD8⁺ T cell epitopes have been well characterized

[112-114]. Furthermore, in tetramer analyses the magnitude and kinetics of CD8⁺ T cell responses to the epitopes have been elegantly characterized [114, 115]. During primary infection, *L. monocytogenes* proliferates *in vivo* for 3 to 4 days following infection and is then cleared by the increasing T cell response within 7 to 8 days post infection. After re-infection with *L. monocytogenes*, memory CD8⁺ T cell populations rapidly respond and clear bacteria from infected tissues. The MHC class I restricted *L. monocytogenes* epitopes are generated from proteins, many of which are also virulence factors, secreted into cytosol. Listeriolysin O, LLO, is one of the most antigenic of the proteins secreted by *L. monocytogenes* [116, 117]. In BALB/c infection, the epitope of LLO (residues 91-99) restricted by H-2K^d has been defined as the most immunodominant CD8⁺ T cell epitope [118].

The ability to quickly and specifically eliminate recurring infections is a hallmark of immunological memory. Thus, the generation of quality memory CD8⁺ T cells is an appealing goal for vaccine design against a variety of infectious diseases. In the *L. monocytogenes* infection model, it has been well known that CD4⁺ T cell help promotes protective memory CD8⁺ T cell development [101-103, 119]. So we tested whether CD4⁺ T cell help can improve the efficacy of SCT DNA vaccine by co-expressing CD4⁺ helper T cell epitopes with the SCT. For this purpose, we compared two known CD4⁺ helper T cell epitopes, a pan CD4⁺ T cell epitope and a well-known CD4⁺ T cell epitope of *L. monocytogenes* that binds to MHC class II I-A^d, LLO 188-201. The pan CD4⁺ T cell epitope (PADRE, AKFVAAWTLKAA), as described in Chapter 2.2, is an engineered peptide that binds to multiple HLA-DR alleles, which also cross-reacts on mouse class II

alleles [86]. *L. monocytogenes* peptide LLO 188-201 (RWNEKYAQAYPNVS) has been reported to be the most immunodominant CD4⁺ T cell epitope binding to I-A^d in the BALB/c model of *L. monocytogenes* infection [113]. Regarding the specificity of CD4⁺ T cell help required for optimal generation and maintenance of memory CD8⁺ T cell responses, it has been proposed that both CD4⁺ and CD8⁺ T cells are required to be specific for the same antigen [120, 121]. However, the recently published data indicate that helper T cell function is not antigen specific and likely results through cytokines [119, 122-125]. The discrepancy between the studies may result from using different experimental systems such as inflammatory or non-inflammatory and/or different precursor frequencies of antigen specific CD8⁺ T cells. Thus, our study not only examined the role of CD4⁺ T cell help in SCT-induced memory immune responses, but also compared *L. monocytogenes*-specific vs. -nonspecific CD4⁺ T cell epitopes for their ability to help protective CD8⁺ T cell responses induced by SCT-based DNA vaccines. Our vaccination approach was attractive conceptually because the CD4⁺ helper T cell epitopes were specifically targeted to the MHC class II antigen presentation pathway using an Ii (invariant chain) expression vector, whereas a CD8⁺ T cell epitope was specifically targeted to the MHC class I antigen presentation pathway using an SCT expression vector.

I generated a H-2K^d SCT incorporating the LLO 91-99 epitope that is recognized by peptide-specific CD8⁺ T cells. DNA vaccination with plasmids encoding K^d/LLO₉₁₋₉₉ SCTs by gene gun induced epitope-specific primary and memory CD8⁺ T cell responses in BALB/c mice and the vaccinated mice showed better control of bacteria upon lethal *L.*

monocytogenes infection. The SCT alone was able to develop functional memory CD8⁺ T cells and the presence of CD4⁺ T cell help, whether it is cognate or non-cognate, marginally enhanced memory CD8⁺ T cell responses. Therefore, our data suggest that a SCT-based DNA vaccine can elicit a potent antibacterial CD8⁺ T cell immunity and thus broaden the application of SCTs in pathogen diseases.

Materials and Methods

1. Cell lines

Transient transfection was performed on 293T human embryonic kidney cells using Lipofectamine 2000 (Invitrogen). LLO 91-99 specific, H-2K^d-restricted T cell hybridoma, 206.15, was a generous gift from Dr. Emil Unanue at Washington University in St. Louis. The hybridoma was maintained in modified DMEM (Invitrogen) supplemented with 10% FBS (HyClone Laboratories, Logan, UT), 1.5mM L-glutamine, 10mM HEPES, 1mM sodium pyruvate, 116mg/L L-arginine, 36mg/L L-asparagine (Sigma) and 100U/mL penicillin/streptomycin (Tissue Culture Support Center, Washington University School of Medicine, St. Louis, MO).

2. SCT construct

To generate H-2K^d/LLO₉₁₋₉₉ SCT, the H-2K^d SCT with HER2/Neu peptide in pcDNA3.1(-) expression vector was used as a template. Nucleotide oligos encoding LLO 91-99 peptide, GYKDGNEYI, flanked by restriction enzyme sites, AgeI and NheI, were designed in order to replace the existing epitope sequence; 5'-ccggtttgtatgctggctataaagatggcaacgaatatattggaggaggtg-3' and 5'-ctagcacctcctccaatatattcgttgccatctttatagccagcatacaaaa -3'. Oligos were annealed to form a double strand and inserted into the vector cut with AgeI and NheI.

To express SCTs and CD4⁺ T cell helper epitopes simultaneously, the pIRES expression vector was used and to direct CD4⁺ T cell helper epitopes to the endosome the invariant chain (Ii) was exploited. The entire sequences encoding SCTs and Ii were

cloned from the original plasmids into the pIRES vector using extended PCR and ligation. Using two step overlapping PCR, the CLIP sequence of Ii was replaced with helper epitopes; PADRE (pan T helper epitope), AKFVAAWTLKAAA, or LLO₁₈₉₋₂₀₁, WNEKYAQAYPNV. For immunization, DNA was prepared using the Plasmid Maxi Prep kit (Qiagen) according to the manufacturer's instructions.

3. Hybridoma activation assay and ELISA

Activation of the T hybridoma was assessed by measuring IL-2 secreted upon activation. T hybridoma cells were co-cultured with 293T cells transiently transfected with SCTs overnight at 37°C. After incubation, the culture supernatants were taken and the amount of IL-2 was measured by ELISA. The supernatant was added to a 96 well plate pre-coated with anti-IL-2 capture antibody, JES6-1A12 (BioLegend, San Diego, CA), overnight at 4°C and blocked with carbonate/bicarbonate coating buffer. After wash with washing buffer, PBS containing 0.05% Tween-20 (Sigma), biotin- anti-IL-2 detection antibody, JES6-5H4 (BioLegend), was added to the plates followed by incubation with avidin-HRP (eBiosciences). Color was developed by adding TMB substrate (eBiosciences) and the reaction was stopped with 2N sulfuric acid. Plates were read on a plate reader (Bio-Rad) at 450nm.

4. *L. monocytogenes* and mouse infection

BALB/c mice were purchased from NCI, maintained under specific pathogen-free conditions at the Washington University School of Medicine and were handled in

accordance with the guidelines set by the Division of Comparative Medicine of Washington University. *Listeria monocytogenes* strain EGD was stored as frozen glycerol stocks at -80°C . All mice were infected intraperitoneally with various doses of *L. monocytogenes* EGD strain in pyrogen-free saline. For primary infection, 10^3 *L. monocytogenes* were injected. Re-immunization was performed with either 2×10^5 or 5×10^4 *L. monocytogenes*.

5. Flow cytometry

Cell culture supernatant containing SF.1-1.1.1, monoclonal anti-H-2K^d antibody, was used to stain K^d/LLO₉₁₋₉₉ SCT-expressing cells. The following mAbs were purchased from eBiosciences: anti-CD8 (53-6.7)-FITC, CD4 (GK1.5)-FITC, CD44 (IM7)-APC, CD62L (MEL-14)-APC, CD3 (145-2C11)-APC or -PE, IL-2 (JES6-5H4)-PE, IFN γ (XMG1.2)-PE, rat IgG1 isotype control-PE, and PE-conjugated goat anti-mouse Ig. PE-conjugated K^d/LLO₉₁₋₉₉ and control tetramer were obtained from the National Institute of Allergy and Infectious Diseases tetramer facility (Emory University, Atlanta, GA). For intracellular cytokine staining, splenocytes were stimulated *in vitro* with peptide at $0.1\mu\text{g}/\text{mL}$ in the presence of GolgiPlug (BD Biosciences, San Jose, CA) for 4 hours at 37°C . Cells were washed and incubated with FcR blocking antibody (2.4G2, eBiosciences), stained with anti-CD8 α , CD4, CD3, and/or CD62L mAb, and fixed with 1% paraformaldehyde (PFA). After washing twice with buffer containing 0.1% saponin, cells were stained with anti-IFN γ , IL-2 mAb, or isotype control antibody. For tetramer staining, cells were stained with tetramers for 30 min at 4°C , and subsequently anti-

CD8 α or CD44 mAb was added for an additional 20 min at 4°C. Propidium iodide (PI) was added shortly before flow cytometry to gate out dead cells. Cells were acquired on FACSCalibur and data were analyzed with FlowJo software (Tree Star).

6. IFN γ ELISpot assay

Spleens were harvested from mice 5 days after the last DNA immunization. After RBC lysis, single cell suspensions were incubated with 1 μ g/mL LLO 91-99 or control peptides in a PVDF filter plate (Millipore, Billerica, MA) pre-coated with 15 μ g/mL of anti-IFN γ capture antibody (AN18, Mabtech Inc, Cincinnati, OH). After overnight stimulation, cells were removed and the plate was incubated with biotinylated anti-IFN γ detection antibody (R4-6A2) and subsequently with streptavidin-ALP. Then spots were developed by adding substrate solution (BCIP/NBT) and counted with an automated ELISpot reader (CTL, Shaker Heights, OH).

7. Colony count

L. monocytogenes numbers in the spleen and liver were estimated by determining colony forming units (CFU) from tissue homogenates on brain heart infusion agar (BHI) plates using standard procedures. Briefly, a spleen or liver was homogenized in buffer containing PBS with 0.05% Triton X-100 (Sigma). Serially diluted tissue homogenates were plated onto BHI plates and incubated for 15-20 hours at 37°C. Colonies on each plate were counted. For all graphs, data were plotted using Prism software (Graphpad). A

Mann-Whitney unpaired test with two-tailed p-values and 95% confidence intervals was used for all statistical analyses.

Chapter 3.1

H-2K^d/LLO₉₁₋₉₉ SCT mediated protection against *L. monocytogenes* infection

Results

H-2K^d SCTs incorporating LLO 91-99 epitope are recognized by peptide-specific CD8⁺ T cells

An SCT construct, which consists of the leader sequence of β_2m , GYKDGNEYI (LLO 91-99, *L. monocytogenes* immunodominant epitope), the first flexible linker of 15 residues (G₄S)₃, the mature mouse β_2m , the second flexible linker of 20 residues (G₄S)₄, and the heavy chain of H-2K^d was generated in the pcDNA3 expression vector. As a control, the plasmid encoding K^d SCTs with HER2/neu peptide, a breast cancer antigen, in the same vector was used. To check the expression at the cell surface, 293T cells were transiently transfected with plasmids encoding K^d/LLO₉₁₋₉₉ SCTs. SCTs were stained with the monoclonal antibody specific for folded K^d, SF1-1.1.1, indicating they were expressed and folded properly on the cell surface after transfection (Fig. 15A). These K^d/LLO₉₁₋₉₉ SCT-expressing cells were incubated with CD8⁺ T hybridomas cells specific for K^d/LLO₉₁₋₉₉ complexes for 24 hours to see whether SCTs can activate T cells. T hybridomas cells secreted IL-2 in response to K^d/LLO₉₁₋₉₉ SCTs but not to control K^d SCTs (Fig. 15B). These results indicate the successful generation of K^d/LLO₉₁₋₉₉ SCTs that are recognized by and activate peptide-specific CD8⁺ T cells.

DNA immunization with K^d/LLO₉₁₋₉₉ SCTs induces specific CD8⁺ T cells

To test the ability of SCT to induce specific CD8⁺ T cells, BALB/c mice were immunized intradermally with plasmids encoding K^d/LLO₉₁₋₉₉ SCTs or control SCTs three times at three day intervals by gene gun. At day 5 after the last immunization, LLO 91-99 specific CD8⁺ T cells were detected in the spleen from mice immunized with K^d/LLO₉₁₋₉₉ SCTs using a tetramer assay (Fig. 16A). In ELISPOT, about the same percentage (~1%) of splenocytes produced IFN γ in response to in vitro peptide re-stimulation, but none from mice immunized with control SCTs (Fig. 16B). Interestingly, I observed a similar or smaller percentage of K^d/LLO₉₁₋₉₉ tetramer positive CD8⁺ T cells in the spleens from mice infected with a sublethal dose of *L. monocytogenes* for 7 days (Fig. 16A). Thus, this indicates that K^d/LLO₉₁₋₉₉ SCT DNA immunization induces an antigen-specific CD8⁺ T cell response which is comparable to that induced by natural infection.

Protection mediated by K^d/LLO₉₁₋₉₉ SCT DNA vaccine against L. monocytogenes infection

How a SCT DNA vaccine influences the outcome of *L. monocytogenes* infection was next determined. After K^d/LLO₉₁₋₉₉ or control SCT DNA vaccination by gene gun as described above, mice were infected intraperitoneally with a lethal dose of *L. monocytogenes* (2×10^5 of strain EGD) at 2 or 4 weeks. For controls to show natural immunity, groups of mice were not infected or were infected with a sublethal amount of *L. monocytogenes* (10^3). Mice were monitored for growth of the *L. monocytogenes* in spleen and liver at 3 days after infection, since, during secondary infection, infected mice usually eliminate *L. monocytogenes* within 3-4 days [126, 127]. K^d/LLO₉₁₋₉₉ SCT DNA

vaccinated mice had one log-fold lower bacteria counts (CFU, colony forming units) than control SCT vaccinated mice in both spleen and liver (statistical significance, *unpaired t test*, $P < 0.05$) whether mice were challenged with *L. monocytogenes* at 2 weeks or 4 weeks after vaccination (Fig. 17). Control SCT DNA vaccinated mice had the same bacteria counts as untreated mice while mice immunized with a sublethal dose of *L. monocytogenes* showed similar or lower bacteria counts than K^d/LLO₉₁₋₉₉ SCT DNA vaccinated mice. This result demonstrates that K^d/LLO₉₁₋₉₉ SCT DNA vaccination can induce a protective immune response against lethal *L. monocytogenes* infection.

Figure Legends

Figure 15. Expression and recognition of K^d/LLO₉₁₋₉₉ SCTs by CD8⁺ T cells

(A) Cell surface expression of K^d/LLO₉₁₋₉₉ SCTs. 293T cells were transfected with K^d/LLO₉₁₋₉₉ SCT DNA and stained with anti-K^d mAb (SF1-1.1.1, solid line). A shaded histogram shows staining of untransfected cells. (B) Activation of hybridomas specific for LLO 91-99/K^d by K^d/LLO₉₁₋₉₉ SCT-expressing cells. Transfected 293T cells were incubated with T hybridomas at the ratios of 8:1, 4:1, or 1:1 for 24 hours and the amounts of IL-2 in the culture supernatant were measured by ELISA. For controls, P815 cells that express endogenous K^d were incubated with hybridomas with or without 1 μg/mL of LLO 91-99 peptide.

Figure 16. K^d/LLO₉₁₋₉₉ SCTs DNA immunization induces peptide-specific CD8⁺ T cells

Mice were immunized with K^d/LLO₉₁₋₉₉ or control K^d SCT DNA three times at 3 day intervals. At 5 days after the last immunization, splenocytes were harvested. (A) Splenocytes from control (*left*), K^d/LLO₉₁₋₉₉ SCT (*middle*), or *L. monocytogenes*-immunized mice [87] were stained with anti-CD8 mAb and LLO 91-99/K^d tetramers. Numbers indicate the percentage of tetramer positive cells among CD3⁺ CD8⁺ cells. Representative figures of the flow cytometry data. (B) Splenocytes from each group were stimulated *in vitro* with LLO 91-99 or irrelevant peptide overnight and IFN γ secretion was measured by ELISPOT. Error bars indicate SE of the experiment. The data presented

are from one representative experiment of two performed independently with each group containing 4~5 mice.

Figure 17. A K^d/LLO₉₁₋₉₉ SCT DNA vaccine lowers bacterial burden in lethal *L. monocytogenes* infection

Mice were immunized with K^d/LLO₉₁₋₉₉ or control K^d SCT DNA by gene gun as described above and infected intraperitoneally with 2×10^5 of *L. monocytogenes* at 2 [86] or 4 weeks (*lower*) post immunization. For controls, mice were infected with 10^3 of *L. monocytogenes* or left uninfected. At 3 days after infection, spleens and livers were harvested and bacteria counts were determined by colony count. Error bars indicate SEM of the experiment. Data were expressed as log₁₀ of colony forming units (CFU). *n.s.*, not significant. *, $p < 0.05$ (unpaired *t* test).

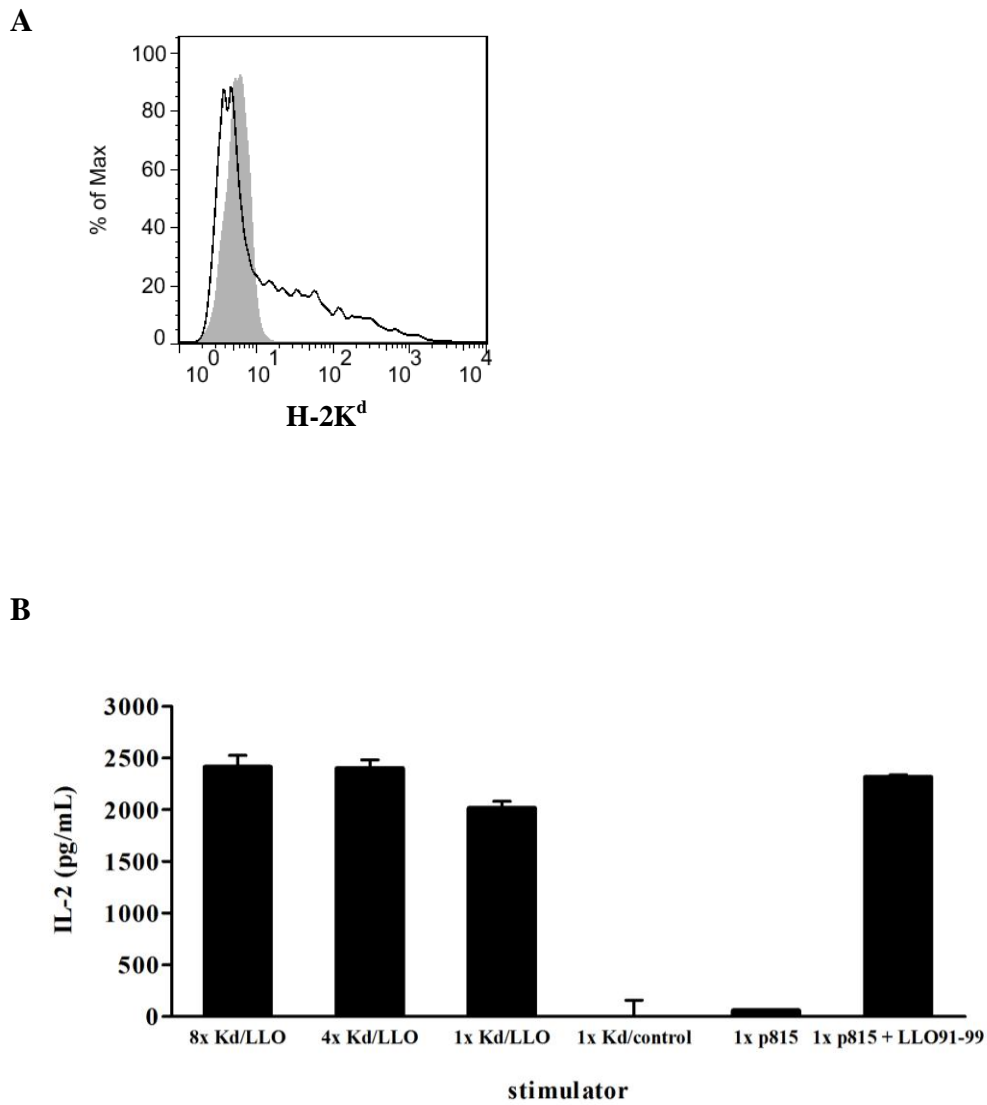


Figure 15. Expression and recognition of K^d/ LLO₉₁₋₉₉ SCTs by CD8⁺ T cells

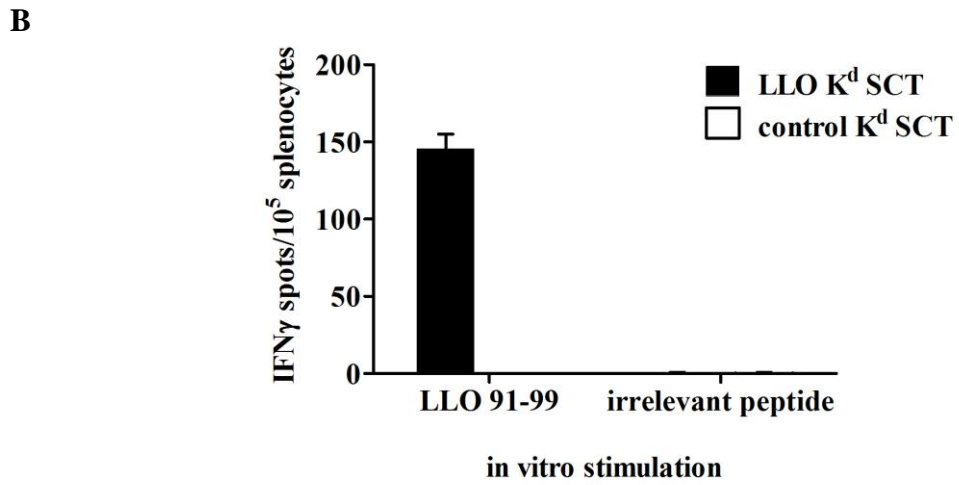
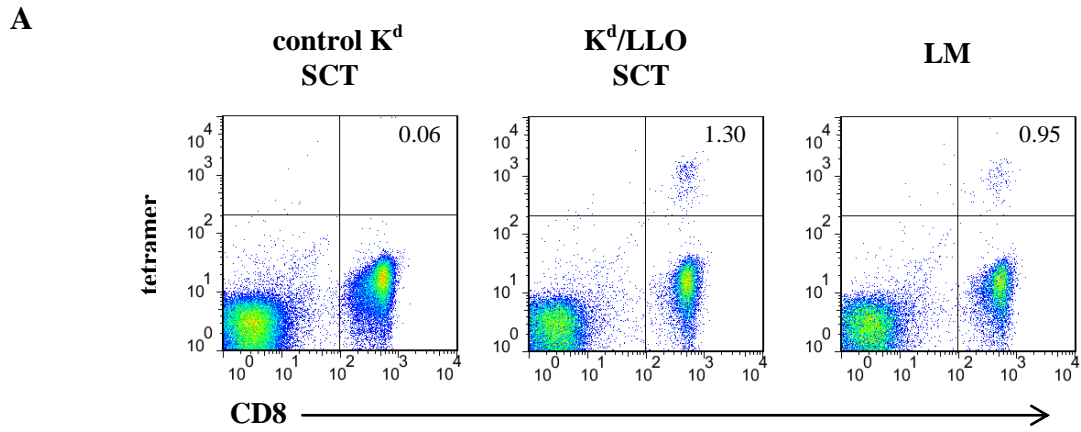
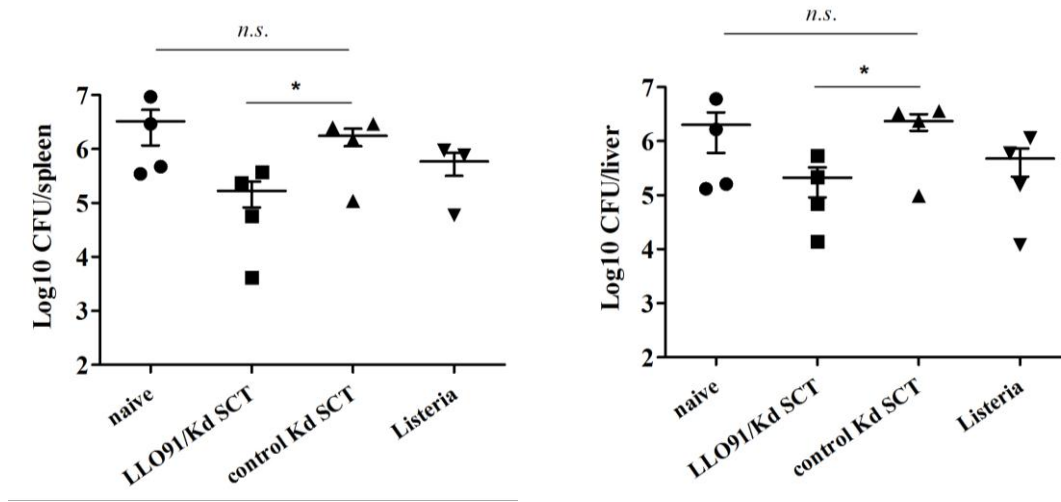


Figure 16. K^d/ LLO₉₁₋₉₉ SCT DNA immunization induces peptide-specific CD8⁺ T cells

2 weeks post-immunization



4 weeks post-immunization

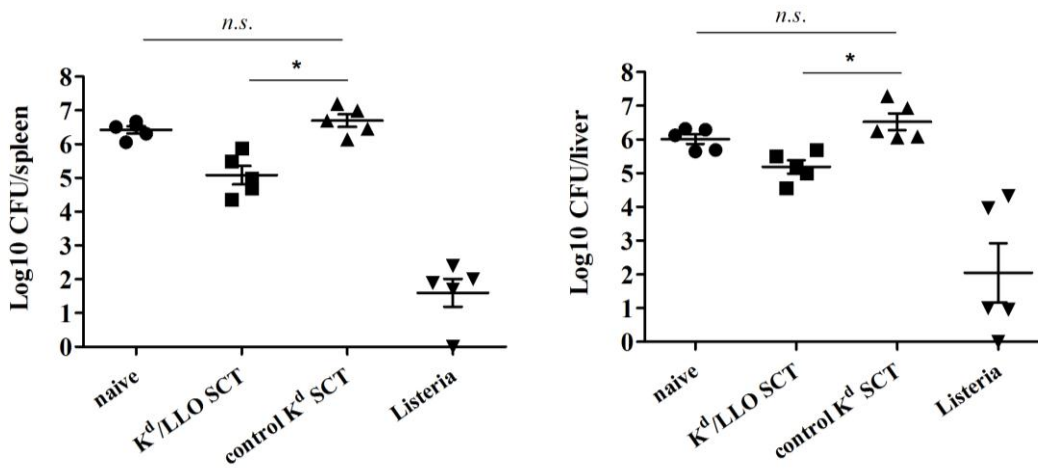


Figure 17. A K^d/LLO₉₁₋₉₉ SCT DNA vaccine lowers bacterial burden in lethal *L. monocytogenes* infection

Chapter 3.2

Role of cognate vs. non-cognate CD4⁺ T cell help for protection

Results

Memory CD8⁺ T cell responses after SCT DNA immunization

Generation of functional memory responses is a critical issue for vaccines against infection. In the previous chapter, I showed that mice have protective immunity at 4 weeks after SCT DNA immunization. But antigens may be still expressed at the time of bacteria challenge because it was reported that antigen expression was still detectable at 10 weeks following intradermal DNA injection [128]. Therefore I examined whether memory CD8⁺ T cells are generated after DNA immunization of SCTs and their functionality at later time points. Mice were immunized with DNA encoding K^d/LLO₉₁₋₉₉ or control SCTs as described above and rested for 5 months before *L. monocytogenes* challenge. 5 months after immunization, K^d/LLO₉₁₋₉₉ tetramer positive CD8⁺ T cells were present in the spleen of resting mice immunized with K^d/LLO₉₁₋₉₉ SCTs, and IFN γ production was detected after peptide stimulation *in vitro* (Fig. 18A and B). The CD8⁺ T cells had memory phenotypes, CD44^{hi} and CD62L^{lo} (Fig. 18A and not shown). These mice were infected with 5×10^4 *L. monocytogenes* and 3 days later bacteria in the spleen and liver were counted. Mice vaccinated with K^d/LLO₉₁₋₉₉ SCTs had 10-fold less bacteria than mice immunized with control SCTs (Fig. 18C). This was a similar result to that from *L. monocytogenes* challenge at 2 or 4 weeks post-immunization described in Chapter 3.1. At the same time, to examine expansion of memory T cells, we infected the vaccinated

mice with 1×10^3 *L. monocytogenes* and compared CD8⁺ T cell responses 7 days later between control, K^d/LLO₉₁₋₉₉ SCTs, and *L. monocytogenes*-immune mice. Mice immunized with K^d/LLO₉₁₋₉₉ SCTs had 4-6 times more tetramer positive CD8⁺ T cells that were CD44^{hi} as well as IFN γ producing CD8⁺ T cells that were CD62L^{lo} than *L. monocytogenes*- or control SCTs -immune mice (Fig. 19). Therefore, the results indicate that DNA immunization of K^d/LLO₉₁₋₉₉ SCTs generates functional memory CD8⁺ T cells that expand rapidly and provide protection against *L. monocytogenes* infection.

Role of CD4⁺ helper T cells for the SCT-induced CD8⁺ T cells

We have observed that expression of only CD8⁺ T cell antigens by SCTs is able to generate functional memory CD8⁺ T cells. Generally, functional memory CD8⁺ T cells are known to require the presence of CD4⁺ helper T cells. Although it is not clear yet how CD4⁺ T cells help to generate and maintain CD8⁺ T cell function, it has been reported that memory CD8⁺ T cell responses are defective when CD4⁺ T cells are absent during the priming phase [102, 103]. In these studies CD8⁺ T cells were primed with infectious antigens, which is not the case in our study. It is possible that the CD8⁺ T cell responses we saw after SCT immunization could be enhanced by the presence of activated CD4⁺ T cells. To determine whether CD4⁺ T cells make SCT-induced CD8⁺ T cell responses better, we designed DNA constructs that express CD4⁺ T cell epitopes with SCTs simultaneously (Fig. 20A). CD4⁺ T cell epitopes were expressed in the context of an invariant chain (Ii) where a CLIP sequence was replaced with a CD4⁺ T cell epitope sequence in order for it to be loaded onto MHC II in the appropriate endocytic

compartment. Expression of CD4⁺ T cell epitopes and induction of specific CD4⁺ T cells using this strategy have been previously reported [41, 129-131]. The CD4⁺ T cell epitope/Ii was co-expressed with SCTs using an internal ribosomal entry site (IRES). Two different CD4⁺ T cell helper epitopes were used in the study. One is the peptide LLO 189-201 (one of the dominant CD4⁺ T cell epitopes of *L. monocytogenes* that binds to MHC II I-A^d) and the other is the pan CD4⁺ helper T cell epitope (PADRE). Mice were immunized as above and CD4⁺ and CD8⁺ T cell responses and bacteria control were compared among groups immunized with SCTs alone, SCTs plus LLO₁₈₉₋₂₀₁, and SCTs plus PADRE after challenge with *L. monocytogenes*.

First, I was able to confirm the induction of epitope-specific CD4⁺ T cells at one week post-immunization by measuring IFN γ and IL-2 production after *in vitro* peptide re-stimulation of splenocytes from the immunized mice (Fig. 20B). Both CD4⁺ helper T cell epitopes induced a comparable level of CD4⁺ T cell response, as monitored after *in vitro* expansion. All three groups showed similar CD8⁺ T cell responses in terms of the number of K^d/LLO₉₁₋₉₉ tetramer positive cells as well as IFN γ production (Fig. 20B). These results indicated that the presence of activated CD4⁺ T cells did not affect the primary CD8⁺ T cell response. Next, memory CD8⁺ T cell responses were examined.

At 6 weeks post-immunization, about the same number of memory phenotype, CD44^{hi}, CD62L^{lo} and K^d/LLO₉₁₋₉₉ tetramer positive CD8⁺ T cells were present in all three groups and they produced a comparable amount of IFN γ upon *in vitro* peptide re-stimulation (Fig. 21A). However, after challenge with 1×10^3 of *L. monocytogenes*, mice that had been vaccinated with SCTs plus LLO₁₈₉₋₂₀₁ or SCTs plus PADRE showed larger

IFN γ -producing CD8⁺ T cell responses than mice vaccinated with SCTs alone (Fig. 21B). SCTs plus LLO₁₈₉₋₂₀₁ and SCTs plus PADRE mounted similar recall responses, indicating that CD4⁺ T cell help is not necessarily antigen-specific. Finally, the vaccinated mice were challenged with 5x10⁴ *L. monocytogenes* and 3 days later bacteria in the spleen and liver were counted. Mice that had been vaccinated with SCTs plus LLO₁₈₉₋₂₀₁ or SCTs plus PADRE showed no significantly different bacteria counts, indicating that they were able to control bacterial infection equally (Fig. 22). However, mice in both groups had about 10-fold less bacteria than mice vaccinated with SCTs alone. Therefore, DNA immunization of K^d/LLO₉₁₋₉₉ SCTs generates functional memory CD8⁺ T cells and expression of CD4⁺ helper T cell epitopes can further enhance the protective efficacy of SCTs.

Figure Legends

Figure 18. A SCT DNA vaccine develops memory CD8⁺ T cells

Mice were vaccinated with K^d/LLO₉₁₋₉₉ SCTs or control K^d SCTs as described above and rested for 5 months before *L. monocytogenes* challenge. (A) At 5 months post-immunization, splenocytes were stained with anti-CD8, -CD44 mAb and SVG9/HLA-A*0201 tetramers. In the left panels CD3 positive cells are shown and the numbers indicate the percentage of CD3⁺ CD8⁺ tetramer⁺ cells. In the right panels CD3⁺ CD8⁺ cells are shown and the numbers indicate the percentage of cells in each quadrant. Representative figures of the flow cytometry data. (B) Splenocytes from each group were stimulated *in vitro* with LLO 91-99 or irrelevant peptide overnight and IFN γ secretion was measured by ELISPOT. Error bars indicate SE of the experiment. The data presented are from one representative experiment of two performed independently with each group containing 4~5 mice. (C) Vaccinated mice were infected with 5×10^4 *L. monocytogenes* and 3 days later spleens and livers were harvested and bacteria growth was determined by colony count. Error bars indicate SEM of the experiment. Data were expressed as log₁₀ of colony forming units (CFU). *n.s.*, not significant. *, $p < 0.05$ (unpaired *t* test).

Figure 19. A SCT DNA vaccine develops functional memory CD8⁺ T cells

Mice were vaccinated with control K^d, K^d/LLO₉₁₋₉₉ SCTs, or 10^3 *L. monocytogenes* and 5 months later challenged with 10^3 *L. monocytogenes*. At 7 days post-infection, splenocytes were stained with anti-CD8, -CD44 mAb, and K^d/LLO₉₁₋₉₉ tetramers (*left*) or with anti-CD8, CD62L and -IFN γ mAb after 4 hour stimulation *in vitro* with LLO or irrelevant

peptide in the presence of Golgi-blocking agent [87]. CD8 positive cells were shown. Numbers indicate the percentage of cells of the gated population among CD8⁺ cells. Representative figures of the flow cytometry data.

Figure 20. Co-expression of a CD4⁺ T cell epitope does not affect primary CD8⁺ T cell responses

(A) Diagrams of the plasmid DNA encoding K^d/LLO₉₁₋₉₉ SCT and a CD4 epitope. PCMV, promoter; IRES, internal ribosomal entry site; Ii, invariant chain. (B) Mice were immunized with DNA encoding K^d/LLO₉₁₋₉₉ SCT only, SCT plus Ii-LLO 198, or SCT plus Ii-PADRE three times at 3 day intervals by gene gun. At 5 days after the last immunization, splenocytes were harvested. Splenocytes were stained with anti-CD8, -CD3 mAb, and K^d/LLO₉₁₋₉₉ tetramers [86] or anti-CD8, -CD3, and -IFN γ mAb after 4 hour stimulation *in vitro* with LLO 91-99 or irrelevant peptide in the presence of Golgi-blocking agent (*middle*). Numbers indicate the percentage of the cells in the quadrant among CD8⁺ cells. Or splenocytes were cultured *in vitro* in the presence of 1 μ g/mL of LLO 198 or PADRE peptide for 5 days and then stained with anti-CD3, -CD4, and -IL-2 mAb after 4 hour re-stimulation with each peptide in the presence of Golgi-blocking agent (*lower*). Numbers indicate the percentage of the gated cells of CD3⁺ cells. CD3⁺ cells are shown. Representative figures of the flow cytometry data.

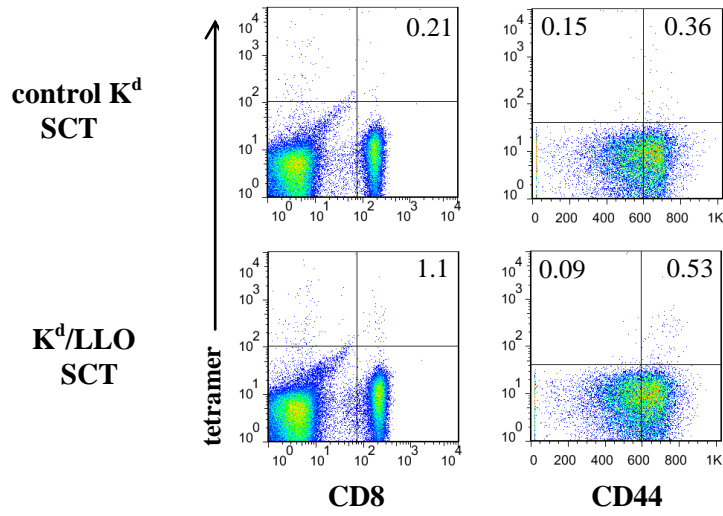
Figure 21. Co-expression of a CD4⁺ T cell epitope increases memory CD8⁺ T cell responses

Mice were immunized with DNA encoding K^d/ LLO₉₁₋₉₉ SCT only, SCT plus Ii-LLO 198, or SCT plus Ii-PADRE as described above. (A) At 6 weeks post-immunization, spleens were harvested and stained with anti-CD8, -CD44 mAb and K^d/LLO₉₁₋₉₉ tetramers. Percentage of tetramer⁺ CD44^{hi}CD8⁺ T cells of four mice in each group was shown (*left*). Or splenocytes were stained with anti-CD8, CD62L and -IFN γ mAb after 4 hour stimulation *in vitro* with LLO or irrelevant peptide in the presence of Golgi-blocking agent [87]. Error bars indicate SD. *n.s.*, not significant (unpaired *t* test). (B) At 6 weeks post-immunization, mice were challenged with 1×10^3 of *L. monocytogenes*. 7 days later, splenocytes were stained with anti-CD8, -CD3, and -IFN γ mAb after 4 hour stimulation *in vitro* with LLO 91-99 or irrelevant peptide in the presence of Golgi-blocking agent (*lower*). CD3 positive cells are shown. Numbers indicate the percentage of the cells in the quadrant among CD8⁺ cells. Representative figures of the flow cytometry data.

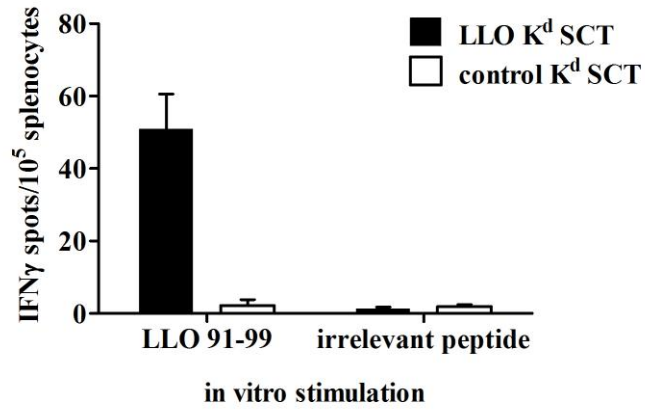
Figure 22. Co-expression of a CD4⁺ T cell epitope enhances the protective efficacy of a SCT DNA vaccine

Mice were immunized with DNA encoding K^d/ LLO₉₁₋₉₉ SCT only, SCT plus Ii-LLO 198, SCT plus Ii-PADRE, or 10^3 *L. monocytogenes* as described above. At 6 weeks post-immunization, mice were infected with 5×10^4 *L. monocytogenes* and 3 days later spleens and livers were harvested and bacteria growth was determined by colony count. Error bars indicate SEM of the experiment. Data were expressed as log₁₀ of colony forming units (CFU). *n.s.*, not significant. *, $p < 0.05$ (unpaired *t* test).

A



B



C

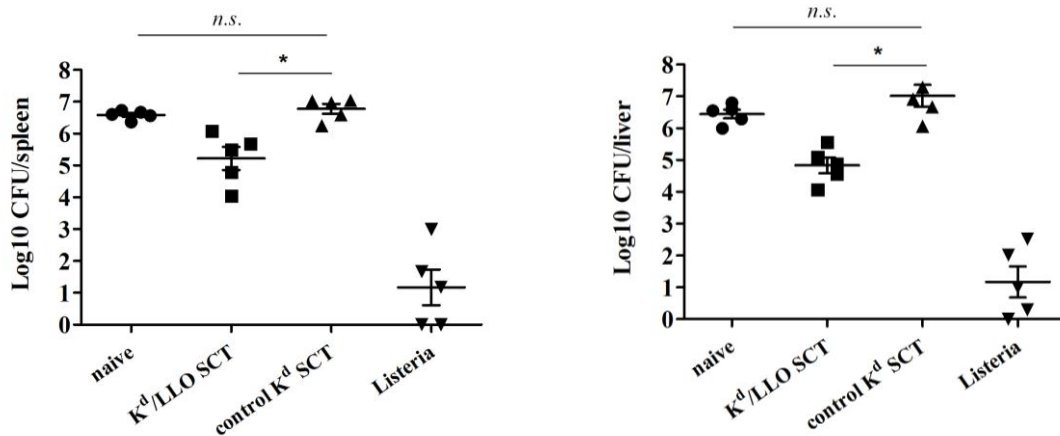


Figure 18. A SCT DNA vaccine develops memory CD8⁺ T cells

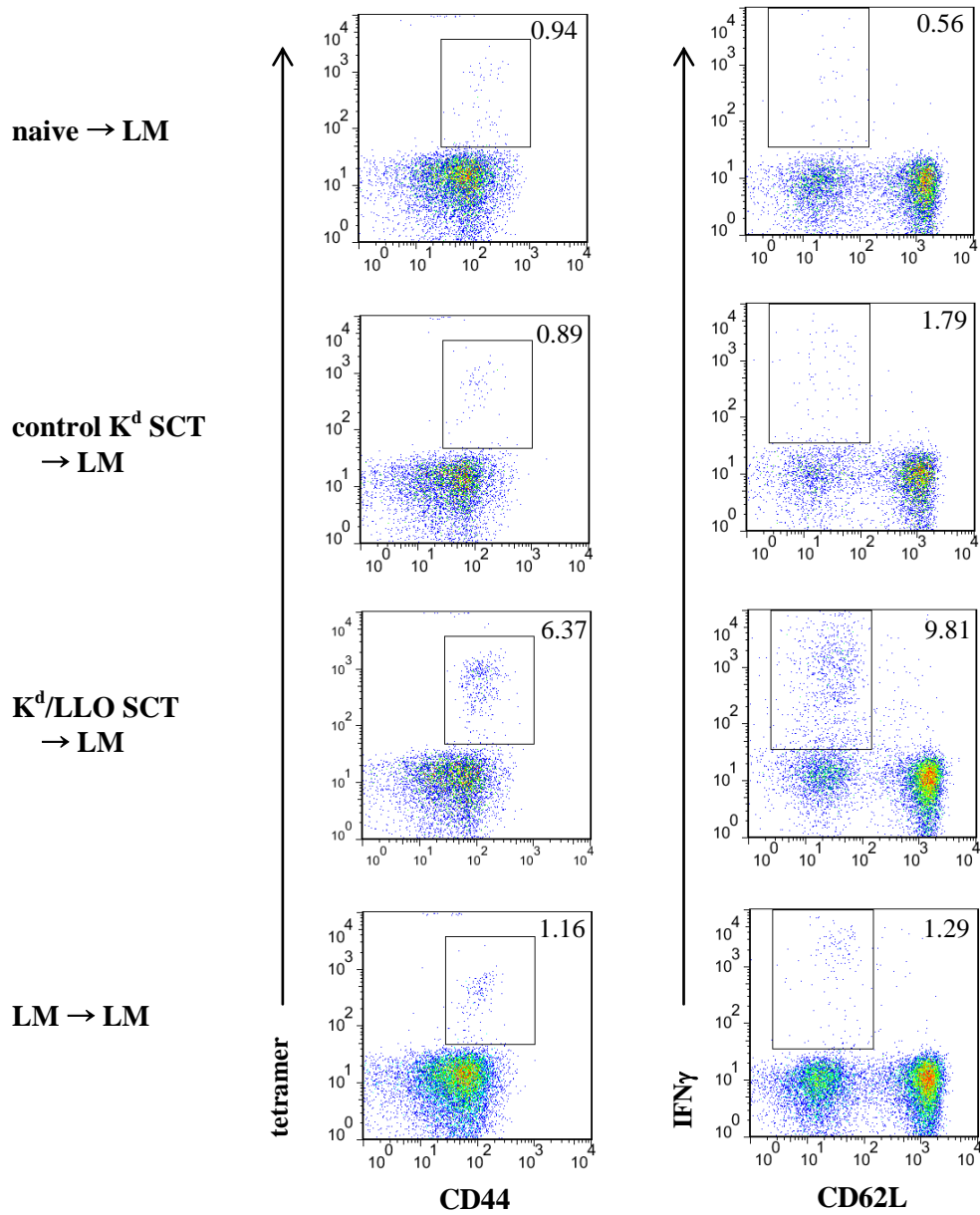
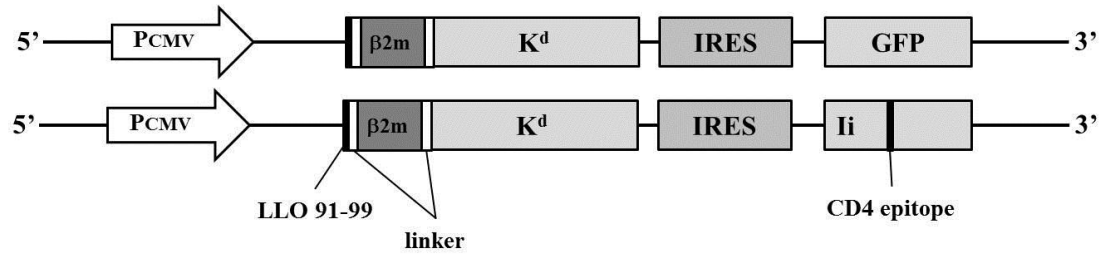


Figure 19. A SCT DNA vaccine develops functional memory CD8⁺ T cells

A



B

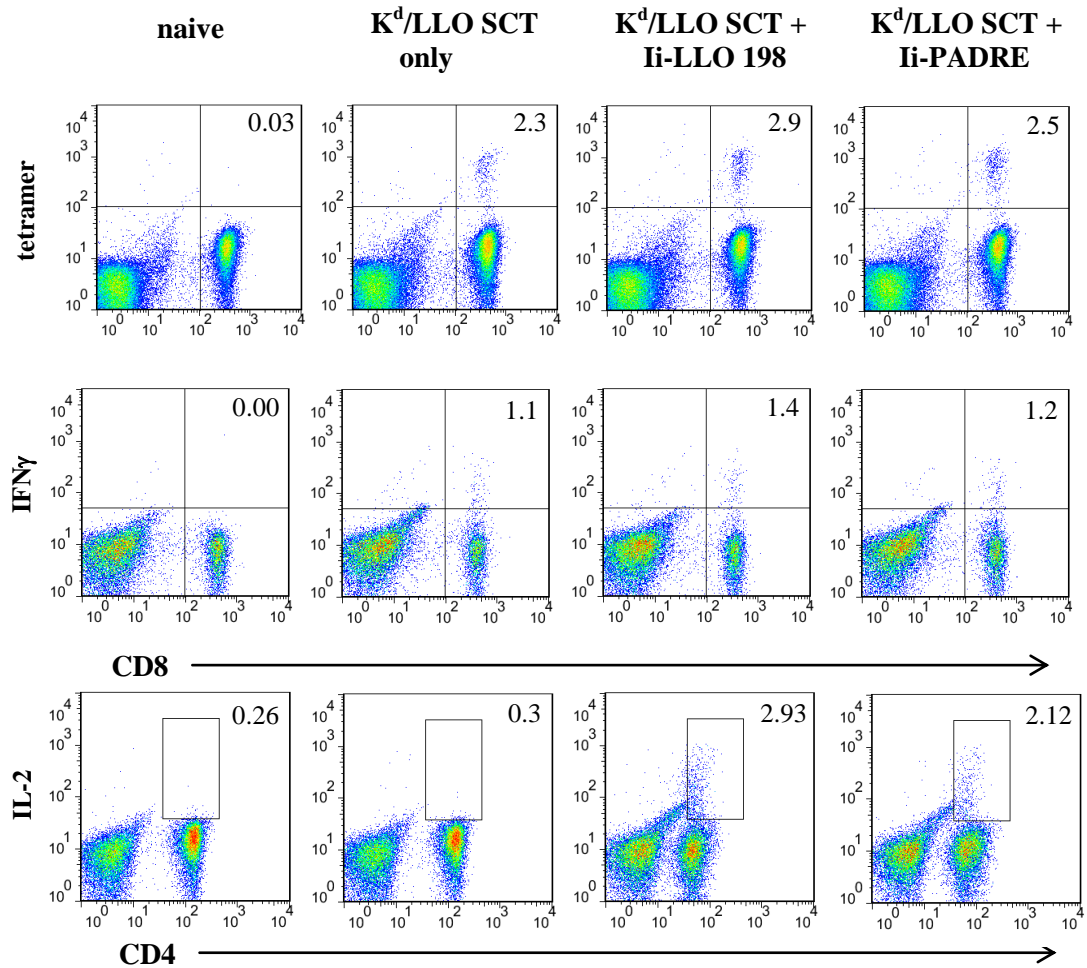
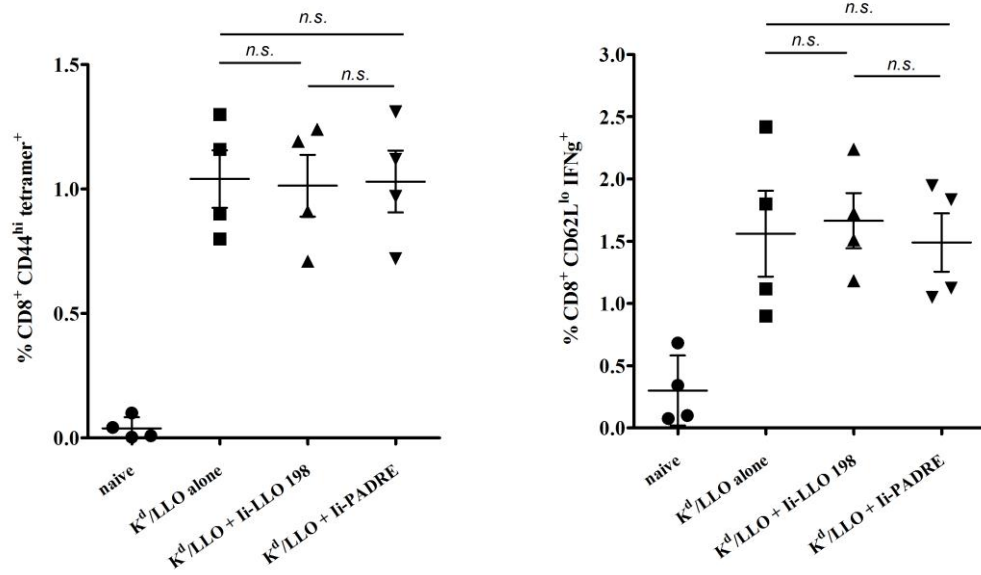


Figure 20. Co-expression of a CD4⁺ T cell epitope does not affect primary CD8⁺ T cell responses

A



B

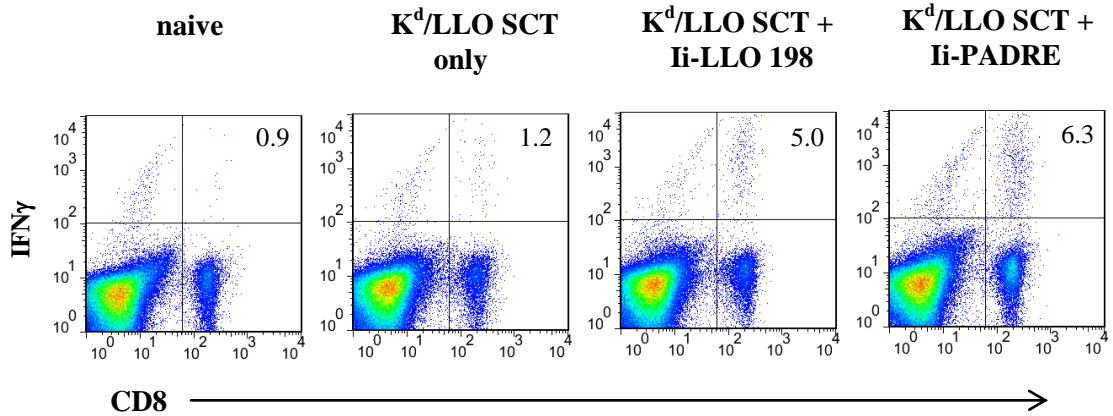


Figure 21. Co-expression of a CD4⁺ T cell epitope increases memory CD8⁺ T cell responses

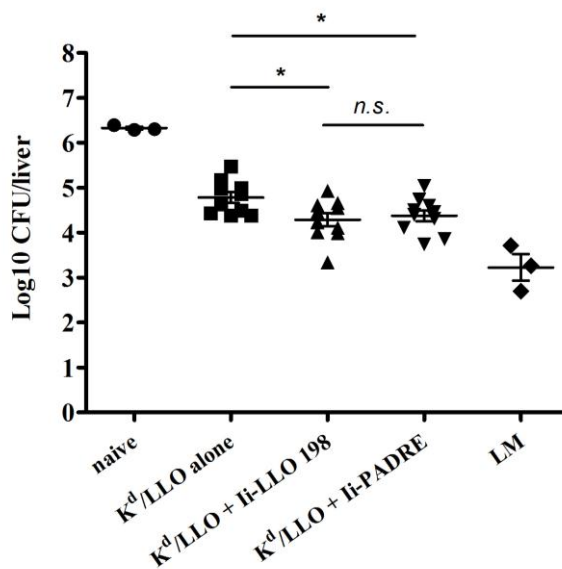
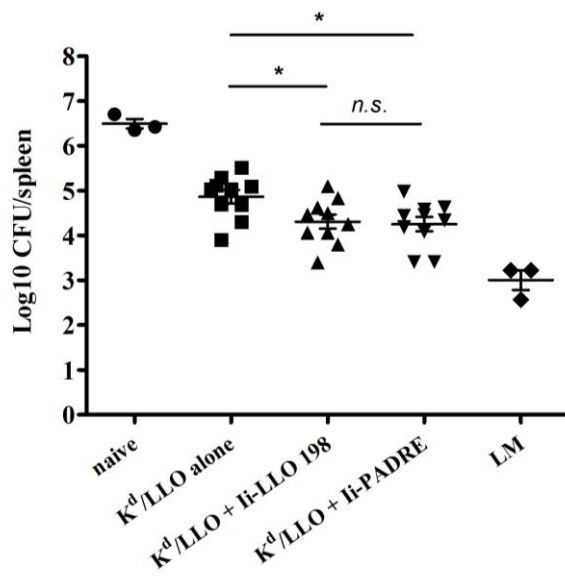


Figure 22. Co-expression of a CD4⁺ T cell epitope enhances the protective efficacy of a SCT DNA vaccine

Discussion

The SCT format has been amenable to different MHC I/peptide complexes, both murine and human, and it is one of the intriguing properties of SCTs. Here, we add to the list a SCT with the H-2K^d haplotype, confirming the potential use of SCTs in clinical applications. Like other SCTs previously reported, K^d/LLO₉₁₋₉₉ SCTs were properly folded and expressed at the cell surface after transfection and activated T cells *in vitro* and primed peptide-specific CD8⁺ T cells *in vivo*. This supports the universal application of SCTs and therefore the potential as a DNA vaccine platform.

I demonstrate that K^d/LLO₉₁₋₉₉ SCT DNA vaccination provides protection against lethal *L. monocytogenes* infection. A partial protection by CTLs specific for LLO 91-99 was previously shown in the study where CTLs from mice vaccinated with plasmid DNA encoding the LLO 91-99 epitope were *in vitro* expanded and adoptively transferred into naïve mice prior to *L. monocytogenes* challenge [132]. As discussed in Chapter 1, SCT-based DNA vaccines have been proven more effective at generating CD8⁺ T cell immunity than epitope-only DNA vaccines due to incorporation of a preprocessed and preloaded peptide [21, 30, 31]. We expect that DNA vaccination with K^d/LLO₉₁₋₉₉ SCTs would be more efficacious at conferring protection than a plasmid encoding LLO 91-99 and it will be interesting to compare these different approaches directly.

Generation of functional memory responses is essential to develop successful vaccines against pathogens and considerable effort has been made in developing strategies to induce high frequencies of memory T cells [133]. I showed that DNA vaccination with K^d/LLO₉₁₋₉₉ SCTs generates functional memory CD8⁺ T cells. In fact,

K^d/LLO₉₁₋₉₉ SCT DNA vaccine developed more memory CD8⁺ T cells and a better recall response than immunization with a low dose of live *L. monocytogenes*. But, the SCT DNA vaccine failed to provide mice the same level of protection as live bacteria-immunization. This might be because LLO 91-99 is just one of the many immunodominant epitopes of *L. monocytogenes* in BALB/c mice. Although LLO 91-99 seems most immunodominant among many others, the immunodominance is not absolute. For example, p60 217-225 derived from p60, a murein hydrolase secreted by bacteria into the cytosol, induces a slightly smaller but substantial CD8⁺ T cell response than LLO 91-99 [113, 114]. Also, other immune components besides CD8⁺ T cells play a role in controlling *L. monocytogenes* infection. For example, neutrophils and macrophages are thought to be the principal mediators of the killing of *L. monocytogenes* at early infection [134-136]. The SCT DNA vaccine is very potent to prime CD8⁺ T cells but it alone may not be sufficient to activate all the players involved in pathogen infection. For this reason, SCTs should be considered in a composite vaccine targeting multiple aspects of the immune system.

Our study shows that SCT DNA immunization induces a primary CD8⁺ T cell response independently of CD4⁺ T cells and it alone can generate functional memory CD8⁺ T cells that provide protection against infection. The presence of CD4⁺ T cell help improved the recall response and protective efficacy marginally. In the literature, there has been agreement that primary CD8⁺ T cell responses do not depend on CD4⁺ T cell help [102, 103, 137], which is consistent with our results. However, role of CD4⁺ T cell help for the generation of stable, protective CD8⁺ T cell memory is still controversial. In

the studies supporting a requirement for CD4⁺ T cell help for the generation of CD8⁺ T cell memory [101-103, 119], CD8⁺ T cells developed in the absence of CD4⁺ T cells using MHC class II- or CD4-knockout mice, whereas CD4⁺ T cells were present during SCT-induced CD8⁺ T cell generation in our study. Indeed, Bevan *et al.* demonstrated that effector CD8⁺ T cells became functionally impaired after transfer into MHC II-deficient recipients, but not into wild-type recipients [119]. My results that co-expression of CD4⁺ helper T cell epitopes increased secondary CD8⁺ T cell responses and protective efficacy support a crucial role of CD4⁺ T cells for the maintenance of memory CD8⁺ T cells [119]. Additionally, the similar extent of augmentation of CD8⁺ T cell responses by LLO 189-201 and PADRE suggest that CD4⁺ T cell function is not antigen specific. Our results are consistent with the study by T. C. Wu *et al.* where co-administration of Ii-PADRE DNA with K^b SCT DNA encoding a tumor epitope further enhanced generation of antigen-specific CD8⁺ T cells and anti-tumor effects against tumor challenge. However, it was not identified in this study whether the activated CD4⁺ T cells affected primary or memory CD8⁺ T cell responses [41].

The mechanism through which CD4⁺ T cells provide help for memory CD8⁺ T cells has not been elucidated. In the cytotoxic T cell response to noninfectious agents such as immunization with protein antigens, activation of CD4⁺ T cells is important in maturation of the antigen presenting cells so that it can promote a CD8⁺ T cell response whether CD4⁺ T cells function solely via activation of the antigen presenting cells through CD40-CD40L interaction or also via direct CD4-CD8 T cell interaction [138-140]. Thus the amount of danger signals produced by the immunization seems to be

important. Accordingly, in the CTL response to virulent pathogens, the generation of memory CD8⁺ T cell precursors is CD4⁺ T cell independent [141, 142]. One of the mechanisms for the immune responses by DNA vaccines is the innate responses directed against the plasmid itself. Because the plasmid is of bacterial origin, its sequences contain CpG oligodeoxynucleotide motifs that bind the pattern recognition receptor Toll-like receptor 9 (TLR9), which is constitutively expressed on dendritic cells, with a resultant augmentation of the immune response against the antigen encoded by the plasmid [143, 144]. Although the role of TLR9 in DNA vaccines is still inconsistent between studies [145, 146], the role of the CpG motifs in activating DCs may be important for generating T cell responses with DNA vaccines.

We hypothesize that SCT DNA immunization may not largely depend on CD4⁺ T cell help because of the adjuvant effect of CpG motifs from bacterial plasmid and/or high density epitope/MHC I expression at the cell surface. It has been reported that gene-gun administration of DNA stimulates a type 2 immune response due to the low amount of DNA injected, consequently fewer CpG motifs, whereas a type 1 immune response is critical to clear intracellular bacteria like *L. monocytogenes* [147-149]. However, our data show that SCT DNA vaccination using the gene-gun method can provide protection against *L. monocytogenes*. We speculate that it is likely that the high density expression of antigens at the cell surface using a SCT format overcomes the limited adjuvant.

In conclusion, our study demonstrates that SCTs can serve as a potent platform for DNA vaccines to develop CD8⁺ T cell immunity in various disease models including

virus as well as bacterial infection. Furthermore, our combined WNV and Listeria data demonstrate that SCT DNA vaccines are largely CD4 helper cell independent.

Chapter 4.

Improvement of SCT-based DNA vaccines

Introduction

Vaccination with plasmid DNA encoding a SCT has been shown to be superior for eliciting CD8⁺ T cell responses compared with DNA encoding an immunodominant peptide or the unprocessed protein from which the immunodominant peptide is derived [21, 30, 31]. However, the capacity of a SCT may be further improved by increasing stability of the SCT at the cell surface or targeting its expression to cell types critical for T cell priming. Improving peptide anchoring within the SCT is especially relevant when the antigenic peptide has very low affinity. Although a weak binding peptide, such as the p5Y variant of OVA_p, was used to make an SCT detected by OT-1 T cells, this SCT was more susceptible to peptide displacement than an SCT incorporating the native OVA_p [23]. These comparisons demonstrated that SCTs incorporating tight binding peptides were more stable suggesting they may also make better vaccines.

Our lab, in collaboration with the Fremont lab, has taken a structure based approach to re-engineer the SCT format to better accommodate a peptide in the peptide binding groove of MHC I. The crystal structure of the H-2K^b/OVA_p SCT showed that the anchoring of the C-terminus of the OVA peptide within the F pocket of K^b was disrupted [25]. More specifically, the peptide-β2m linker extending from the C terminal peptide residue disrupts the canonical hydrogen binding network conserved among all published structures of MHC I/protein complexes. Most significantly, a protrusion of the peptide-

β 2m linker was imposed by the highly conserved MHCI residue Tyr-84 that is integrally involved in C terminal peptide anchoring. These observations of the SCT structure explain why the K^b/OVAp SCT is more susceptible to peptide exchange than native K^b/OVAp complexes [22]. To improve linker accommodation and peptide binding with the SCT, a disulfide bond judiciously incorporated between the linker and a residue at the C-terminal end of the peptide binding groove of heavy chain (disulfide trap- or dt- SCT) enhanced the stability of the original K^b/OVAp SCT while preserving TCR interactions [23-25]. Here, I examined whether a disulfide trap can improve SCTs that are poorly recognized by T cells. Collaborative efforts of the Hansen, Diamond, and Fremont labs and others have published immunodominant WNV epitopes presented by H-2K^b molecules of C57BL/6 mice to CD8⁺ T cells [72, 73]. WNVp3, IALTFLAV, is one of the immunodominant CD8⁺ T cell epitopes that binds to H-2K^b and is processed from the viral E protein. A H-2K^b/WNVp3 SCT was constructed and a high level of surface expression of this SCT was achieved after transfection *in vitro*. Surprisingly, the SCT was not recognized by peptide-specific CD8⁺ T cells. This failure was surprising because our lab and others have reported the universal application of the SCT format to all MHC I/peptide complexes studied thus far. These reported SCTs included 3 made with K^b and different antigenic peptides [18]. It is noteworthy that WNVp3 is not a particularly avid binder compared to SIINFEKL of ovalbumin that also binds to H-2K^b. Thus, a K^b/WNVp3 dtSCT was considered a good model to determine whether a difficult SCT can be improved by incorporating a disulfide trap.

Targeting of delivery, not just to the antigen processing pathway but to particular cells or subsets of cells is an important factor for increasing the potency of vaccines. It can be achieved better with DNA plasmids as vaccine vectors which are relatively easy to manipulate. However, the mechanism by which antigens are presented after DNA vaccination is controversial. While some studies suggested direct presentation where transfected APCs, i.e. dendritic cells (DCs), trafficking to the draining lymph nodes express and present antigens to T cells [49], many studies have speculated that cross-presentation is involved in priming T cells following DNA vaccination [50, 51, 150-152]. If T cell priming occurs via cross-presentation of antigens after DNA vaccination, SCTs would still induce specific T cells but it is not clear why they should be better than a peptide or a protein as reported [21, 30, 31]. If the antigen with the SCT is indeed cross-presented, it is possible that the SCT may only stabilize the peptide within the original cell taking up the DNA or that a mechanism of cross-presentation involves the transfer of the entire SCT complex. To probe the mechanism by which antigen is presented by the SCT, we used a dtSCT and an original SCT using peptides that cannot be cross-presented.

In this chapter, I demonstrated that K^b/WNVp3 SCT became more resistant to replacement by exogenous competitor peptides and its recognition by T cells improved with a disulfide trap. Also my data showed that the SCT with a weak binding peptide OVAp5Y, which did not prime T cells when introduced as cDNA, induced CD8⁺ T cell responses after DNA vaccination, indicating SCTs are presented as intact molecules.

Materials and Methods

1. SCT construct

SCTs consist of the leader sequence of β_2m followed by the epitope sequence, then a linker of 15 residues $(G_4S)_3$, and the mature mouse β_2m sequence. The β_2m was followed by the second linker of 20 residues $(G_4S)_4$ and the heavy chain of H-2K^b. To generate H-2K^b/WNVp3 SCT, H-2K^b SCT with SIINFEKL peptide was used as a template. Nucleotide oligos encoding West Nile virus peptide, p3 (IALTFLAV), flanked by AgeI and NheI restriction enzyme sites were designed; 5'-CCGGTTTGTATGCTATCGCCCTCACCTTCCTAGCCGTCGGAGGAGGTG -3' and 5'-CTAGCACCTCCTCCGACGGCTAGGAAGGTGAGGGCGATAGCATACAAA -3'. Oligos were annealed to form double strands and inserted into the pIRESneo.OVA.mB2mb.etK^b cut with AgeI and NheI. Then the fragment containing p3 sequence was excised using NotI and EcoRI, and inserted into pMIN.OVA.mB2mb.K^b cut with the same restriction enzymes. To introduce a disulfide bond between the linker and the heavy chain, the second amino acid, glycine, of the first linker was mutated to cysteine and tyrosine at residue 84 of K^b heavy chain was also mutated to cysteine by site-directed mutagenesis. The correct sequence was confirmed by DNA sequencing using BigDye 3.1 (Washington University, St. Louis, MO).

Generation of HLA-A2/WNV SVG9 SCTs was described in Chapter 2.2. The original and disulfide trap SCT of H-2K^b/OVAp5Y have been previously described [21, 23].

2. Generation of stable cell line expressing SCTs

Transient transfection was performed on 293T human embryonic kidney cells using Lipofectamine 2000 (Invitrogen) to generate retrovirus-containing supernatants for infection and mouse fibroblast LM1.8 cells were used for retroviral transduction of SCTs. SCT-expressing cells were sorted through flow cytometry post transduction. All cells were maintained in DMEM (Invitrogen) supplemented with 10% FBS (HyClone Laboratories, Logan, UT), 2mM L-glutamine, 0.1mM non-essential amino acids, 1.25mM HEPES, 1mM sodium pyruvate, and 100U/mL penicillin/streptomycin (all from the Tissue Culture Support Center, Washington University School of Medicine, St. Louis, MO).

3. Antibodies and flow cytometry

Cell culture supernatant containing the following monoclonal antibodies were used to stain SCTs at the surface; anti-H-2K^b (B8-24-3), anti-K^b/OVA_p (SIINFEKL) (25-D1.16), anti-H-2D^k or K^k (15-5-5). About 10⁶ cells per sample were incubated on ice in microtiter plates with primary mAb for 30min. After washing with PBS containing 1% BSA, PE-conjugated goat anti-mouse IgG (BD Pharmingen) was added as secondary Ab for 20min. Analyses were performed using a FACSCalibur (BD Biosciences). Dead cells and debris were excluded from analysis on the basis of forward-angle and side-scatter light gating. Data were analyzed using FlowJo software (Tree Star).

4. Generation of a CD8⁺ T cell line

For generation of bulk CTL clones, C57BL/6 mice were infected subcutaneously by footpad injection with 10^2 PFU of WNV (strain 3000.0259). 4 weeks after infection, splenocytes were harvested, washed with medium (RPMI 1640 containing 10% FBS), and resuspended at 7.5×10^6 cells/mL. In parallel, splenocytes from uninfected congenic TAP^{-/-} C57BL/6 mice were harvested, depleted of erythrocytes with ACK buffer (0.15 M NH₄Cl, 10 mM KHCO₃, 0.1 mM Na₂EDTA), washed with RPMI medium, irradiated (2000 rad), and counted. TAP^{-/-} splenocytes were resuspended at 3.5×10^6 cells/mL and 2 μ M peptide, WNVp3, was added. CTL were generated by incubating immune splenocytes with peptide-pulsed TAP^{-/-} splenocytes at a final peptide concentration of 1 μ M in a 24-well tissue culture plate. Seven days later, CTL were restimulated with 3.5×10^6 irradiated TAP^{-/-} splenocytes pulsed with 1 μ M WNVp3. At day 14 and thereafter, bulk CTL against WNVp3 were stimulated at weekly intervals with irradiated wild-type splenocytes, 1 μ M peptide, and 10 U/mL rIL-2.

5. CTL assay

At day 5 after stimulation, CTLs were assayed for their ability to lyse target cells. To perform a ⁵¹Cr release assay, target cells were labeled with 0.2 mCi of ⁵¹Cr (PerkinElmer Life Sciences, Waltham, MI) for 1 hour and incubated with CTLs with or without peptides for 4 ½ hours at 37°C. To determine maximum lysis, Triton-X 100 was added to control wells. To determine spontaneous lysis, target cells were incubated without CTLs. Supernatants were collected and read by an Isomedic γ -counter (ICN Biomedicals). The percentage of ⁵¹Cr release was calculated by [(experimental ⁵¹Cr

release-spontaneous ^{51}Cr release)/(maximum ^{51}Cr release-spontaneous ^{51}Cr release)]
x100.

6. Peptide competition assay

For the competition assay, serially diluted SIINFEKL peptide from 250 to 0.24 μM was incubated with 2×10^5 LM1.8 cells expressing SCTs in a 96 well round-bottom plate for 4 hours at 37°C. Cells were then washed three times with PBS containing 1% BSA and stained with B8-24-3 for total K^b or 25-D1.16 for K^b/SIINFEKL.

7. Mice and DNA immunization

For the immunization of HLA-A2/WNV SVG9 SCTs, HHDII transgenic (B6; Cg-B2M^{tm1Unc} H2-D1^{tm1Bpe}-Tg (HLA-A/H2-D/B2M)1Bpe) mice were used (described in Chapter 2.1). For the immunization of H-2K^b/OVAp or H-2K^b/WNVp3 SCTs, C57BL/6 mice were purchased from the Jackson Laboratory (Bar Harbor, Maine). All mice were bred and housed at the Washington University Animal Facility and all animal procedures were approved by the Animal Studies Committee at Washington University.

DNA-coated gold particle-mediated DNA vaccination was performed using a helium-driven gene gun (Bio-Rad). DNA-coated gold particles (diameter, 1 μm) and cartridges were prepared according to the manufacturer's instructions so that each cartridge contained 1 μg of DNA. The DNA-coated gold particles were delivered to the shaved abdomen of mice with a discharge pressure of 200 psi. Mice were immunized with 4 μg of DNA three times at 3 day intervals.

8. IFN γ ELISpot assay

Spleens were harvested from mice 5 days after the last DNA immunization. After RBC lysis, single cell suspensions were incubated with 1 μ g/mL SVG9 or control peptides in a PVDF filter plate (Millipore) pre-coated with 15 μ g/mL of anti-IFN γ capture antibody (AN18, Mabtech Inc, Cincinnati, OH). After overnight stimulation, cells were removed and the plate was incubated with biotinylated anti-IFN γ detection antibody (R4-6A2) and subsequently with streptavidin-ALP. Then spots were developed by adding substrate solution (BCIP/NBT) and counted with an automated ELISpot reader.

Chapter 4.1

Trapping peptide by disulfide bond can improve difficult SCTs

Results

Peptide binding groove of K^b/WNVp3 SCTs is readily accessible

K^b/WNVp3 SCTs were expressed in LM1.8 cells, which express H-2^k endogenously, by viral transduction. SCTs were properly folded and expressed at the cell surface, which was determined by staining with mAb specific for K^b with a folded conformation (Fig. 23A). To examine whether SCTs are recognized by peptide-specific CD8⁺ T cells, a stable cell line was generated after sorting of high K^b expressers by FACS. After sorting, SCT (K^b) expression at the cell surface was as high as the expression level of endogenous MHC I, D^k (Fig. 23A). However, K^b/WNVp3 SCTs showed no killing by WNVp3-specific CD8⁺ T cells (Fig. 23B). It was surprising that SCTs were not recognized by T cells despite their high surface expression and properly folded conformation. Thus we speculated that the peptide in the peptide binding groove of SCT may be rapidly displaced by other peptides and/or extrusion of the peptide-β2m linker somehow obstructs optimal interaction with the TCR. To examine how secure the epitope binding to K^b in SCTs is, I performed a peptide competition assay using OVA_p, SIINFEKL. If the binding of WNVp3 to the binding groove of heavy chain is stable, peptides added exogenously would be able to displace WNVp3 and bind to MHC of SCT only at high concentration. Although it was not as easily accessible as K^b alone, WNVp3 in K^b/WNVp3 SCT was certainly being displaced by exogenous SIINFEKL at as low a

concentration as 2 μ M (Fig. 23C). Thus, weak binding of the peptide in the SCT is likely one reason for the failure of T cell recognition.

Securing WNVp3 into the peptide binding groove of the SCT with a disulfide-trap potentiates CTL recognition

It is likely that insecurely bound peptide and protrusion of the attached linker hinders the proper engagement of SCTs with TCR. We knew from western blot analysis that the majority of K^b/WNVp3 SCTs are still expressed as one polyprotein with a covalently linked β 2m (data not shown). Thus, to lock the peptide in the binding groove of the MHC heavy chain, a disulfide trap was introduced. A glycine residue at the first linker and a tyrosine residue, Y⁸⁴, in the MHC I heavy chain, which is located at the C-terminal end of the peptide-binding cleft, were mutated to cysteine so that a disulfide bond was formed between the two residues (Fig. 24). This disulfide bond would close the C-terminal end of the binding groove and secure the peptide [23, 25]. The addition of a disulfide bond did not increase the expression of K^b/WNVp3 dtSCT at the surface in comparison with K^b/WNVp3 SCTs as analyzed by flow cytometry (Fig. 25A). However, K^b/WNVp3 dtSCTs were resistant to displacement by exogenous OVAp (Fig. 25B) and now peptide-specific CD8⁺ T cells were able to lyse cells expressing K^b/WNVp3 dtSCTs, indicating that the SCT was recognized (Fig. 25C). Thus, our data suggest that engineering with a disulfide trap can increase peptide occupancy and recognition of SCTs by T cells. Interestingly, these data represent the first example we are aware of where a disulfide trap is required for CD8⁺ T cell detection of an SCT. Mechanistically, this is a

very intriguing observation, because as shown in the next section, an SCT made with a poor binding variant of the OVA_p is detected by CD8⁺ T cells with and without a disulfide trap. Implications of these combined findings are included the Discussion section of this chapter.

Figure Legends

Figure 23. K^b/WNVp3 SCTs are expressed but do not activate peptide-specific CD8⁺ T cells

LM1.8 cells expressing K^b/WNVp3 SCTs were generated by virus transduction and selection through FACS sorting. (A) Cell surface expression of K^b/WNVp3 SCTs. Cells were stained with anti-K^b mAb (B8-24-3, solid line) or anti-K^k mAb (15-5-5, dotted line). A shaded histogram shows staining of non-transduced LM1.8 cells with anti-K^b mAb. (B) LM1.8 cells expressing K^b or K^b/WNVp3 SCTs were used as targets in a ⁵¹Cr-release assay with WNVp3-specific CTLs. For a control, K^b-expressing LM1.8 cells pulsed with WNVp3 were also used as targets. (C) LM1.8 cells expressing K^b (circle) or K^b/WNVp3 SCTs (square) were incubated with serially diluted SIINFEKL peptide from 250 to 0.24μM for 4 hours. Total amount of K^b at the cell surface was measured by staining with anti-K^b mAb (B8-24-3) and the amount of K^b/SIINFEKL complexes were measured by staining with anti-OVAp/K^b mAb (25-D1.16). Data were presented as the percentage of K^b/SIINFEKL molecules of total K^b molecules at the cell surface.

Figure 24. Diagram of the H-2K^b/OVAp dtSCT

Figures were taken from the article, ‘Structural engineering of p MHC reagents for T cell vaccines and diagnostics’ by Mistaksov V. and Truscott S. [25]. (A) Diagram of K^b/OVAp SCTs with a disulfide trap (dtSCT). In the ribbon diagram, OVAp and the peptide-β2m linker were rendered as ball-and-stick models and colored as follows; OVAp and linker carbon atoms, yellow and orange, respectively; nitrogen atoms, blue; oxygen atoms, red.

The possible conformation for the $\beta 2m$ -heavy chain linker was represented as small orange balls. (B) CPK model of the surface of the peptide binding grooves of K^b /OVAp SCT (*left*) and K^b /OVAp dtSCT (*right*). The solvent-accessible surfaces of the peptide-binding grooves were displayed as blue dotted surface. K^b pocket locations were indicated underneath each surface. The peptide- $\beta 2m$ linker residues were labeled L1 through L6 or L9.

Figure 25. A disulfide trap improves stability and T cell recognition of K^b /WNVp3 SCTs

(A) Cell surface expression of K^b /WNVp3 dtSCTs. LM1.8 cells were transfected with K^b /WNVp3 SCTs with (dotted line) or without a disulfide trap (solid line) and stained with anti- K^b mAb (B8-24-3). A shaded histogram shows staining of untransfected LM1.8 cells with anti- K^b mAb. (B) LM1.8 cells expressing K^b (circle) or K^b /WNVp3 dtSCTs (square) were incubated with serially diluted SIINFEKL peptide from 250 to $0.24\mu\text{M}$ for 4 hours. Total amount of K^b at the cell surface was measured by staining with anti- K^b mAb (B8-24-3) and the amount of K^b /SIINFEKL complexes were measured by staining with anti-OVAp/ K^b mAb (25-D1.16). Data were presented as the percentage of K^b /SIINFEKL molecules of total K^b molecules at the cell surface. (C) LM1.8 cells expressing K^b , K^b /WNVp3 SCTs, or dtSCTs were used as targets in a ^{51}Cr -release assay with WNVp3-specific CTLs. For a control, K^b -expressing LM1.8 cells pulsed with WNVp3 were also used as targets.

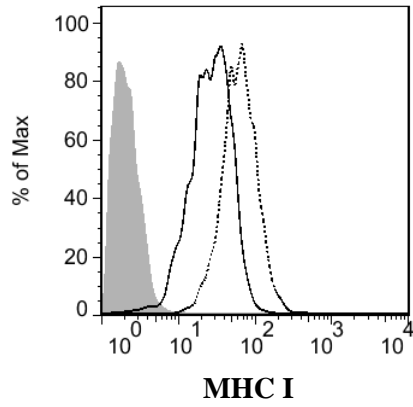
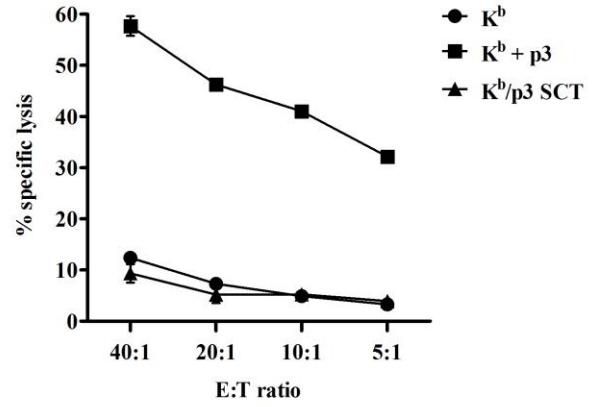
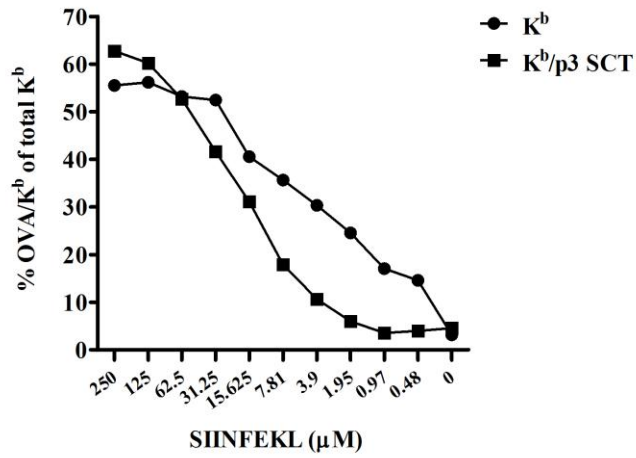
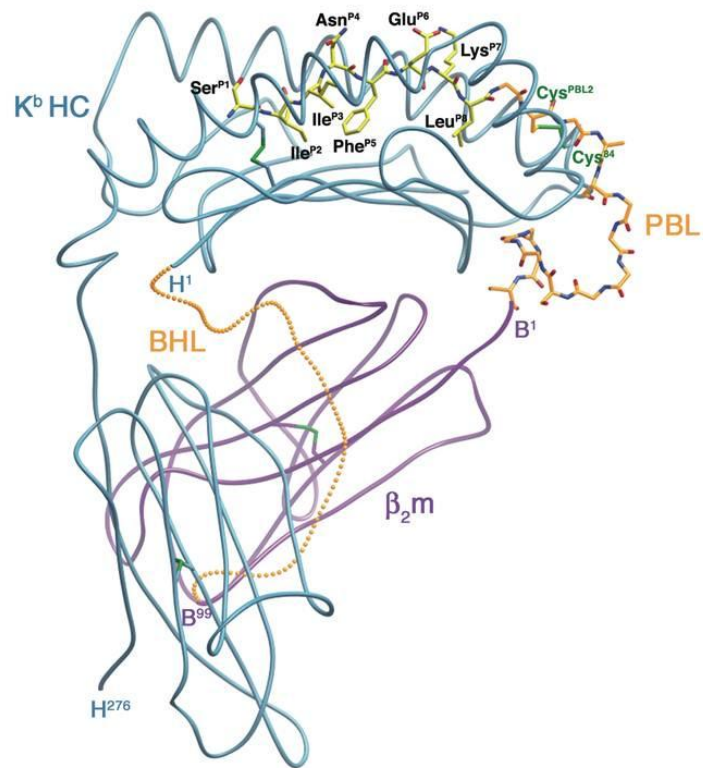
A**B****C**

Figure 23. K^b/WNVp3 SCTs are expressed but do not activate peptide-specific CD8⁺

T cells

A



B

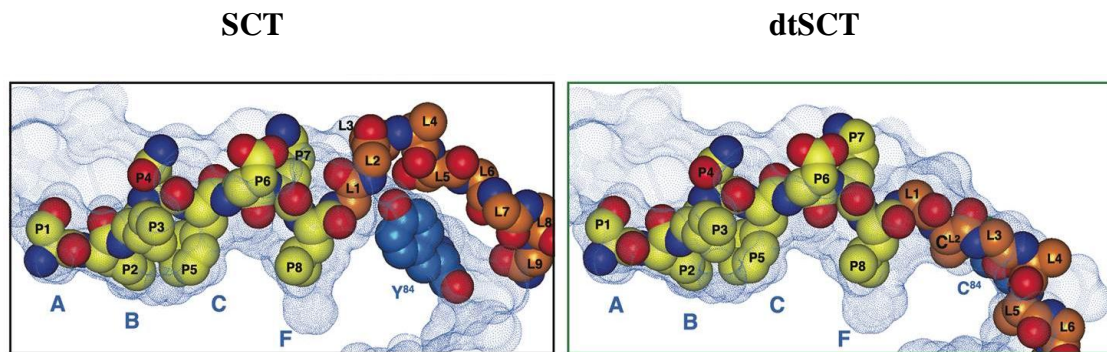
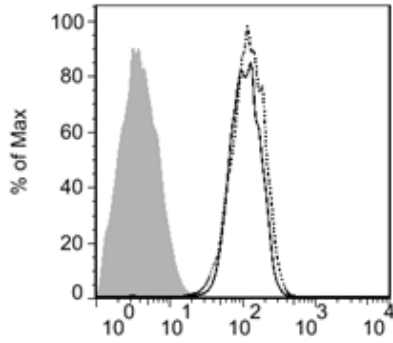
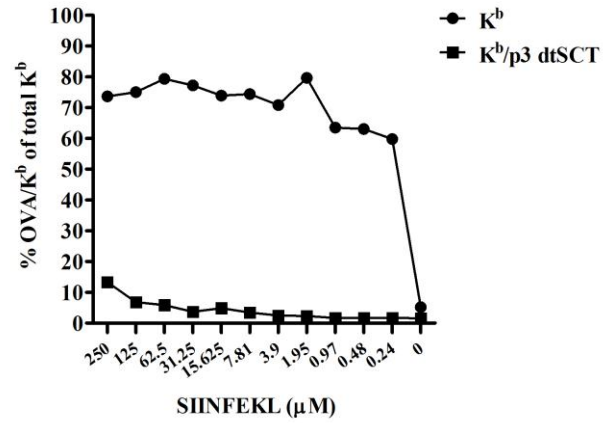


Figure 24. Diagram of the H-2K^b/OVAp dtSCT

A



B



C

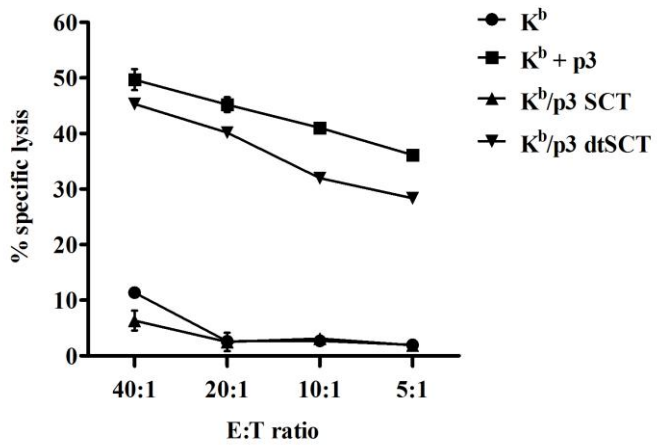


Figure 25. A disulfide trap improves stability and T cell recognition of K^b/WNVp3 SCTs

Chapter 4.2

SCTs are presented as intact structures

Results

Chimeric HLA-A2/D^b α 3 SCTs are better than intact HLA-A2 SCTs for induction of CD8⁺ T cells by DNA immunization in HHDII mice

In Chapter 2.2, I showed that the SCT of a West Nile virus epitope SVG9 and HLA-A2 induces epitope-specific CD8⁺ T cell responses after DNA immunization in HLA-A2 transgenic (HHDII) mice. Because the HHDII mouse expresses no human CD8 but does express mouse CD8 co-receptors and chimeric HLA-A2 molecules, in which the α 3 domain is replaced with that of H-2D^b, SCTs for DNA immunization were also constructed to have the same chimeric A2/D^b α 3. It has been reported that the interaction between a CD8 co-receptor of a TCR complex and α 3 domain of MHC I heavy chain is required to prime naïve CD8⁺ T cells and there is some species specificity in the interaction of CD8 with the α 3 domain of the class I molecule [153-155]. Especially, Engelhard *et al.* demonstrated that CTL lines from HLA-A2 transgenic mice preferentially recognize class I molecules with a murine α 3 domain at low concentrations of peptide *in vitro* [154]. Thus, it is expected that a chimeric A2/D^b α 3 SCT DNA vaccine would prime naïve CD8⁺ T cells better than an intact HLA-A2 SCT in the HHDII HLA-A2 transgenic mouse, but only if the SCTs remain intact for presentation. However, if the SCTs require processing and re-loading onto the endogenous MHC class I of an APC not taking up the DNA, i.e. cross-presentation, both chimeric A2/D^b α 3 SCTs and intact A2

SCTs would result in priming CD8⁺ T cells equally in the transgenic mice. To determine whether SCTs are presented as intact molecules or cross-presented to T cells after DNA vaccination, I immunized HHDII mice with either chimeric A2/D^b α 3/ or intact A2/SVG9 SCT DNA using the gene gun, as described in the previous chapters, and compared IFN γ responses of CD8⁺ T cells upon *in vitro* peptide re-stimulation at 5 days post immunization. The results show that the chimeric A2/D^b α 3/SVG9 SCTs induced stronger CD8⁺ T cell responses than intact A2/SVG9 SCTs, indicating SCTs were presented to T cells as intact molecules (Fig. 26).

H-2K^b/p5Y SCTs, but not p5Y, induce OVA-specific CD8⁺ T cells after DNA immunization

OVAp5Y, SIINYEKL, is an altered peptide ligand of SIINFEKL, that binds poorly to H-2K^b because of a mutation at position 5, an anchor residue for MHC I binding. Half-time for dissociation of SIINYEKL from K^b at the cell surface is 120 minutes while half-time of SIINFEKL is 360 minutes, indicating SIINYEKL has very low binding affinity to K^b [156]. But OVAp5Y is still recognized by SIINFEKL-specific OT-1 T cells in the context of K^b [157, 158]. Studies in our lab showed that K^b/OVAp5Y dtSCTs are expressed well at the cell surface after transfection and efficiently exclude exogenous competitor peptides from binding [23]. Thus, we speculated that a K^b/OVAp5Y dtSCT would be able to prime peptide-specific CD8⁺ T cells if it were presented intact following DNA immunization. We also speculated that the p5Y peptide from the K^b/OVAp5Y dtSCT DNA would be incapable of cross-presentation by a native K^b molecule due to its poor binding affinity. To test whether this was indeed the case, as a

control I immunized mice with DNA encoding the OVAp5Y peptide (kindly provided by Dr. Lijin Li). As shown in Fig 27, C57BL/6 mice were immunized with DNA encoding OVAp5Y, K^b/OVA SCTs, or K^b/OVAp5Y SCTs with or without a disulfide trap using gene gun. IFN γ production of OVA-specific T cells in the spleen upon *in vitro* peptide restimulation was measured at day 5. Indeed, OVAp5Y cDNA did not induce any detectable T cell responses, demonstrating the p5Y cannot be cross-presented. However, all three of the SCT DNA constructs induced equally strong OVA-specific CD8⁺ T cell responses (Fig. 27). Therefore, the data demonstrates that SCTs are presented as intact structures to T cells following DNA immunization.

H-2K^b/WNVp3 dtSCTs induce a more robust CD8⁺ T cell response than the H-2K^b/WNVp3 SCTs without disulfide trap after DNA immunization.

With the same logic as above, I compared K^b/WNVp3 SCTs and K^b/WNVp3 dtSCTs for their ability to induce peptide-specific CD8⁺ T cells after DNA immunization. C57BL/6 mice were immunized with K^b/WNVp3 SCTs or K^b/WNVp3 dtSCT DNA using the gene gun and T cell responses were assessed by measuring IFN γ production upon *in vitro* peptide restimulation. K^b/WNVp3 SCTs without a disulfide trap induced a few IFN γ -producing cells (Fig. 28), which was consistent with the observation that K^b/WNVp3 SCTs did not activate peptide-specific CD8⁺ T cells *in vitro* as described in Chapter 4.1. On the contrary, K^b/WNVp3 dtSCTs DNA immunization induced many more T cells producing IFN γ than K^b/WNVp3 SCTs. Thus all three of the above

experimental results in this section present cumulative evidence that SCTs are presented as intact molecules following DNA immunization.

Figure Legends

Figure 26. Chimeric HLA-A2/D^b α 3 SCTs induce stronger CD8⁺ T cell responses than intact HLA-A2 SCTs in HHDII mice

HHDII mice were immunized with chimeric A2/Db α 3/ or intact A2/SVG9 SCT DNA using gene gun as described above. At day 5 after the last immunization, splenocytes from each group were stimulated *in vitro* with SVG9 or irrelevant peptide overnight and IFN γ secretion was measured by ELISPOT. Error bars indicate SE of the experiment. The data presented are from one representative experiment of two performed independently with each group containing 4~5 mice. *, $p < 0.05$ (unpaired *t* test).

Figure 27. H-2K^b/OVAp5Y SCT DNA but not OVAp5Y cDNA immunization primes CD8⁺ T cells

C57BL/6 mice were immunized with OVAp5Y, control K^b SCTs, K^b/OVA SCTs, K^b/OVAp5Y SCTs or K^b/OVAp5Y dtSCTs using gene gun as described above. At day 5 after the last immunization, splenocytes from each group were stimulated *in vitro* with OVAp or irrelevant peptide overnight and IFN γ secretion was measured by ELISPOT. Error bars indicate SE of the experiment. The data presented are from one representative experiment of two performed independently with each group containing 4 mice. *n.s.*, not significant., *, $p < 0.05$ (unpaired *t* test).

Figure 28. H-2K^b/WNVp3 dtSCTs induce a more robust CD8⁺ T cell response than the H-2K^b/WNVp3 SCTs.

C57BL/6 mice were immunized with control K^b SCTs, K^b/WNVp3 SCTs, or K^b/WNVp3 dtSCTs using gene gun as described above. At day 5 after the last immunization, splenocytes from each group were stimulated *in vitro* with WNVp3 or irrelevant peptide overnight and IFN γ secretion was measured by ELISPOT. Error bars indicate SE of the experiment. The data presented are from one representative experiment of two performed independently with each group containing 4~5 mice. *, $p < 0.05$ (unpaired t test).

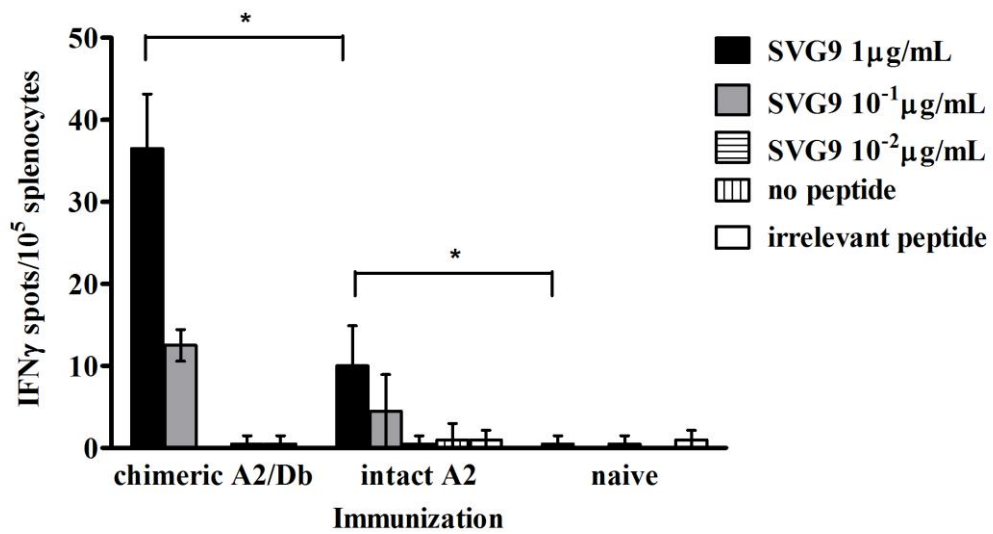


Figure 26. Chimeric HLA-A2/D^b α 3 SCTs induce stronger CD8⁺ T cell responses than intact HLA-A2 SCTs in HHDII mice

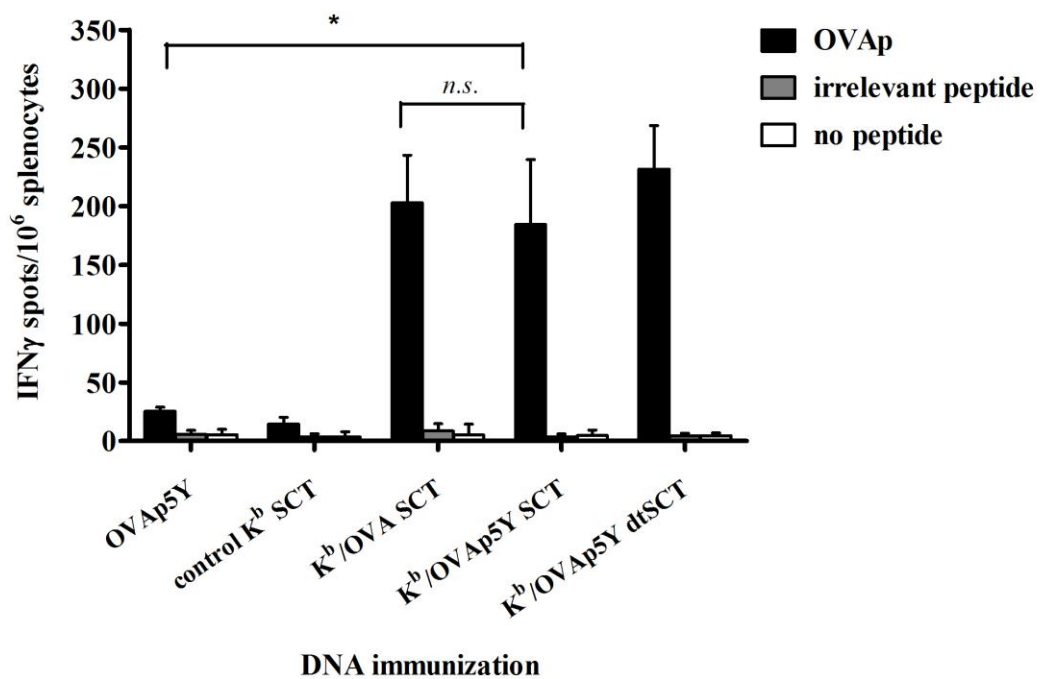


Figure 27. H-2K^b/OVAp5Y SCTs DNA but not OVAp5Y cDNA immunization primes CD8⁺ T cells

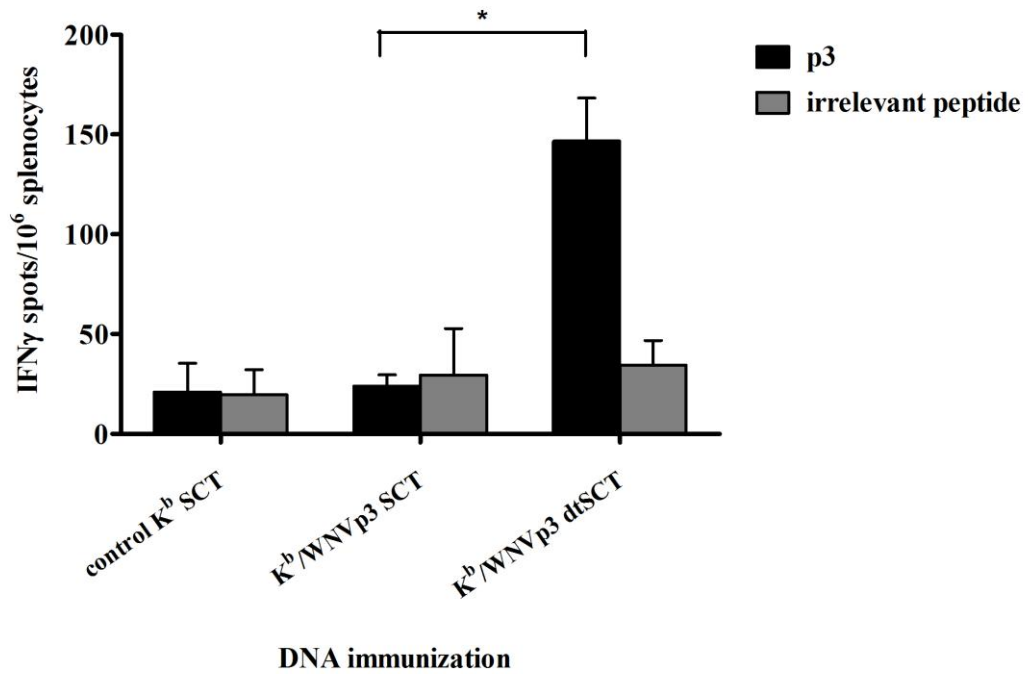


Figure 28. H-2K^b/WNVp3 dtSCTs induce a more robust CD8⁺ T cell response than the H-2K^b/WNVp3 SCTs.

Discussion

From the previous studies in our lab, we knew that the linker attached antigenic peptide in the SCT is constantly rebinding to the peptide binding groove of the MHC heavy chain [22, 23, 25]. Structural analyses in collaboration with the Fremont lab showed that the impaired peptide binding is due to the first linker of the SCT that extends beyond the peptide binding groove. Normally the F pocket in the MHC I heavy chain anchors the C terminus of the peptide through conserved interactions, but the first peptide- β 2m linker disrupts many of the conserved interactions. Despite this fact, the H-2K^b/OVAp SCT is more stable at the cell surface than native MHC I/peptide complexes and exhibits a high level of steady state peptide occupancy. This is because OVAp is a particularly high affinity binder and the covalently attached peptide is efficiently rebinding after dissociation occurs [22, 23]. Also the continuous rebinding of peptide does not seem to affect T cell recognition of K^b/OVAp SCT. However, our current study with a WNV epitope, WNVp3, showed that exogenous peptides can gain access to the peptide binding groove of K^b/WNVp3 SCTs even at a low concentration, implying peptide accommodation is severely impaired. Moreover, T cell recognition of SCTs was also impaired. It is not likely that the peptide is cleaved from the heavy chain because K^b/WNVp3 SCTs were expressed at high levels at the cell surface and were more resistant to displacement by exogenous OVAp than K^b/ β 2m with endogenous peptides. This result indicates the peptide binding groove of the K^b/WNVp3 SCT was occupied, but not necessarily with the linker attached peptide. Thus, the failure of the K^b/WNVp3 SCT to be detected by CTL could result from i) relatively low affinity of WNVp3 to K^b,

ii) hindrance of TCR engagement by peptide- β 2m linker extrusion, and/or iii) peptide registry shift due to the extended C terminus of the peptide. Regarding the first possibility, low affinity alone is not likely the explanation, because the OVAp5Y peptide is a poor binder yet the SCT incorporating p5Y peptide is detected by T cells. Regarding the second possibility, our lab previously showed from analysis of the crystal structure of K^b/OVAp SCT that the extruded peptide- β 2m linker traverses over the C terminal TCR proximal surface of the MHC α helix where a conserved TCR recognition region is [25]. Regarding the third possibility, peptide registry shift within the peptide binding groove of MHC has been proposed particularly for MHC class II which allows a wide range of peptide lengths, which vary between 13 and 17 amino acids although shorter or longer lengths are not uncommon, for binding because of the open-ended peptide binding groove [159-163]. Peptides are hypothesized to shift within the MHC class II peptide-binding groove, changing which 9mer register sits directly within the groove. For example, Goverman *et al.* demonstrated that processing of myelin basic protein (MBP) produces MBPAc1-18 peptide which utilizes two binding registers to bind I-A^u [162]. Also Kappler *et al.* demonstrated that I-A^b binds an immunogenic peptide variant stably by creating unique interactions, indicating MHC can bind peptide stably in more than one way [161]. Because in SCTs the peptide available for binding is extended by its covalently attached linker, it is possible that peptides bind the groove with different registers so that it cannot be recognized same by peptide-specific T cells.

Failure of the K^b/WNVp3 SCT to be recognized by T cells was overcome by introducing a disulfide trap in the area of the F pocket of the peptide binding groove. The

disulfide trap is engineered to bind the first linker to Y⁸⁴ at the C terminal end of the peptide-binding groove of heavy chain so that it locks in the linker-attached peptide and keeps the extrusion of the peptide and linker away from TCR interaction surface. Structural studies with H-2K^b/OVAp SCTs showed that the mutation of a heavy chain residue, Y⁸⁴, to make a disulfide bond, opens the C terminal end of the peptide-binding groove and allows the linker to freely extrude from the peptide-binding platform [22, 23, 25]. A SCT with a disulfide trap (dtSCT) was more stable and refractory to exogenous peptide binding than a SCT without a disulfide trap. Here, I found that the disulfide trap rendered K^b/WNVp3 SCT more resistant to exogenous peptide binding and potentiated recognition by T cells. Our finding is of importance in that it suggests a low affinity or suboptimal peptide can also activate T cells in the context of a dtSCT. Thus the dtSCT format has a great potential for broadening the application of SCT DNA vaccines for diseases in which critical antigenic peptides are weak binders to MHC. For example, many tumor associated antigens (TAA) show low immunogenicity because of low binding affinity to MHC I and this fact has limited the efficacy of cancer vaccines and immunotherapeutics [34]. A dtSCT strategy will increase the potency of a vaccine by increasing the level of MHC I/tumor epitope complexes on the antigen presenting cell surface.

Future improvements using SCT based vaccines will require a better understanding of the mechanism by which they present antigen. Indeed, the mechanisms by which DNA vaccines induce antigen specific immunity *in vivo* are under intense investigation. After the plasmid is delivered to the skin, subcutaneum or to the muscle

depending on the delivery method, it enters the nucleus of transfected cells using the host cellular machinery followed by expression of the antigen of interest [24]. Antigen presenting cells (APCs) play a dominant role in priming naïve antigen specific T cells by presenting MHC I/peptide complexes in combination with co-stimulatory molecules. Two models have been proposed for how APCs obtain and present antigens following DNA vaccination. It can be either direct transfection of professional APCs by the plasmid or cross-presentation of antigens transferred from transfected nonprofessional cells such as keratinocytes or myocytes to APCs [2, 33-39]. Our study provides evidence that SCTs are presented as intact molecules after immunization, suggesting that cross-presentation involving re-processing of antigens is not the major mechanism for antigen presentation after DNA vaccination. Gene-gun delivers plasmids to the epidermis where epidermal keratinocytes and also epidermal dendritic cells (Langerhans cells) can be directly transfected [34, 48, 93]. Langerhans cells were shown to migrate to draining lymph nodes and prime naïve CD8⁺ T cells efficiently [49]. Thus, in our case, professional APCs, i.e. dendritic cells (DCs), directly transfected with plasmids may express and present SCTs directly to T cells. Alternatively, APCs may obtain intact SCT molecules from transfected cells through intercellular transfer of cell surface molecules. This phenomenon of transfer of plasma membrane fragments including proteins between lymphocytes, called trans-endocytosis or trogocytosis, has been reported for a long time [51, 58-65, 164]. This process allows rapid transfer of intact cell surface proteins between cells in contact with one another and transfer of intact MHC/peptide complexes between APCs or from dying cells to APCs, recently termed ‘cross-dressing’, has been

demonstrated although the molecular processes involved need to be clarified. Relevant to our study, Ostrand-Rosenberg *et al.* reported that DCs utilize both cross-presentation and cross-dressing mechanisms to prime CD8⁺ T cells [59]. And Lechler *et al.* demonstrated *in vitro* that splenic CD8 α ⁺ DCs can acquire MHC/peptide complexes from other DCs and stimulate CD8⁺ T cells [61]. More recently, Bevan *et al.* demonstrated that this cross-dressing does occur *in vivo* during virus infection [58]. It is plausible to think SCTs are presented through a cross-dressing mechanism, considering that our data indicate presentation of intact SCT molecules and that it has been reported that targeting antigen presentation to DCs was insufficient to optimally prime T cells in gene gun DNA immunization [50]. Thus, in our case, DCs may present SCTs that are obtained from transfected epidermal keratinocytes or epidermal dendritic cells via a cross-dressing mechanism. In any case, our unique approach using SCTs adds to the growing evidence of the importance of intercellular transfer of intact MHC/peptide for T cell priming.

Chapter 5

Concluding Remarks and Future Directions

I have learned in my dissertation studies that unexpected results can sometimes be more insightful for future directions than expected results. More specifically for many experiments there are clear expectations or biases based on previously reported findings. However, during my dissertation research I came upon several instances where expected results were not obtained forcing us to re-think paradigms. In this final chapter I give three examples of my experiments that resulted in unexpected and unresolved findings; indeed the first two were unexpected negative findings. I then speculate on the significance of these findings and what might be done to resolve outstanding questions raised by these three observations.

Unexpected diversity of TCR V β chain usage of MAIT cells after MR1 selection

The first unexpected findings concern MR1, the project I worked on when I joined the Hansen lab. MR1 is a class Ib MHC molecule that restricts the development and activation of a novel T cell subset referred to as MAIT (mucosal-associated invariant T) cells [165-167]. MR1 is remarkably conserved among mammalian species, especially in its $\alpha 1$ and $\alpha 2$ domains. Indeed, the $\alpha 1/\alpha 2$ domains are 90% identical between human and mouse, suggesting an evolutionarily conserved function for MR1, perhaps binding a conserved ligand [168, 169]. Mouse MAIT cells express an invariant V $\alpha 19$ -J $\alpha 33$ chain and limited V β chains, preferentially V $\beta 8.1$, V $\beta 8.2$, or V $\beta 6$. Although MR1-restricted

MAIT cells have been recently implicated in bacterial responses [167], their mechanism of detection of bacteria is unknown. MAIT cells are one of only two mammalian T cell populations with an invariant TCR α chain. The other invariant T cells are the extensively studied iNKT cells that recognize glycolipid antigens presented with CD1d molecules [170]. On the basis of the expression of an invariant TCR and the restriction to the highly conserved MR1 of MAIT cells, we hypothesized that TCR V β chains of MAIT cells have limited diversity. To examine this, we determined the importance of the TCR V β chain diversity of polyclonal mouse MAIT cells using a sequencing approach of the CDR3 region. These studies were done with the expert advice of Dr. Chyi-Song Hsieh. Surprisingly, the usage of V β chains of MAIT cells was highly diverse in both amino acid sequence and length of the CDR3 region. This result suggested that i) MAIT cells do not discriminate ligands, and/or ii) the orientation of the interaction of MAIT cell TCR and MR1 is different from that of conventional $\alpha\beta$ TCR and classical MHC I. It has been reported that iNKT cells are able to recognize many different self- and non-self glycolipid variants [87, 170, 171]. iNKT cells also express a limited number of TCR β chains with variable CDR3 β regions paired with an invariant V α 14-J α 18. Importantly, structural and mutational studies showed that the iNKT cell TCR uses the unique mode of antigen recognition where germline-encoded residues are involved in antigen recognition and CDR3 β is unlikely to contact directly with antigens, indicating limited antigen discrimination [172-175]. Thus, my finding seemed to suggest that MAIT cells also may not discriminate antigens or CDR3 β is not directly involved in antigen recognition. Recently, two groups reported that human and mouse polyclonal MAIT cells are

activated in an MR1-dependent manner by a wide variety of microbes including *E. coli*, *Mycobacteria*, *Pseudomonas*, *Klebsiella*, *Lactobacillus*, *Staphylococcus*, *Saccharomyces* and *Candida*, but not *Streptococcus A* and virus [176, 177], suggesting that MAIT cells have limited ligand discrimination. To elucidate the antigen recognition of MAIT cells, it will be critical to identify the nature of the MR1 ligand and whether it is a self-ligand induced by infection or a microbial ligand. Elution and characterization of the ligand from MR1 at the surface of cells infected with microbes should be able to answer to this question.

Failure to construct a WNVp33/D^b SCT even with a disulfide trap

Our lab and others have made SCTs with several different human, mouse, or rat MHC I heavy chains bound by different antigenic peptides. The reported SCTs include ones made with the class Ib molecule HLA-E bound by two different antigenic peptides. Thus, we considered that the SCT was likely universally applicable prior to my findings that include the WNVp3/K^b SCT described in Chapter 4.1. Besides the WNVp3/K^b SCT, I found the D^b SCT that incorporates another immunodominant WNV epitope p33, SSVWNATTA, is also not recognized by T cells. More surprisingly, the recognition of WNVp33/D^b SCT was not improved by a disulfide trap. Even with a disulfide trap, this SCT appears accessible to the exogenous peptide because CTLs were able to kill the cells when WNVp33 was exogenously added to WNVp33/D^b dtSCT-expressing cells. To solve the problem, with advice from Dr. Fremont, I first tried mutation of the anchor residue of WNVp33 to increase the peptide binding to the groove. D^b binding peptides

usually have a hydrophilic C terminal residue, Met, Ile, or Leu, which WNVp33 does not have [178, 179]. Our hypothesis was that the mutation of P9 alanine to one of the common anchor residues might enhance the peptide binding and T cell recognition. However, my result showed that four different WNVp33 variant/D^b SCTs still do not activate T cells. Alternatively, I re-positioned the disulfide trap using either Thr⁸⁰ or Tyr⁸⁴ in the heavy chain and Gly¹ or Gly² in the peptide-β2m linker to find a better combination to provide the best anchoring of peptide. Thr⁸⁰ in the heavy chain locates at the C terminal end of the peptide binding groove along with Tyr⁸⁴ and studies in our lab previously showed that a disulfide trap using this residue did not alter the surface expression or antibody recognition of the K^b/OVAp SCT [23]. But to our disappointment, none of the disulfide trap locations made WNVp33/D^b SCT refractory to exogenous peptide binding nor did they promote T cell detection. The failure of this SCT is still puzzling to us, but clearly indicates that not every MHC I/peptide complex can be made as a SCT without modifications. To resolve the problem with WNVp33/D^b SCT, detailed analyses of the SCT at the cell surface such as conformation, β2m binding, and the linker association might be helpful. Also different lengths of the peptide-β2m linker and/or combinations of the approaches that have been tried above may need to be considered. Resolution of this enigma may provide novel insights into peptide binding to MHC proteins or at least to the D^b allele.

Implication of intercellular membrane exchange in Ag presentation following DNA vaccine

Our data supporting the importance of intercellular membrane exchange as a mechanism for cross-presentation following DNA vaccination was unexpected based on its inefficiency. Membrane exchange between cells, frequently referred to as trogocytosis, has been reported in cellular interactions such as APCs with T cells or NK cells [64]. However, in these examples the membrane transfer is receptor-mediated, i.e. MHC transfer from APCs to T cells by the TCR or to NK cells by the Ly49 receptors. If membrane exchange is involved in the antigen presentation after DNA vaccination by gene gun, it presumably involves transfer of MHC/peptide complexes from the cells taking up the DNA to the APCs that prime the CD8⁺ T cells.

Accumulating reports in the literature document the importance of cross-presentation *in vivo* as a mechanism for detection of pathogens and tumors [55-57]. Also significant is recent evidence suggesting that the APCs required for priming of CD8⁺ T cells are LN resident CD8 α ⁺ DC [56]. In addition, a recent report in *Science* from the Murphy lab clearly demonstrates the *in vivo* importance of CD8 α ⁺ DCs in responses to pathogens and tumors in that T cell responses are absent in *Batf3*-deficient mice that specifically lack CD8 α ⁺ DCs [54]. Their findings define the critical importance of this cell type for physiologic cross-presentation. Thus the initial outstanding questions are which cells express the antigen after DNA vaccination and which cells transfer the antigen to the CD8 α ⁺ DCs. From studies of the cross-presentation after subcutaneous virus infection, a current model is that a migratory DC transports the antigen from the skin to the regional LN where it is then transferred to the CD8 α ⁺ DC for activation of CD8⁺ T cells [55, 56]. However, what is unclear in this model is how antigens are

efficiently transferred between cells. Most studies probing the mechanism of cross-presentation have used *in vitro* approaches to address the cellular processes that allow APCs to take up exogenous antigens and transfer them to the cytosol where TAP transports the antigens into the ER to compete with other peptides for loading into MHC I molecules. This mechanism of re-presentation of the antigen is very unlikely to be efficient particularly because most current *in vivo* models of cross-presentation require multiple transfers between different cells, making it difficult to achieve sufficient levels of the surface antigen display to activate CD8⁺ T cells.

Could the transfer of intact MHC/peptide complexes represent a more efficient mechanism of cross-presentation than re-presentation of the antigen between different cells? Conceptually, it might seem so because transfer of an intact MHC/peptide complex bypasses inefficiencies of retro-grade intracellular transport into the ER as well as competition within the ER for peptide loading. However, based again solely on *in vitro* assays, the transfer of intact MHC/peptide complexes between cells (i.e cross-dressing) appears marginal at best [62, 63]. Typically, in these *in vitro* membrane exchange assays, freeze/thaw lysates of the antigen-fed cells of one MHC haplotype are incubated with cells of an alternative MHC haplotype. CD8⁺ T cells specific for the donor MHC/antigen are then used to monitor exchange of the intact MHC/peptide molecules. It is noteworthy that in these *in vitro* assays the level of MHC/peptide complexes that are exchanged is barely detectable by FACS. Thus, like with conventional cross-presentation mechanisms, the efficiency of the transfer of intact MHC/peptide complexes seems marginal.

What has been missing is *in vivo* evidence that cross-dressing is an important mechanism of CD8⁺ T cell activation. In this regard, the recent paper by Wakim and Bevan is important in that they make several relevant observations [58]. First, they showed that cross-dressing is 3 orders of magnitude less efficient than the direct presentation by donor DCs for inducing proliferation of naïve or memory T cells. They then used the diphtheria toxin system to eliminate the cross-dressed DCs and showed data implicating cross-dressing in expansion of resting memory cells and not naïve cells. Somewhat surprisingly, they also report that CD4⁺ DCs are the subset involved in cross-dressing. These intriguing findings certainly help to focus future investigations on the *in vivo* mechanism of cross-dressing.

As reported here in Chapter 4.2, we took a unique approach to study the importance of cross-dressing using SCT-based DNA vaccines. Our rationale was, if SCTs really are superior to the peptide or minigene based vaccines, then they are presumably presented by APCs to CD8⁺ T cells as intact structures. Mechanistically, this would imply either that the APC taking up the plasmid encoding the SCT directly presents the SCT, or that the SCT is transferred from the cell making the SCT protein to a DC capable of CD8⁺ T cell activation. It is also noteworthy that in collaboration with the Gillanders and Murphy labs we have shown that CD8 α ⁺ DCs are required for gene gun DNA vaccination in general and SCT-based vaccination specifically. Thus, like other models where cross-presentation has been implicated, the CD8 α ⁺ DC appears to be the requisite APC. Our evidence that SCTs are presented as intact structures is based on the two different lines of evidence (Chapter 4.2 and unpublished observations from the

Gillanders' lab). First, a mutation in the SCT that blocks TCR or CD8 engagement ablates its ability to prime T cells after DNA vaccination. Second, the SCTs with poor binding peptides that cannot be re-presented elicit robust CD8⁺ T cell responses after DNA vaccination. Although our findings like the aforementioned Wakim and Bevan's study support the importance of cross-dressing, they have significant differences. Most notably, our findings, in contrast to theirs, suggest the importance of cross-dressing for priming naïve CD8⁺ T cell responses and implicate the importance of CD8α⁺ DCs in cross-dressing.

Thus there are several outstanding questions where SCT approaches can be used to address mechanisms of cross-presentation in CD8⁺ T cell responses including DNA vaccination. Because of the published disconnect between the *in vitro* and *in vivo* evidence regarding mechanisms of cross-presentation, it will be critical to focus future studies on *in vivo* approaches. For example, in the OT-1 model, expression of OVAp/K^b SCTs to certain cell types using different promoters and expressing SCTs that can or cannot (OVAp5Y/K^b) be cross-primed may be informative for addressing mechanistic questions. For example, this approach might be useful for determining which cells express the SCT after DNA vaccination and which APCs are required for priming naïve *vs.* memory CD8⁺ T cells. This approach might also be used to address the relative importance of cross-dressing *vs.* peptide re-presentation. It might also be insightful to use *in vivo* imaging to track the SCT following DNA vaccination.

References

1. Berzofsky, J.A., J.D. Ahlers, and I.M. Belyakov, Strategies for designing and optimizing new generation vaccines. *Nat Rev Immunol*, 2001. 1(3): p. 209-19.
2. Kutzler, M.A. and D.B. Weiner, DNA vaccines: ready for prime time? *Nat Rev Genet*, 2008. 9(10): p. 776-88.
3. Bijker, M.S., et al., Superior induction of anti-tumor CTL immunity by extended peptide vaccines involves prolonged, DC-focused antigen presentation. *Eur J Immunol*, 2008. 38(4): p. 1033-42.
4. Welters, M.J., et al., Induction of tumor-specific CD4+ and CD8+ T-cell immunity in cervical cancer patients by a human papillomavirus type 16 E6 and E7 long peptides vaccine. *Clin Cancer Res*, 2008. 14(1): p. 178-87.
5. Speetjens, F.M., et al., Induction of p53-specific immunity by a p53 synthetic long peptide vaccine in patients treated for metastatic colorectal cancer. *Clin Cancer Res*, 2009. 15(3): p. 1086-95.
6. Bijker, M.S., et al., CD8+ CTL priming by exact peptide epitopes in incomplete Freund's adjuvant induces a vanishing CTL response, whereas long peptides induce sustained CTL reactivity. *J Immunol*, 2007. 179(8): p. 5033-40.
7. Zwaveling, S., et al., Established human papillomavirus type 16-expressing tumors are effectively eradicated following vaccination with long peptides. *J Immunol*, 2002. 169(1): p. 350-8.

8. Melief, C.J. and S.H. van der Burg, Immunotherapy of established (pre)malignant disease by synthetic long peptide vaccines. *Nat Rev Cancer*, 2008. 8(5): p. 351-60.
9. Rock, K.L., I.A. York, and A.L. Goldberg, Post-proteasomal antigen processing for major histocompatibility complex class I presentation. *Nat Immunol*, 2004. 5(7): p. 670-7.
10. Mottez, E., et al., Cells expressing a major histocompatibility complex class I molecule with a single covalently bound peptide are highly immunogenic. *J Exp Med*, 1995. 181(2): p. 493-502.
11. Yu, Y.Y., et al., Cutting edge: single-chain trimers of MHC class I molecules form stable structures that potently stimulate antigen-specific T cells and B cells. *J Immunol*, 2002. 168(7): p. 3145-9.
12. White, J., et al., Soluble class I MHC with beta2-microglobulin covalently linked peptides: specific binding to a T cell hybridoma. *J Immunol*, 1999. 162(5): p. 2671-6.
13. Mage, M.G., et al., A recombinant, soluble, single-chain class I major histocompatibility complex molecule with biological activity. *Proc Natl Acad Sci U S A*, 1992. 89(22): p. 10658-62.
14. Uger, R.A. and B.H. Barber, Creating CTL targets with epitope-linked beta 2-microglobulin constructs. *J Immunol*, 1998. 160(4): p. 1598-605.
15. Uger, R.A., S.M. Chan, and B.H. Barber, Covalent linkage to beta2-microglobulin enhances the MHC stability and antigenicity of suboptimal CTL epitopes. *J Immunol*, 1999. 162(10): p. 6024-8.

16. Kim, S., et al., Licensing of natural killer cells by host major histocompatibility complex class I molecules. *Nature*, 2005. 436(7051): p. 709-13.
17. Elliott, J.M., J.A. Wahle, and W.M. Yokoyama, MHC class I-deficient natural killer cells acquire a licensed phenotype after transfer into an MHC class I-sufficient environment. *J Exp Med*, 2010. 207(10): p. 2073-9.
18. Hansen, T., Y.Y. Yu, and D.H. Fremont, Preparation of stable single-chain trimers engineered with peptide, beta2 microglobulin, and MHC heavy chain. *Curr Protoc Immunol*, 2009. Chapter 17: p. Unit17 5.
19. Hansen, T.H. and L. Lybarger, Exciting applications of single chain trimers of MHC-I molecules. *Cancer Immunol Immunother*, 2006. 55(2): p. 235-6.
20. Kim, S., et al., Single-chain HLA-A2 MHC trimers that incorporate an immunodominant peptide elicit protective T cell immunity against lethal West Nile virus infection. *J Immunol*, 2010. 184(8): p. 4423-30.
21. Li, L., et al., Engineering superior DNA vaccines: MHC class I single chain trimers bypass antigen processing and enhance the immune response to low affinity antigens. *Vaccine*, 2010. 28(8): p. 1911-8.
22. Lybarger, L., et al., Enhanced immune presentation of a single-chain major histocompatibility complex class I molecule engineered to optimize linkage of a C-terminally extended peptide. *J Biol Chem*, 2003. 278(29): p. 27105-11.
23. Truscott, S.M., et al., Disulfide bond engineering to trap peptides in the MHC class I binding groove. *J Immunol*, 2007. 178(10): p. 6280-9.

24. Truscott, S.M., et al., Human major histocompatibility complex (MHC) class I molecules with disulfide traps secure disease-related antigenic peptides and exclude competitor peptides. *J Biol Chem*, 2008. 283(12): p. 7480-90.
25. Mitaksov, V., et al., Structural engineering of pMHC reagents for T cell vaccines and diagnostics. *Chem Biol*, 2007. 14(8): p. 909-22.
26. Cheung, Y.K., et al., Induction of T-cell response by a DNA vaccine encoding a novel HLA-A*0201 severe acute respiratory syndrome coronavirus epitope. *Vaccine*, 2007. 25(32): p. 6070-7.
27. Crew, M.D., et al., An HLA-E single chain trimer inhibits human NK cell reactivity towards porcine cells. *Mol Immunol*, 2005. 42(10): p. 1205-14.
28. Greten, T.F., et al., Peptide-beta2-microglobulin-MHC fusion molecules bind antigen-specific T cells and can be used for multivalent MHC-Ig complexes. *J Immunol Methods*, 2002. 271(1-2): p. 125-35.
29. Zhang, Y., et al., Hepatitis B virus core antigen epitopes presented by HLA-A2 single-chain trimers induce functional epitope-specific CD8⁺ T-cell responses in HLA-A2.1/Kb transgenic mice. *Immunology*, 2007. 121(1): p. 105-12.
30. Huang, C.H., et al., Cancer immunotherapy using a DNA vaccine encoding a single-chain trimer of MHC class I linked to an HPV-16 E6 immunodominant CTL epitope. *Gene Ther*, 2005. 12(15): p. 1180-6.
31. Palmowski, M.J., et al., A single-chain H-2Db molecule presenting an influenza virus nucleoprotein epitope shows enhanced ability at stimulating CD8⁺ T cell responses in vivo. *J Immunol*, 2009. 182(8): p. 4565-71.

32. Lu, S., S. Wang, and J.M. Grimes-Serrano, Current progress of DNA vaccine studies in humans. *Expert Rev Vaccines*, 2008. 7(2): p. 175-91.
33. Sykes, K., Progress in the development of genetic immunization. *Expert Rev Vaccines*, 2008. 7(9): p. 1395-404.
34. Fioretti, D., et al., DNA vaccines: developing new strategies against cancer. *J Biomed Biotechnol*, 2010. 2010: p. 174378.
35. Garmory, H.S., K.A. Brown, and R.W. Titball, DNA vaccines: improving expression of antigens. *Genet Vaccines Ther*, 2003. 1(1): p. 2.
36. Gurunathan, S., D.M. Klinman, and R.A. Seder, DNA vaccines: immunology, application, and optimization*. *Annu Rev Immunol*, 2000. 18: p. 927-74.
37. Ingolotti, M., et al., DNA vaccines for targeting bacterial infections. *Expert Rev Vaccines*, 2010. 9(7): p. 747-63.
38. Kowalczyk, D.W. and H.C. Ertl, Immune responses to DNA vaccines. *Cell Mol Life Sci*, 1999. 55(5): p. 751-70.
39. Liu, M.A., DNA vaccines: a review. *J Intern Med*, 2003. 253(4): p. 402-10.
40. Hung, C.F., et al., A DNA vaccine encoding a single-chain trimer of HLA-A2 linked to human mesothelin peptide generates anti-tumor effects against human mesothelin-expressing tumors. *Vaccine*, 2007. 25(1): p. 127-35.
41. Hung, C.F., et al., DNA vaccines encoding Ii-PADRE generates potent PADRE-specific CD4+ T-cell immune responses and enhances vaccine potency. *Mol Ther*, 2007. 15(6): p. 1211-9.

42. Stoecklinger, A., et al., Langerin⁺ dermal dendritic cells are critical for CD8⁺ T cell activation and IgH gamma-1 class switching in response to gene gun vaccines. *J Immunol*, 2011. 186(3): p. 1377-83.
43. Park, B., et al., Human cytomegalovirus inhibits tapasin-dependent peptide loading and optimization of the MHC class I peptide cargo for immune evasion. *Immunity*, 2004. 20(1): p. 71-85.
44. Jones, T.R., et al., Human cytomegalovirus US3 impairs transport and maturation of major histocompatibility complex class I heavy chains. *Proc Natl Acad Sci U S A*, 1996. 93(21): p. 11327-33.
45. Corr, M., et al., Gene vaccination with naked plasmid DNA: mechanism of CTL priming. *J Exp Med*, 1996. 184(4): p. 1555-60.
46. Doe, B., et al., Induction of cytotoxic T lymphocytes by intramuscular immunization with plasmid DNA is facilitated by bone marrow-derived cells. *Proc Natl Acad Sci U S A*, 1996. 93(16): p. 8578-83.
47. Iwasaki, A., et al., The dominant role of bone marrow-derived cells in CTL induction following plasmid DNA immunization at different sites. *J Immunol*, 1997. 159(1): p. 11-4.
48. Raz, E., et al., Intradermal gene immunization: the possible role of DNA uptake in the induction of cellular immunity to viruses. *Proc Natl Acad Sci U S A*, 1994. 91(20): p. 9519-23.

49. Porgador, A., et al., Predominant role for directly transfected dendritic cells in antigen presentation to CD8⁺ T cells after gene gun immunization. *J Exp Med*, 1998. 188(6): p. 1075-82.
50. Lauterbach, H., et al., Insufficient APC capacities of dendritic cells in gene gun-mediated DNA vaccination. *J Immunol*, 2006. 176(8): p. 4600-7.
51. Corr, M., et al., In vivo priming by DNA injection occurs predominantly by antigen transfer. *J Immunol*, 1999. 163(9): p. 4721-7.
52. Schulz, O., et al., Toll-like receptor 3 promotes cross-priming to virus-infected cells. *Nature*, 2005. 433(7028): p. 887-92.
53. Belz, G.T., et al., CD8alpha⁺ dendritic cells selectively present MHC class I-restricted noncytolytic viral and intracellular bacterial antigens in vivo. *J Immunol*, 2005. 175(1): p. 196-200.
54. Hildner, K., et al., Batf3 deficiency reveals a critical role for CD8alpha⁺ dendritic cells in cytotoxic T cell immunity. *Science*, 2008. 322(5904): p. 1097-100.
55. Allan, R.S., et al., Epidermal viral immunity induced by CD8alpha⁺ dendritic cells but not by Langerhans cells. *Science*, 2003. 301(5641): p. 1925-8.
56. Allan, R.S., et al., Migratory dendritic cells transfer antigen to a lymph node-resident dendritic cell population for efficient CTL priming. *Immunity*, 2006. 25(1): p. 153-62.
57. Bedoui, S., et al., Cross-presentation of viral and self antigens by skin-derived CD103⁺ dendritic cells. *Nat Immunol*, 2009. 10(5): p. 488-95.

58. Wakim, L.M. and M.J. Bevan, Cross-dressed dendritic cells drive memory CD8+ T-cell activation after viral infection. *Nature*, 2011. 471(7340): p. 629-32.
59. Dolan, B.P., K.D. Gibbs, Jr., and S. Ostrand-Rosenberg, Dendritic cells cross-dressed with peptide MHC class I complexes prime CD8+ T cells. *J Immunol*, 2006. 177(9): p. 6018-24.
60. Dolan, B.P., K.D. Gibbs, Jr., and S. Ostrand-Rosenberg, Tumor-specific CD4+ T cells are activated by "cross-dressed" dendritic cells presenting peptide-MHC class II complexes acquired from cell-based cancer vaccines. *J Immunol*, 2006. 176(3): p. 1447-55.
61. Smyth, L.A., et al., The relative efficiency of acquisition of MHC:peptide complexes and cross-presentation depends on dendritic cell type. *J Immunol*, 2008. 181(5): p. 3212-20.
62. Qu, C., et al., MHC class I/peptide transfer between dendritic cells overcomes poor cross-presentation by monocyte-derived APCs that engulf dying cells. *J Immunol*, 2009. 182(6): p. 3650-9.
63. Zhang, Q.J., et al., Trogocytosis of MHC-I/peptide complexes derived from tumors and infected cells enhances dendritic cell cross-priming and promotes adaptive T cell responses. *PLoS One*, 2008. 3(8): p. e3097.
64. Davis, D.M., Intercellular transfer of cell-surface proteins is common and can affect many stages of an immune response. *Nat Rev Immunol*, 2007. 7(3): p. 238-43.

65. Herrera, O.B., et al., A novel pathway of alloantigen presentation by dendritic cells. *J Immunol*, 2004. 173(8): p. 4828-37.
66. Klinman, D.M., et al., Contribution of cells at the site of DNA vaccination to the generation of antigen-specific immunity and memory. *J Immunol*, 1998. 160(5): p. 2388-92.
67. Diamond, M.S., et al., The host immunologic response to West Nile encephalitis virus. *Front Biosci*, 2009. 14: p. 3024-34.
68. Diamond, M.S., Evasion of innate and adaptive immunity by flaviviruses. *Immunol Cell Biol*, 2003. 81(3): p. 196-206.
69. Wang, T. and E. Fikrig, Immunity to West Nile virus. *Curr Opin Immunol*, 2004. 16(4): p. 519-23.
70. King, N.J. and A.M. Kesson, Interaction of flaviviruses with cells of the vertebrate host and decoy of the immune response. *Immunol Cell Biol*, 2003. 81(3): p. 207-16.
71. Weaver, S.C. and A.D. Barrett, Transmission cycles, host range, evolution and emergence of arboviral disease. *Nat Rev Microbiol*, 2004. 2(10): p. 789-801.
72. Brien, J.D., J.L. Uhrlaub, and J. Nikolich-Zugich, Protective capacity and epitope specificity of CD8(+) T cells responding to lethal West Nile virus infection. *Eur J Immunol*, 2007. 37(7): p. 1855-63.
73. Purtha, W.E., et al., Antigen-specific cytotoxic T lymphocytes protect against lethal West Nile virus encephalitis. *Eur J Immunol*, 2007. 37(7): p. 1845-54.

74. McMurtrey, C.P., et al., Epitope discovery in West Nile virus infection: Identification and immune recognition of viral epitopes. *Proc Natl Acad Sci U S A*, 2008. 105(8): p. 2981-6.
75. Pascolo, S., et al., HLA-A2.1-restricted education and cytolytic activity of CD8(+) T lymphocytes from beta2 microglobulin (beta2m) HLA-A2.1 monochain transgenic H-2Db beta2m double knockout mice. *J Exp Med*, 1997. 185(12): p. 2043-51.
76. Diamond, M.S., et al., B cells and antibody play critical roles in the immediate defense of disseminated infection by West Nile encephalitis virus. *J Virol*, 2003. 77(4): p. 2578-86.
77. Verma, B., et al., Direct discovery and validation of a peptide/MHC epitope expressed in primary human breast cancer cells using a TCRm monoclonal antibody with profound antitumor properties. *Cancer Immunol Immunother*, 2010. 59(4): p. 563-73.
78. Verma, B., et al., TCR mimic monoclonal antibody targets a specific peptide/HLA class I complex and significantly impedes tumor growth in vivo using breast cancer models. *J Immunol*, 2010. 184(4): p. 2156-65.
79. Diamond, M.S., et al., Innate and adaptive immune responses determine protection against disseminated infection by West Nile encephalitis virus. *Viral Immunol*, 2003. 16(3): p. 259-78.

80. Samuel, M.A. and M.S. Diamond, Pathogenesis of West Nile Virus infection: a balance between virulence, innate and adaptive immunity, and viral evasion. *J Virol*, 2006. 80(19): p. 9349-60.
81. Henderson, R.A., et al., HLA-A2.1-associated peptides from a mutant cell line: a second pathway of antigen presentation. *Science*, 1992. 255(5049): p. 1264-6.
82. Bai, A., J. Broen, and J. Forman, The pathway for processing leader-derived peptides that regulate the maturation and expression of Qa-1b. *Immunity*, 1998. 9(3): p. 413-21.
83. Fernandez-Garcia, M.D., et al., Pathogenesis of flavivirus infections: using and abusing the host cell. *Cell Host Microbe*, 2009. 5(4): p. 318-28.
84. Fields, B.N., D.M. Knipe, and P.M. Howley, *Fields virology*. 5th ed2007, Philadelphia: Wolters Kluwer Health/Lippincott Williams & Wilkins.
85. Shrestha, B. and M.S. Diamond, Role of CD8+ T cells in control of West Nile virus infection. *J Virol*, 2004. 78(15): p. 8312-21.
86. Alexander, J., et al., Development of high potency universal DR-restricted helper epitopes by modification of high affinity DR-blocking peptides. *Immunity*, 1994. 1(9): p. 751-61.
87. Gadola, S.D., et al., Structure and binding kinetics of three different human CD1d-alpha-galactosylceramide-specific T cell receptors. *J Exp Med*, 2006. 203(3): p. 699-710.

88. Jaramillo, A., et al., Recognition of HLA-A2-restricted mammaglobin-A-derived epitopes by CD8⁺ cytotoxic T lymphocytes from breast cancer patients. *Breast Cancer Res Treat*, 2004. 88(1): p. 29-41.
89. Wilson, C.C., et al., Development of a DNA vaccine designed to induce cytotoxic T lymphocyte responses to multiple conserved epitopes in HIV-1. *J Immunol*, 2003. 171(10): p. 5611-23.
90. Doan, T., et al., A polytope DNA vaccine elicits multiple effector and memory CTL responses and protects against human papillomavirus 16 E7-expressing tumour. *Cancer Immunol Immunother*, 2005. 54(2): p. 157-71.
91. Li, X., et al., A novel HBV DNA vaccine based on T cell epitopes and its potential therapeutic effect in HBV transgenic mice. *Int Immunol*, 2005. 17(10): p. 1293-302.
92. Bins, A.D., et al., A rapid and potent DNA vaccination strategy defined by in vivo monitoring of antigen expression. *Nat Med*, 2005. 11(8): p. 899-904.
93. Yoshida, A., et al., Advantage of gene gun-mediated over intramuscular inoculation of plasmid DNA vaccine in reproducible induction of specific immune responses. *Vaccine*, 2000. 18(17): p. 1725-9.
94. Oliphant, T., et al., Development of a humanized monoclonal antibody with therapeutic potential against West Nile virus. *Nat Med*, 2005. 11(5): p. 522-30.
95. Oliphant, T., et al., Induction of epitope-specific neutralizing antibodies against West Nile virus. *J Virol*, 2007. 81(21): p. 11828-39.

96. Diamond, M.S., T.C. Pierson, and D.H. Fremont, The structural immunology of antibody protection against West Nile virus. *Immunol Rev*, 2008. 225: p. 212-25.
97. Hansen, T.H. and M. Bouvier, MHC class I antigen presentation: learning from viral evasion strategies. *Nat Rev Immunol*, 2009. 9(7): p. 503-13.
98. Primeau, T., et al., Applications of major histocompatibility complex class I molecules expressed as single chains. *Immunol Res*, 2005. 32(1-3): p. 109-21.
99. Vijh, S., I.M. Pilip, and E.G. Pamer, Effect of antigen-processing efficiency on in vivo T cell response magnitudes. *J Immunol*, 1998. 160(8): p. 3971-7.
100. Sitati, E.M. and M.S. Diamond, CD4⁺ T-cell responses are required for clearance of West Nile virus from the central nervous system. *J Virol*, 2006. 80(24): p. 12060-9.
101. Bourgeois, C., B. Rocha, and C. Tanchot, A role for CD40 expression on CD8⁺ T cells in the generation of CD8⁺ T cell memory. *Science*, 2002. 297(5589): p. 2060-3.
102. Sun, J.C. and M.J. Bevan, Defective CD8 T cell memory following acute infection without CD4 T cell help. *Science*, 2003. 300(5617): p. 339-42.
103. Shedlock, D.J. and H. Shen, Requirement for CD4 T cell help in generating functional CD8 T cell memory. *Science*, 2003. 300(5617): p. 337-9.
104. Wang, Y., et al., CD8⁺ T cells mediate recovery and immunopathology in West Nile virus encephalitis. *J Virol*, 2003. 77(24): p. 13323-34.
105. Shrestha, B., M.A. Samuel, and M.S. Diamond, CD8⁺ T cells require perforin to clear West Nile virus from infected neurons. *J Virol*, 2006. 80(1): p. 119-29.

106. Shrestha, B., et al., The relative contribution of antibody and CD8+ T cells to vaccine immunity against West Nile encephalitis virus. *Vaccine*, 2008. 26(16): p. 2020-33.
107. Ureta-Vidal, A., et al., Phenotypical and functional characterization of the CD8+ T cell repertoire of HLA-A2.1 transgenic, H-2KbnullDbnull double knockout mice. *J Immunol*, 1999. 163(5): p. 2555-60.
108. Pamer, E.G., Immune responses to *Listeria monocytogenes*. *Nat Rev Immunol*, 2004. 4(10): p. 812-23.
109. Shen, H., C.M. Tato, and X. Fan, *Listeria monocytogenes* as a probe to study cell-mediated immunity. *Curr Opin Immunol*, 1998. 10(4): p. 450-458.
110. Finelli, A., et al., MHC class I restricted T cell responses to *Listeria monocytogenes*, an intracellular bacterial pathogen. *Immunol Res*, 1999. 19(2-3): p. 211-23.
111. Zenewicz, L.A. and H. Shen, Innate and adaptive immune responses to *Listeria monocytogenes*: a short overview. *Microbes Infect*, 2007. 9(10): p. 1208-15.
112. Pamer, E.G., et al., MHC class I antigen processing of *Listeria monocytogenes* proteins: implications for dominant and subdominant CTL responses. *Immunol Rev*, 1997. 158: p. 129-36.
113. Geginat, G., et al., A novel approach of direct ex vivo epitope mapping identifies dominant and subdominant CD4 and CD8 T cell epitopes from *Listeria monocytogenes*. *J Immunol*, 2001. 166(3): p. 1877-84.

114. Vijh, S. and E.G. Pamer, Immunodominant and subdominant CTL responses to *Listeria monocytogenes* infection. *J Immunol*, 1997. 158(7): p. 3366-71.
115. Busch, D.H., et al., Coordinate regulation of complex T cell populations responding to bacterial infection. *Immunity*, 1998. 8(3): p. 353-62.
116. Pamer, E.G., Direct sequence identification and kinetic analysis of an MHC class I-restricted *Listeria monocytogenes* CTL epitope. *J Immunol*, 1994. 152(2): p. 686-94.
117. Sijts, A.J., et al., Two *Listeria monocytogenes* CTL epitopes are processed from the same antigen with different efficiencies. *J Immunol*, 1996. 156(2): p. 683-92.
118. Pamer, E.G., J.T. Harty, and M.J. Bevan, Precise prediction of a dominant class I MHC-restricted epitope of *Listeria monocytogenes*. *Nature*, 1991. 353(6347): p. 852-5.
119. Sun, J.C., M.A. Williams, and M.J. Bevan, CD4⁺ T cells are required for the maintenance, not programming, of memory CD8⁺ T cells after acute infection. *Nat Immunol*, 2004. 5(9): p. 927-33.
120. Ramsburg, E.A., et al., Requirement for CD4 T cell help in maintenance of memory CD8 T cell responses is epitope dependent. *J Immunol*, 2007. 178(10): p. 6350-8.
121. Gao, F.G., et al., Antigen-specific CD4(+) T-cell help is required to activate a memory CD8(+) T cell to a fully functional tumor killer cell. *Cancer Research*, 2002. 62(22): p. 6438-6441.

122. Tsukamoto, T., et al., Impact of cytotoxic-T-lymphocyte memory induction without virus-specific CD4+ T-Cell help on control of a simian immunodeficiency virus challenge in rhesus macaques. *J Virol*, 2009. 83(18): p. 9339-46.
123. Hao, S., J. Yuan, and J. Xiang, Nonspecific CD4(+) T cells with uptake of antigen-specific dendritic cell-released exosomes stimulate antigen-specific CD8(+) CTL responses and long-term T cell memory. *J Leukoc Biol*, 2007. 82(4): p. 829-38.
124. de Goer de Herve, M.G., et al., Heterospecific CD4 help to rescue CD8 T cell killers. *J Immunol*, 2008. 181(9): p. 5974-80.
125. Hamilton, S.E. and S.C. Jameson, The nature of the lymphopenic environment dictates protective function of homeostatic-memory CD8+ T cells. *Proc Natl Acad Sci U S A*, 2008. 105(47): p. 18484-9.
126. Carrero, J.A., B. Calderon, and E.R. Unanue, Type I interferon sensitizes lymphocytes to apoptosis and reduces resistance to *Listeria* infection. *J Exp Med*, 2004. 200(4): p. 535-40.
127. Carrero, J.A., B. Calderon, and E.R. Unanue, Lymphocytes are detrimental during the early innate immune response against *Listeria monocytogenes*. *J Exp Med*, 2006. 203(4): p. 933-40.
128. Hovav, A.H., et al., Duration of antigen expression in vivo following DNA immunization modifies the magnitude, contraction, and secondary responses of CD8+ T lymphocytes. *J Immunol*, 2007. 179(10): p. 6725-33.

129. Kim, D., et al., Role of IL-2 secreted by PADRE-specific CD4+ T cells in enhancing E7-specific CD8+ T-cell immune responses. *Gene Ther*, 2008. 15(9): p. 677-87.
130. Nagata, T., et al., Induction of protective immunity to *Listeria monocytogenes* by immunization with plasmid DNA expressing a helper T-cell epitope that replaces the class II-associated invariant chain peptide of the invariant chain. *Infect Immun*, 2002. 70(5): p. 2676-2680.
131. van Bergen, J., et al., Efficient loading of HLA-DR with a T helper epitope by genetic exchange of CLIP. *Proc Natl Acad Sci U S A*, 1997. 94(14): p. 7499-502.
132. Yoshida, A., et al., Protective CTL response is induced in the absence of CD4+ T cells and IFN-gamma by gene gun DNA vaccination with a minigene encoding a CTL epitope of *Listeria monocytogenes*. *Vaccine*, 2001. 19(30): p. 4297-306.
133. Sallusto, F., et al., From Vaccines to Memory and Back. *Immunity*, 2010. 33(4): p. 451-463.
134. Czuprynski, C.J., et al., Administration of anti-granulocyte mAb RB6-8C5 impairs the resistance of mice to *Listeria monocytogenes* infection. *J Immunol*, 1994. 152(4): p. 1836-46.
135. Conlan, J.W. and R.J. North, Neutrophils are essential for early anti-*Listeria* defense in the liver, but not in the spleen or peritoneal cavity, as revealed by a granulocyte-depleting monoclonal antibody. *J Exp Med*, 1994. 179(1): p. 259-68.

136. Rogers, H.W. and E.R. Unanue, Neutrophils are involved in acute, nonspecific resistance to *Listeria monocytogenes* in mice. *Infect Immun*, 1993. 61(12): p. 5090-6.
137. Bourgeois, C. and C. Tanchot, Mini-review CD4 T cells are required for CD8 T cell memory generation. *Eur J Immunol*, 2003. 33(12): p. 3225-31.
138. Bennett, S.R., et al., Help for cytotoxic-T-cell responses is mediated by CD40 signalling. *Nature*, 1998. 393(6684): p. 478-80.
139. Ridge, J.P., F. Di Rosa, and P. Matzinger, A conditioned dendritic cell can be a temporal bridge between a CD4⁺ T-helper and a T-killer cell. *Nature*, 1998. 393(6684): p. 474-8.
140. Schoenberger, S.P., et al., T-cell help for cytotoxic T lymphocytes is mediated by CD40-CD40L interactions. *Nature*, 1998. 393(6684): p. 480-3.
141. Sun, J.C. and M.J. Bevan, Cutting edge: long-lived CD8 memory and protective immunity in the absence of CD40 expression on CD8 T cells. *J Immunol*, 2004. 172(6): p. 3385-9.
142. Lee, B.O., L. Hartson, and T.D. Randall, CD40-deficient, influenza-specific CD8 memory T cells develop and function normally in a CD40-sufficient environment. *J Exp Med*, 2003. 198(11): p. 1759-64.
143. Krieg, A.M., CpG motifs in bacterial DNA and their immune effects. *Annu Rev Immunol*, 2002. 20: p. 709-60.
144. Klinman, D.M., et al., CpG DNA as a vaccine adjuvant. *Expert Rev Vaccines*, 2011. 10(4): p. 499-511.

145. Babiuk, S., et al., TLR9^{-/-} and TLR9^{+/+} mice display similar immune responses to a DNA vaccine. *Immunology*, 2004. 113(1): p. 114-20.
146. Rottembourg, D., et al., Essential role for TLR9 in prime but not prime-boost plasmid DNA vaccination to activate dendritic cells and protect from lethal viral infection. *J Immunol*, 2010. 184(12): p. 7100-7.
147. Feltquate, D.M., et al., Different T helper cell types and antibody isotypes generated by saline and gene gun DNA immunization. *J Immunol*, 1997. 158(5): p. 2278-84.
148. Strugnell, R.A., et al., DNA vaccines for bacterial infections. *Immunol Cell Biol*, 1997. 75(4): p. 364-9.
149. Fensterle, J., et al., Effective DNA vaccination against listeriosis by prime/boost inoculation with the gene gun. *J Immunol*, 1999. 163(8): p. 4510-8.
150. Bedoui, S., et al., Equivalent stimulation of naive and memory CD8 T cells by DNA vaccination: a dendritic cell-dependent process. *Immunol Cell Biol*, 2009. 87(3): p. 255-9.
151. Cho, J.H., J.W. Youn, and Y.C. Sung, Cross-priming as a predominant mechanism for inducing CD8(+) T cell responses in gene gun DNA immunization. *J Immunol*, 2001. 167(10): p. 5549-57.
152. Radcliffe, J.N., et al., Prime-boost with alternating DNA vaccines designed to engage different antigen presentation pathways generates high frequencies of peptide-specific CD8⁺ T cells. *J Immunol*, 2006. 177(10): p. 6626-33.

153. Connolly, J.M., et al., Recognition by CD8 on cytotoxic T lymphocytes is ablated by several substitutions in the class I alpha 3 domain: CD8 and the T-cell receptor recognize the same class I molecule. *Proc Natl Acad Sci U S A*, 1990. 87(6): p. 2137-41.
154. Newberg, M.H., et al., Species specificity in the interaction of CD8 with the alpha 3 domain of MHC class I molecules. *J Immunol*, 1992. 149(1): p. 136-42.
155. Takeshita, T., et al., Role of conserved regions of class I MHC molecules in the activation of CD8+ cytotoxic T lymphocytes by peptide and purified cell-free class I molecules. *Int Immunol*, 1993. 5(9): p. 1129-38.
156. Howarth, M., et al., Tapasin enhances MHC class I peptide presentation according to peptide half-life. *Proc Natl Acad Sci U S A*, 2004. 101(32): p. 11737-42.
157. Saito, Y., P.A. Peterson, and M. Matsumura, Quantitation of peptide anchor residue contributions to class I major histocompatibility complex molecule binding. *J Biol Chem*, 1993. 268(28): p. 21309-17.
158. Lipford, G.B., et al., In vivo CTL induction with point-substituted ovalbumin peptides: immunogenicity correlates with peptide-induced MHC class I stability. *Vaccine*, 1995. 13(3): p. 313-20.
159. Bankovich, A.J., et al., Peptide register shifting within the MHC groove: theory becomes reality. *Mol Immunol*, 2004. 40(14-15): p. 1033-1039.
160. Kozono, H., et al., Production of Soluble Mhc Class-Ii Proteins with Covalently Bound Single Peptides. *Nature*, 1994. 369(6476): p. 151-154.

161. Liu, X., et al., Alternate interactions define the binding of peptides to the MHC molecule IA(b). *Proc Natl Acad Sci U S A*, 2002. 99(13): p. 8820-5.
162. Seamons, A., et al., Competition between two MHC binding registers in a single peptide processed from myelin basic protein influences tolerance and susceptibility to autoimmunity. *J Exp Med*, 2003. 197(10): p. 1391-7.
163. Chang, S.T., et al., Peptide length-based prediction of peptide-MHC class II binding. *Bioinformatics*, 2006. 22(22): p. 2761-7.
164. Hudrisier, D., et al., T cell activation correlates with an increased proportion of antigen among the materials acquired from target cells. *Eur J Immunol*, 2005. 35(8): p. 2284-94.
165. Chua, W.J. and T.H. Hansen, Bacteria, mucosal-associated invariant T cells and MR1. *Immunol Cell Biol*, 2010. 88(8): p. 767-9.
166. Tilloy, F., et al., An invariant T cell receptor alpha chain defines a novel TAP-independent major histocompatibility complex class Ib-restricted alpha/beta T cell subpopulation in mammals. *J Exp Med*, 1999. 189(12): p. 1907-21.
167. Treiner, E., et al., Selection of evolutionarily conserved mucosal-associated invariant T cells by MR1. *Nature*, 2003. 422(6928): p. 164-9.
168. Huang, S., et al., MR1 antigen presentation to mucosal-associated invariant T cells was highly conserved in evolution. *Proc Natl Acad Sci U S A*, 2009. 106(20): p. 8290-5.
169. Huang, S., et al., Evidence for MR1 antigen presentation to mucosal-associated invariant T cells. *J Biol Chem*, 2005. 280(22): p. 21183-93.

170. Mattner, J., et al., Exogenous and endogenous glycolipid antigens activate NKT cells during microbial infections. *Nature*, 2005. 434(7032): p. 525-9.
171. Zajonc, D.M., et al., Structure and function of a potent agonist for the semi-invariant natural killer T cell receptor. *Nat Immunol*, 2005. 6(8): p. 810-8.
172. Wei, D.G., et al., Mechanisms imposing the Vbeta bias of Valpha14 natural killer T cells and consequences for microbial glycolipid recognition. *J Exp Med*, 2006. 203(5): p. 1197-207.
173. Scott-Browne, J.P., et al., Germline-encoded recognition of diverse glycolipids by natural killer T cells. *Nat Immunol*, 2007. 8(10): p. 1105-13.
174. Kjer-Nielsen, L., et al., A structural basis for selection and cross-species reactivity of the semi-invariant NKT cell receptor in CD1d/glycolipid recognition. *J Exp Med*, 2006. 203(3): p. 661-73.
175. Ronet, C., et al., Role of the complementarity-determining region 3 (CDR3) of the TCR-beta chains associated with the V alpha 14 semi-invariant TCR alpha-chain in the selection of CD4+ NK T Cells. *J Immunol*, 2001. 166(3): p. 1755-62.
176. Gold, M.C., et al., Human mucosal associated invariant T cells detect bacterially infected cells. *PLoS Biol*, 2010. 8(6): p. e1000407.
177. Le Bourhis, L., et al., Antimicrobial activity of mucosal-associated invariant T cells. *Nat Immunol*, 2010. 11(8): p. 701-8.
178. Falk, K., et al., Allele-specific motifs revealed by sequencing of self-peptides eluted from MHC molecules. *Nature*, 1991. 351(6324): p. 290-6.

179. Hudrisier, D., et al., Binding of viral antigens to major histocompatibility complex class I H-2Db molecules is controlled by dominant negative elements at peptide non-anchor residues. Implications for peptide selection and presentation. *J Biol Chem*, 1996. 271(30): p. 17829-36.

Curriculum Vitae

Sojung Kim

21 Crabapple Ct

St.Louis, MO 63132

(314) 703-9149

sojungkim@go.wustl.edu

Education

Washington University in St. Louis, St. Louis, Missouri USA

Ph.D, Immunology, expected Aug 2011

- Advisor: Ted Hansen
- Dissertation: Single chain MHC trimer (SCT)-based DNA vaccines for pathogen protection

Ewha Womans University, Seoul, South Korea

M.S., Molecular and life sciences, Feb 2002

- Advisor: Kil-hyun Kim
- Dissertation: Telomerase activity is constitutively expressed in the murine CD8 T lymphocytes and controlled transcriptionally and post-translationally.

B.S. Pharmacy, Feb 2000

- *Magna Cum Laude*

Teaching experience

Washington University in St. Louis, St. Louis, Missouri USA

Teaching Assistant, Division of Biology and Biomedical sciences

- Foundations in Immunology, Fall 2005

Research experience

National Cancer Center, South Korea

Research fellow, 2002 – 2004,

Bukwang Pharm.Co.Ltd., South Korea

Internship, 1999 summer

Publication

- Chua WJ, Kim S, Myers N, Huang S, Yu L, Fremont DH, Diamond MS, Hansen TH. Endogenous MHC-related protein 1 is transiently expressed on the plasma membrane in a conformation that activates mucosal-associated invariant T cells. *J Immunol.* 2011 186(8) :4744-50
- Kim S, Li L, McMurtrey CP, Hildebrand WH, Weidanz JA, Gillanders WE, Diamond MS, Hansen TH. Single-chain HLA-A2 MHC trimers that incorporate an immunodominant peptide elicit protective T cell immunity against lethal West Nile virus infection. *J Immunol.* 2010 184(8) :4423-30.
- Huang S, Martin E, Kim S, Yu L, Soudais C, Fremont DH, Lantz O, Hansen TH. MR1 antigen presentation to mucosal-associated invariant T cells was highly conserved in evolution. *Proc Natl Acad Sci U S A.* 2009 106(20) :8290-5

- Huang S, Gilfillan S, Kim S, Thompson B, Wang X, Sant AJ, Fremont DH, Lantz O, Hansen TH. MR1 uses an endocytic pathway to activate mucosal-associated invariant T cells. *J Exp Med.* 2008 205(5) :1201-11.
- Baek KH, Park HY, Kang CM, Kim SJ, Jeong SJ, Hong EK, Park JW, Sung YC, Suzuki T, Kim CM, Lee CW. Overexpression of Hepatitis C virus NS5A protein induces chromosome instability via mitotic cell cycle dysregulation., *J Mol. Biol.* 2006 (359) :22-34
- Shin HJ, Baek KH, Jeon AH, Kim SJ, Jang KL, Sung YC, Kim CM, Lee CW, Inhibition of histone deacetylase activity increases chromosomal instability by the aberrant regulation of mitotic checkpoint activation., *Oncogene* 2003 (22) :3853-3858

Certification

Certificate of Pharmacist, South Korea, Oct 2000